



**Calhoun: The NPS Institutional Archive**  
**DSpace Repository**

---

Theses and Dissertations

1. Thesis and Dissertation Collection, all items

---

2002-03

# On the capacity of a cellular CDMA system reverse channel

Klitorakis, Petros

Monterey, Calif. Naval Postgraduate School

---

<http://hdl.handle.net/10945/5993>

*Downloaded from NPS Archive: Calhoun*



Calhoun is a project of the Dudley Knox Library at NPS, furthering the precepts and goals of open government and government transparency. All information contained herein has been approved for release by the NPS Public Affairs Officer.

**Dudley Knox Library / Naval Postgraduate School**  
**411 Dyer Road / 1 University Circle**  
**Monterey, California USA 93943**

<http://www.nps.edu/library>

# NAVAL POSTGRADUATE SCHOOL Monterey, California



## THESIS

**ON THE CAPACITY OF A CELLULAR CDMA SYSTEM  
REVERSE CHANNEL**

by

Petros Klitorakis

March 2002

Thesis Advisor:

Thesis Co-Advisor:

Second Reader:

Tri T. Ha

Jan E. Tighe

David C. Jenn

**Approved for public release; distribution is unlimited**

THIS PAGE INTENTIONALLY LEFT BLANK

<b>REPORT DOCUMENTATION PAGE</b>			Form Approved OMB No. 0704-0188
Public reporting burden for this collection of information is estimated to average 1 hour per response, including the time for reviewing instruction, searching existing data sources, gathering and maintaining the data needed, and completing and reviewing the collection of information. Send comments regarding this burden estimate or any other aspect of this collection of information, including suggestions for reducing this burden, to Washington headquarters Services, Directorate for Information Operations and Reports, 1215 Jefferson Davis Highway, Suite 1204, Arlington, VA 22202-4302, and to the Office of Management and Budget, Paperwork Reduction Project (0704-0188) Washington DC 20503.			
<b>1. AGENCY USE ONLY (Leave blank)</b>	<b>2. REPORT DATE</b> March 2002	<b>3. REPORT TYPE AND DATES COVERED</b> Master's Thesis	
<b>4. TITLE AND SUBTITLE:</b> On the Capacity of a Cellular CDMA System Reverse Channel			<b>5. FUNDING NUMBERS</b>
<b>6. AUTHOR(S)</b> Petros Klitorakis			<b>8. PERFORMING ORGANIZATION REPORT NUMBER</b>
<b>7. PERFORMING ORGANIZATION NAME(S) AND ADDRESS(ES)</b> Naval Postgraduate School Monterey, CA 93943-5000			<b>10. SPONSORING / MONITORING AGENCY REPORT NUMBER</b>
<b>9. SPONSORING / MONITORING AGENCY NAME(S) AND ADDRESS(ES)</b> N/A			<b>11. SUPPLEMENTARY NOTES</b> The views expressed in this thesis are those of the author and do not reflect the official policy or position of the Department of Defense or the U.S. Government.
<b>12a. DISTRIBUTION / AVAILABILITY STATEMENT</b> Approved for public release; distribution is unlimited			<b>12b. DISTRIBUTION CODE</b>
<b>13. ABSTRACT (maximum 200 words)</b> In this thesis, the reverse channel model for a seven-cell cluster DS-CDMA cellular communications system operating in a slow-flat Nakagami fading and lognormal shadowing environment is developed. The aforementioned system uses imperfect power control to combat the near-far effect and the lognormal shadowing. Forward error correction is applied by using convolutional encoding and soft decision decoding. The probability of bit error is estimated by using a Gaussian approximation, sectoring antennas and a rake receiver at the base station in order to enhance the system's performance. The performance of the system is examined under several values of the standard deviation of lognormal shadowing and the power control error for various numbers of users and values of the Nakagami-m variable by using simulations. Finally, a barrage noise jammer will be introduced and its effect seen in the performance of the cellular communication system for a specific value of $\frac{E_b}{N_0}$ .			
<b>14. SUBJECT TERMS</b> Reverse Channel Cellular Communications			<b>15. NUMBER OF PAGES</b> 119
			<b>16. PRICE CODE</b>
<b>17. SECURITY CLASSIFICATION OF REPORT</b> Unclassified	<b>18. SECURITY CLASSIFICATION OF THIS PAGE</b> Unclassified	<b>19. SECURITY CLASSIFICATION OF ABSTRACT</b> Unclassified	<b>20. LIMITATION OF ABSTRACT</b> UL

THIS PAGE INTENTIONALLY LEFT BLANK

**Approved for public release; distribution is unlimited**

**ON THE CAPACITY OF A CELLULAR CDMA SYSTEM REVERSE CHANNEL**

Petros Klitorakis  
Lieutenant Junior Grade, Hellenic Navy  
B.S., Hellenic Naval Academy, 1993

Submitted in partial fulfillment of the  
requirements for the degrees

**MASTER OF SCIENCE IN ELECTRICAL ENGINEERING  
and  
MASTER OF SCIENCE IN SYSTEMS ENGINEERING**

from the

**NAVAL POSTGRADUATE SCHOOL  
March 2002**

Author: Petros Klitorakis

Approved by: Tri T. Ha  
Thesis Advisor

Jan E. Tighe  
Thesis Co-Advisor

David C. Jenn  
Second Reader

Dan C. Boger  
Chairman, Department of Information Sciences

Jeffrey B. Knorr  
Chairman, Department of Electrical and Computer  
Engineering

THIS PAGE INTENTIONALLY LEFT BLANK

## ABSTRACT

In this thesis, the reverse channel model for a seven-cell cluster DS-CDMA cellular communications system operating in a slow-flat Nakagami fading and lognormal shadowing environment is developed. The aforementioned system uses imperfect power control to combat the near-far effect and the lognormal shadowing. Forward error correction is applied by using convolutional encoding and soft decision decoding. The probability of bit error is estimated by using a Gaussian approximation, sectoring antennas and a rake receiver at the base station in order to enhance the system's performance.

The performance of the system is examined under several values of the standard deviation of lognormal shadowing and the power control error for various numbers of users and values of the Nakagami-m variable by using simulations.

Finally, a barrage noise jammer will be introduced and its effect seen in the performance of the cellular communication system for a specific value of  $\frac{E_b}{N_0}$ .



THIS PAGE INTENTIONALLY LEFT BLANK

## TABLE OF CONTENTS

<b>I.</b>	<b>INTRODUCTION.....</b>	<b>1</b>
	<b>A. BACKGROUND.....</b>	<b>1</b>
	<b>B. OBJECTIVE.....</b>	<b>1</b>
	<b>C. RELATED WORK .....</b>	<b>2</b>
	<b>D. THESIS OUTLINE.....</b>	<b>2</b>
<b>II.</b>	<b>DIRECT SEQUENCE SPREAD SPECTRUM CDMA .....</b>	<b>5</b>
	<b>A. SPREAD SPECTRUM .....</b>	<b>5</b>
	<b>B. WALSH FUNCTIONS .....</b>	<b>6</b>
	<b>C. PSEUDO-NOISE SEQUENCES.....</b>	<b>8</b>
<b>III.</b>	<b>REVERSE CHANNEL MODEL.....</b>	<b>11</b>
	<b>A. BUILDING THE DS-CDMA REVERSE SIGNAL .....</b>	<b>12</b>
	<b>1. DS-CDMA Spreading and Despreading .....</b>	<b>13</b>
	<b>2. The Transmitted Signal .....</b>	<b>15</b>
	<b>3. Free Space Propagation .....</b>	<b>16</b>
	<b>B. NAKAGAMI FADING CHANNEL .....</b>	<b>18</b>
	<b>1. Small Scale Fading due to Multiple Paths .....</b>	<b>19</b>
	<b>2. Log-Normal Shadowing.....</b>	<b>19</b>
	<b>3. Power Control and Power Control Error .....</b>	<b>20</b>
	<b>C. NAKAGAMI-LOGNORMAL CHANNEL MODEL .....</b>	<b>21</b>
	<b>1. The Reverse Signal <math>S_0(t)</math> .....</b>	<b>21</b>
	<b>2. Intracell Interference .....</b>	<b>22</b>
	<b>3. Co-Channel or Intercell Interference.....</b>	<b>24</b>
	<b>4. The Received Signal <math>r(t)</math> .....</b>	<b>26</b>
	<b>D. SUMMARY.....</b>	<b>27</b>
	<b>APPENDIX III. LOGNORMAL RANDOM VARIABLE.....</b>	<b>29</b>
<b>IV.</b>	<b>DS-CDMA PERFORMANCE ANALYSIS .....</b>	<b>31</b>
	<b>A. PERFORMANCE OF THE BASIC SYSTEM.....</b>	<b>32</b>
	<b>1. The Demodulated Signal <math>y(t)</math> .....</b>	<b>32</b>
	<b>2. The Decision Statistic <math>Y</math> .....</b>	<b>34</b>
	<b>3. Signal-to-Noise plus Interference Ratio .....</b>	<b>36</b>
	<b>B. CONVOLUTIONAL ENCODING.....</b>	<b>38</b>
	<b>C. BIT ERROR ANALYSIS OF DS-CDMA.....</b>	<b>44</b>
	<b>APPENDIX IV-A. CALCULATION OF THE VARIANCE OF THE INTERCELL INTERFERENCE .....</b>	<b>49</b>
	<b>APPENDIX IV-B. CALCULATION OF THE VARIANCE OF THE NOISE COMPONENT .....</b>	<b>53</b>
	<b>APPENDIX IV-C. PROBABILITY OF BIT ERROR.....</b>	<b>55</b>

APPENDIX IV-D. PLOTS OF THE PERFORMANCE OF THE SYSTEM FOR VARIOUS USERS AND PARAMETERS.....	57
V. VARIOUS TECHNIQUES TO IMPROVE THE PERFORMANCE OF OUR SYSTEM .....	63
A. RAKE RECEIVER.....	63
B. SECTORING.....	65
APPENDIX V. PLOTS OF THE PERFORMANCE OF THE SYSTEM WITH THE USE OF RAKE RECEIVER AND SECTORING.....	69
VI. JAMMING.....	89
A. PERFORMANCE OF BPSK IN BARRAGE NOISE JAMMING .....	89
B. PERFORMANCE OF DS SPREAD SPECTRUM SYSTEMS IN BARRAGE NOISE JAMMING .....	89
C. PERFORMANCE OF REVERSE CHANNEL OF A DS SPREAD SPECTRUM SYSTEM WITH FEC IN BARRAGE NOISE JAMMING.....	92
VII. CONCLUSIONS.....	95
LIST OF REFERENCES .....	97
INITIAL DISTRIBUTION LIST .....	99

## LIST OF FIGURES

Figure 2.1.	Power Spectral Density for the BPSK Signal and the DS for $N=2$ .....	6
Figure 3.1.	Reverse Channel.....	11
Figure 3.2.	Seven-Cell Cluster Cellular System.....	12
Figure 3.3.	Baseband Spreading and Dispersing for One Data Bit from User One by a Factor of $N=8$ . ....	13
Figure 3.4.	The Transmitted Signal. ....	15
Figure 3.5.	The Reverse Signal.....	22
Figure 3.5.	Mobile User $ij$ in Adjacent Cell $i$ . ....	25
Figure 3.6.	Memoryless System. ....	29
Figure 4.1.	Seven-Cell Cluster Cellular System.....	31
Figure 4.2.	Base Station Receiver.....	32
Figure 4.3.	Trellis Diagram. ....	39
Figure 4.4.	Coded Nakagami for Lognormal Shadowing $\sigma = 7$ and Power Control Error $\sigma_{1dB} = 1, 2, 3, 4$ for $m = 1$ and 20 Users per Cell.....	44
Figure 4.5.	Coded Nakagami for Lognormal Shadowing $\sigma = 9$ and Power Control Error $\sigma_{1dB} = 1, 2, 3, 4$ for $m = 1$ and 20 Users per Cell.....	45
Figure 4.6.	Coded Nakagami for Lognormal Shadowing $\sigma = 7$ and Power Control Error $\sigma_{1dB} = 4$ for $m = 0.5, 0.75, 1, 1.5, 2$ and 20 Users per Cell. ....	46
Figure 4.7.	Coded Nakagami for Lognormal Shadowing $\sigma = 9$ and Power Control Error $\sigma_{1dB} = 4$ for $m = 0.5, 0.75, 1, 1.5, 2$ and 20 Users per Cell. ....	47
Figure 4.8.	Coded Nakagami for Lognormal Shadowing $\sigma = 7$ and Power Control Error $\sigma_{1dB} = 4$ for $m = 1$ . ....	48
Figure 4.9.	Transformation of the Limits of Integration. ....	50
Figure 4.10.	Coded Nakagami for Lognormal Shadowing $\sigma = 7$ and Power Control Error $\sigma_{1dB} = 4$ for $m = 0.5$ . ....	57
Figure 4.11.	Coded Nakagami for Lognormal Shadowing $\sigma = 7$ and Power Control Error $\sigma_{1dB} = 4$ for $m = 0.75$ . ....	58
Figure 4.12.	Coded Nakagami for Lognormal Shadowing $\sigma = 7$ and Power Control Error $\sigma_{1dB} = 1, 2, 3, 4$ for $m = 0.5$ and 20 Users per Cell.....	59
Figure 4.13.	Coded Nakagami for Lognormal Shadowing $\sigma = 9$ and Power Control Error $\sigma_{1dB} = 1, 2, 3, 4$ for $m = 0.5$ and 20 Users per Cell.....	60
Figure 4.14.	Coded Nakagami for Lognormal Shadowing $\sigma = 7$ and Power Control Error $\sigma_{1dB} = 1, 2, 3, 4$ for $m = 2$ and 20 Users per Cell.....	61
Figure 4.15.	Coded Nakagami for Lognormal Shadowing $\sigma = 9$ and Power Control Error $\sigma_{1dB} = 1, 2, 3, 4$ for $m = 2$ and 20 Users per Cell.....	62
Figure 5.1.	Typical Rake Receiver for $L=3$ .....	64

Figure 5.2.	Coded Nakagami with and without Rake Receiver for 30 Users per Cell and for Lognormal Shadowing $\sigma = 7$ and Power Control Error $\sigma_{1dB} = 4$ and $m=1$ .	65
Figure 5.3.	120° Sectoring.	66
Figure 5.4.	60° Sectoring.	67
Figure 5.5.	Coded Nakagami with and without Sectoring for 100 Users per Cell and for Lognormal Shadowing $\sigma = 7$ and Power Control Error $\sigma_{1dB} = 4$ and $m=1$ .	68
Figure 5.6.	Coded Nakagami with and without Sectoring for 60 Users per Cell and for Lognormal Shadowing $\sigma = 9$ and Power Control Error $\sigma_{1dB} = 4$ and $m=1$ .	69
Figure 5.7.	Coded Nakagami for Lognormal Shadowing $\sigma = 7$ and Power Control Error $\sigma_{1dB} = 4$ for $m=0.5$ and Various Users for 120° Sectoring.	70
Figure 5.8.	Coded Nakagami for Lognormal Shadowing $\sigma = 7$ and Power Control Error $\sigma_{1dB} = 4$ for $m=0.75$ and Various Users for 120° Sectoring.	71
Figure 5.9.	Coded Nakagami for Lognormal Shadowing $\sigma = 7$ and Power Control Error $\sigma_{1dB} = 4$ for $m=0.75$ and Various Users for 120° Sectoring and Rake Receiver.	72
Figure 5.10.	Coded Nakagami for Lognormal Shadowing $\sigma = 7$ and Power Control Error $\sigma_{1dB} = 4$ for $m=1$ and Various Users for 120° Sectoring.	73
Figure 5.11.	Coded Nakagami for Lognormal Shadowing $\sigma = 7$ and Power Control Error $\sigma_{1dB} = 4$ for $m=1$ and Various Users for 120° Sectoring and Rake Receiver.	74
Figure 5.12.	Coded Nakagami for Lognormal Shadowing $\sigma = 7$ and Power Control Error $\sigma_{1dB} = 4$ for $m=1.5$ and Various Users for 120° Sectoring.	75
Figure 5.13.	Coded Nakagami for Lognormal Shadowing $\sigma = 7$ and Power Control Error $\sigma_{1dB} = 4$ for $m=2$ and Various Users for 120° Sectoring.	76
Figure 5.14.	Coded Nakagami for Lognormal Shadowing $\sigma = 7$ and Power Control Error $\sigma_{1dB} = 4$ for $m=0.5$ and Various Users for 60° Sectoring.	77
Figure 5.15.	Coded Nakagami for Lognormal Shadowing $\sigma = 7$ and Power Control Error $\sigma_{1dB} = 4$ for $m=0.75$ and Various Users for 60° Sectoring.	78
Figure 5.16.	Coded Nakagami for Lognormal Shadowing $\sigma = 7$ and Power Control Error $\sigma_{1dB} = 4$ for $m=0.75$ and Various Users for 60° Sectoring and Rake Receiver.	79
Figure 5.17.	Coded Nakagami for Lognormal Shadowing $\sigma = 7$ and Power Control Error $\sigma_{1dB} = 4$ for $m=1$ and Various Users for 60° Sectoring.	80
Figure 5.18.	Coded Nakagami for Lognormal Shadowing $\sigma = 7$ and Power Control Error $\sigma_{1dB} = 4$ for $m=1$ and Various Users for 60° Sectoring with Rake Receiver.	81

Figure 5.19.	Coded Nakagami for Lognormal Shadowing $\sigma = 7$ and Power Control Error $\sigma_{1dB} = 4$ for $m=1.5$ and Various Users for $60^\circ$ Sectoring.....	82
Figure 5.20.	Coded Nakagami for Lognormal Shadowing $\sigma = 7$ and Power Control Error $\sigma_{1dB} = 4$ for $m=2$ and Various Users for $60^\circ$ Sectoring.....	83
Figure 5.21.	Coded Nakagami for Lognormal Shadowing $\sigma = 7$ and Power Control Error $\sigma_{1dB} = 3$ for $m=0.5$ and Various Users for $120^\circ$ Sectoring.....	84
Figure 5.22.	Coded Nakagami for Lognormal Shadowing $\sigma = 7$ and Power Control Error $\sigma_{1dB} = 3$ for $m=0.75$ and Various Users for $120^\circ$ Sectoring.....	85
Figure 5.23.	Coded Nakagami for Lognormal Shadowing $\sigma = 7$ and Power Control Error $\sigma_{1dB} = 3$ for $m=1$ and Various Users for $120^\circ$ Sectoring.....	86
Figure 5.24.	Coded Nakagami for Lognormal Shadowing $\sigma = 7$ and Power Control Error $\sigma_{1dB} = 3$ for $m=1.5$ and Various Users for $120^\circ$ Sectoring.....	87
Figure 5.25.	Coded Nakagami for Lognormal Shadowing $\sigma = 7$ and Power Control Error $\sigma_{1dB} = 3$ for $m=2$ and Various Users for $120^\circ$ Sectoring.....	88
Figure 6.1.	Coded Nakagami for 100 Users per Cell with $120^\circ$ Sectoring, Lognormal Shadowing $\sigma = 7$ , Power Control Error $\sigma_{1dB} = 4$ and $m=1$ . ....	93
Figure 6.2.	Coded Jammed Nakagami for 100 Users per Cell with $120^\circ$ Sectoring, SNR=15, Lognormal Shadowing $\sigma = 7$ , Power Control Error $\sigma_{1dB} = 4$ and $m=1$ . ....	94

THIS PAGE INTENTIONALLY LEFT BLANK

## LIST OF TABLES

Table 3.1.	Spreading of Information Bit $b_{01}$ of the Desired Cell.....	14
Table 3.2.	Extracting Information Bit $b_{01}$ from the Received Spreaded Signal.....	14
Table 3.3.	Values of the Path Loss Exponent for Various Types of Environment. ....	17



THIS PAGE INTENTIONALLY LEFT BLANK

## **ACKNOWLEDGMENTS**

I would like to initially thank: Professor Tri T. Ha for his sound, knowledgeable and practical guidance that helped me to complete this thesis.

On a personal level, a huge thank you to: my wife, Maria Papageorgiou for her support and love through it all, my daughter Sophia Anastasia for being a patient toddler and my parents who may be abroad but who always lent a sympathetic and an encouraging ear.

THIS PAGE INTENTIONALLY LEFT BLANK

## EXECUTIVE SUMMARY

Currently, the third-generation cellular systems (3G) are already being used in Japan and Europe and soon they will dominate in the field of wireless cellular communications. The third-generation system supports data-type traffic at higher data rates than the second-generation systems (GSM, IS-95), over 144 kbps and up to 2 Mbps.

The third-generation cellular systems use a multiple access technique called Direct Sequence Code Division multiple Access (DS-CDMA), which provides an efficient use of the bandwidth in order to support many users. In DS-CDMA systems every mobile user uses orthogonal Walsh codes to spread its signal. All the user traffic arrives at the base station as a composite reverse signal. The base station extracts the traffic for each user from the composite signal by using the preassigned code for each one separately.

In this thesis, we present the advantages of the use of Spread Spectrum systems and the properties of Walsh codes. We specifically address the reverse channel, which carries traffic from the wireless mobile users to the base station. The performance of the reverse channel is very critical because it is used to upload data to the Internet. In this analysis, it is assumed that the reverse channel is a frequency-selective one and that the multi-path fading signal is characterized by the Nakagami- $m$  probability density function (pdf).

In DS-CDMA cellular systems, the total signal that the base station receives includes the reverse signal from the mobile users of its cell and from the six adjacent cells (for a seven-cell cluster). All the signals from the mobile users of the center cell arrive roughly at the same power-level at the central base station due to the power control technique employed by the base station. The reverse signals from all the other mobile users except the user of interest (user 1) constitute the intracell interference. The reverse signals from all the other mobile users of the six adjacent cells constitute the intercell or co-channel interference. There is also the problem of additive noise that the base station must overcome. To improve the chances of correctly decoding the desired signal, we use Forward Error Correction (FEC) with soft decision decoding. Furthermore, we include

the technique of sectoring to reduce the intracell and intercell interference, and the use of Rake receiver at the base station to address the multi-path fading problem. We develop the probability of bit error, for the reverse channel of a cellular system operating in a Nakagami fading and lognormal shadowing environment, with power control error that employs FEC, sectoring and Rake receiver. We examine the performance of our system under a range of operating conditions, such as the value of the Nakagami  $m$ -variable, the number of mobile users and the value of the power control error and the lognormal shadowing. Finally, we present the effects of Jamming in the performance of the system and the benefits of using a DS system instead of an ordinary BPSK one, and we develop the probability of bit error.

# **I. INTRODUCTION**

## **A. BACKGROUND**

In the beginning of the new millennium it is very important for people, especially businessmen, to be always informed and kept up-to-date even if they are not at work or home. Therefore, wireless and mobile communication networks are, presently, playing a very important role in the supply of a great number of services to both mobile and fixed users such as instant Internet access.

The need for higher data rates for faster downloading and uploading of files, such as e-mails, make the existing first and second-generation of cellular systems obsolete. First-generation systems such as AMPS and N-AMPS are simple FM systems, which, unfortunately, cannot provide access to a large number of users. Second-generation cellular systems such as IS-95 in United States and GSM in Europe offer data rates of 10 kbps, which is fairly good for voice-type communications. However, these systems offer much lower data rates when compared to the data rates that the current modems offer through ordinary telephone lines, and therefore perform inadequately.

Manufacturers believe that they can achieve higher data rates over 144 kbps and up to 2 Mbps with the third-generation systems which would be sufficient to meet the expectations of mobile users.

The third-generation systems use Wideband Code Division Multiple Access techniques, which are already being used in Japan and have recently been tested in Europe (England, 2001).

## **B. OBJECTIVE**

In this thesis, an attempt will be made to examine the operation of the reverse channel of a Direct Sequence Code Division Multiple Access cellular system, which operates in a slow flat Nakagami-fading environment and uses power control with error.

The reverse channel carries data from the mobile user to the base station and its performance is very critical, especially for the uploading of files or the sending of e-mails.

The system's performance is increased by applying Forward Error Correction (FEC) with convolutional encoding and soft decision decoding and by using 120° and 60° sectoring. Rake receivers at base stations are also used to counter multipath fading.

### **C. RELATED WORK**

Most of this analysis is based on the previous work done in the DS-CDMA forward channel of a cellular system operating in a slow-flat Rayleigh fading and lognormal shadowing environment as in [1]. This thesis will examine the reverse channel and especially Nakagami fading which is more general and includes the Rayleigh environment.

Some previous analyses examine only the reverse channel of a single-cell cellular system [2] where there is no inter-cell interference while others do not include the effects of Forward Error Correction (FEC) or imperfect power control [3].

From [3], the results for the SNIR of the reverse channel of a seven-cell system with Nakagami-fading channel and power control error are borrowed which does not include FEC.

None of the above considers the impact that a jammer might have on the performance of our system. This will be examined in Chapter VI and is based on class notes for the jamming of DS-CDMA systems [4].

### **D. THESIS OUTLINE**

In Chapter II, the Direct Sequence Spread Spectrum CDMA system is introduced and its advantages over conventional BPSK systems are discussed. Walsh functions and Pseudo Noise sequences are also introduced, which are basically used for spreading. Their properties are examined and are used in our system.

In Chapter III, the Reverse Channel model for our seven-cell cluster cellular communication system is developed. In this model, large and small-scale propagation effects, Nakagami-fading, lognormal shadowing and power control error problems are handled. In addition, the composite signal that the base station of the center cell receives is developed which is comprised of the desired signal from mobile user 1 located in the coverage area of the center cell, the signals from the other active users in the center cell

(intra-cell interference), the signals from all the active mobile users that are in the coverage area of the six adjacent cells (inter-cell or co-channel interference) and also Additive White Gaussian Noise (AWGN).

In Chapter IV, the Forward Error Correction with convolutional encoding of rate  $\frac{1}{2}$  and soft decision decoding into our Nakagami-lognormal reverse channel is applied and an upper bound on the probability of bit error is also developed. Then, by using Monte Carlo techniques, the performance of our system for several values of the Nakagami- $m$  variable and for various numbers of users per cell is simulated.

In Chapter V, the Rake receiver and the technique of sectoring and their benefits are introduced and briefly discussed. Sectoring angles of  $120^\circ$  and  $60^\circ$  and several values of the standard deviation of the lognormal power control error are also used.

In Chapter VI, an attempt is made to jam our communication system and demonstrate the effects of Barrage Noise Jamming for a specific value of the  $E_b/N_0$ .

In Chapter VII, our observations are summarized a conclusion is reached.



THIS PAGE INTENTIONALLY LEFT BLANK

## II. DIRECT SEQUENCE SPREAD SPECTRUM CDMA

### A. SPREAD SPECTRUM

Spread spectrum is a modulation scheme that produces more transmission bandwidth than the bandwidth required for an information signal and is described in [4] and [5].

Spread spectrum was developed during World War II and until recently was used explicitly for military purposes. Recently, spread spectrum communication systems have been used in many applications because of their numerous advantages. The most important advantages are the following:

- Increased resistance to signal interference from multiple transmission paths
- Capability for multiple access applications such as CDMA
- Low probability to be intercepted (LPI) and low probability of detection (LPD) which is very important for military purposes
- Increased resistance to interference and jamming which is very important for both military and commercial applications
- Capability to measure ranges (DS spread spectrum is used for the global positioning system GPS)

The disadvantages are that more complex transmitters and receivers and much more bandwidth than for conventional systems are needed. In DS CDMA systems, Walsh codes and Pseudo Noise sequences (PN sequences) are used to spread the information signal of each user. The spreading waveform  $c(t)$  is called chipping signal and each chip (the bit of the spreading waveform) has a duration of  $T_c$  seconds.

In order to have a correct spreading of the BPSK information signal  $b(t)$ , which has a duration of  $T_b$  seconds, there must be an integer  $N$  such as  $T_b = N \cdot T_c$ . A synchronization between the baseband and the chipping signal, such as the beginning of a chip interval is the beginning of a bit interval, is also required.

The transmission bandwidth would now be  $N$  times greater than that of the BPSK signal and so the original power spectral density PSD has been also spread out  $N$  times.

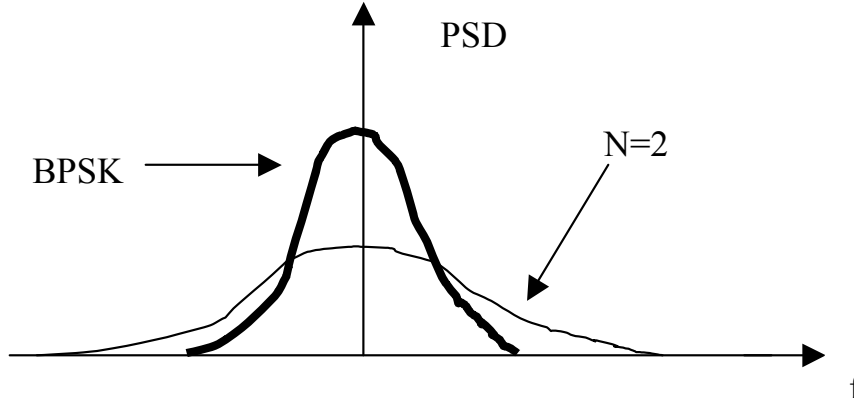


Figure 2.1. Power Spectral Density for the BPSK Signal and the DS for  $N=2$ .

Now for a large  $N$  (in our case  $N=128$ ) even an initially very strong signal will have a small PSD. It would be very hard for someone to detect this signal since the noise power might be greater than the signal's power. For this reason, the DS-SS is called a LPD system. However, even if the signal is detected, the correct spreading sequence  $c(t)$  is needed in order to extract the information signal  $b(t)$ . Therefore, it will be classified as a LPI system.

However, in our case, the spreading waveform  $c_{ij}(t)$  of each user is the product of the user's Walsh code  $w_j(t)$  and the cell's PN sequence  $c_i(t)$ , which is another PN sequence.

## B. WALSH FUNCTIONS

Walsh functions are used for both the reverse and forward channel in a DS-SS cellular communication system. In the forward channel, they provide orthogonal cover and therefore help to overcome the problem of intra-cell interference. In the reverse channel, Walsh functions are used for more spreading and in W-SS where a user can transmit pilot symbols and several data signals simultaneously with different Walsh codes. They provide orthogonality for the several signals of the same user.

There are various ways to generate a set of Walsh functions but in this case, the generation of Walsh functions with the use of Hadamard matrices will be generated. The Hadamard matrix  $H_2$  is as follows:

$$H_2 = \begin{bmatrix} 00 \\ 01 \end{bmatrix}$$

The next Hadamard matrix  $H_4$  is as follows:

$$H_4 = \begin{bmatrix} H_2 H_2 \\ H_2 \bar{H}_2 \end{bmatrix} = \begin{bmatrix} 0000 \\ 0101 \\ 0011 \\ 0110 \end{bmatrix}$$

where  $\bar{H}_2$  is the complement of  $H_2$  which means that a 0 is replaced with a 1 and a 1 is replaced with a 0.

The next Hadamard matrix  $H_8$  is as follows:

$$H_8 = \begin{bmatrix} H_4 H_4 \\ H_4 \bar{H}_4 \end{bmatrix} = \begin{bmatrix} 00000000 \\ 01010101 \\ 00110011 \\ 01100110 \\ 00001111 \\ 01011010 \\ 00111100 \\ 01101001 \end{bmatrix}$$

and in general for the Hadamard Matrix  $H_{2^m}$ :

$$H_{2^m} = \begin{bmatrix} H_{2^{m-1}} & H_{2^{m-1}} \\ H_{2^{m-1}} & \bar{H}_{2^{m-1}} \end{bmatrix}$$

Now each row of the Hadamard code is a block code and the set of  $2^{m+1}$   $2^m$  tuples consisting of the rows of  $H_{2^m}$  and  $\bar{H}_{2^m}$  form a  $(n, k) = (n, m + 1)$  block code called the Hadamard code. Except for the all zero and all one code word, each of the other  $2^{m+1}$  code words has  $2^{m-1}$  ones and  $2^{m-1}$  zeros. Walsh functions are easily reproduced which means low security if they are used alone for spreading.

### C. PSEUDO-NOISE SEQUENCES

Pseudo-Noise (PN) sequences should have, as much as possible, the same characteristics as a True Random Binary Sequence. For a true random binary wave, the probability of a logical one or a logical zero is the same and equal to a half:

$$\Pr[c(t) = 1] = \Pr[c(t) = -1] = \frac{1}{2}$$

The expected value of  $c(t)$  must be equal to zero:

$$E[c(t)] = \frac{1 + (-1)}{2} = 0$$

A bit is not dependent on the value of the previous bit or the next bit and generally is independent of all the other bits.

The autocorrelation function  $R_{c(t)}$  is given by:

$$R_{c(t)} = \begin{cases} \left(1 - \frac{|\tau|}{T_c}\right) & \text{for } |\tau| \leq T_c \\ 0 & \text{for } |\tau| > T_c \end{cases}$$

PN sequences are usually generated with the use of an n-stage shift register. For higher security, a non-linear PN generator is used.

PN sequences are deterministic and periodic with period  $N' \cdot T_c$  where  $N'$  is an integer and  $T_c$  is the chipping bit interval.

Now if  $N'$  is much greater than  $N$  ( $N' \gg N$ ) then there is a long PN code and if  $N' = N$ , there is a short PN code. A short PN code means that the period of the PN sequence is  $T_b$  (bit duration) and so it repeats itself every bit interval. In the cellular system of concern, and generally in all modern systems, a long PN code is used.

THIS PAGE INTENTIONALLY LEFT BLANK

### III. REVERSE CHANNEL MODEL

The reverse channel in a DS-CDMA cellular system is the channel used to convey traffic from the mobile user to the base station as shown in Figure 3.1.

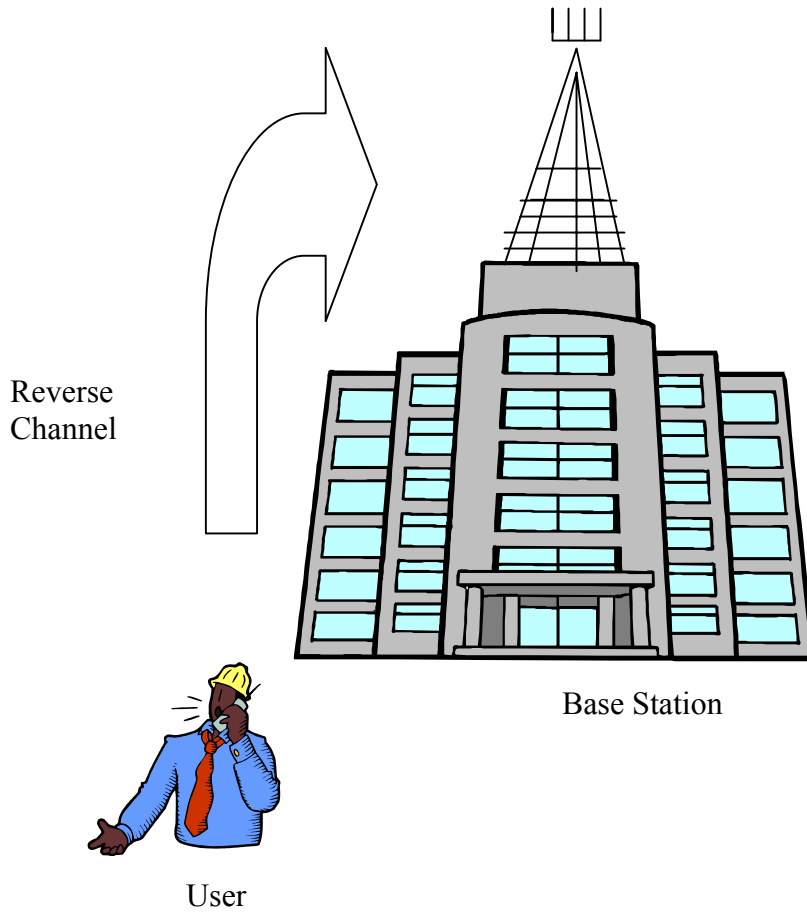


Figure 3.1. Reverse Channel.

The cellular system with higher data rates in the reverse channel will provide the user with the notable benefit of the fast uploading of files including e-mails or video conferencing.



In Chapter III, a reverse channel model will be built for a typical DS-CDMA cellular system. Our analysis is complicated because the channel is wireless and the base stations receive signals from all mobile users. The propagation of the signal is affected by reflection, diffraction, and scattering. Furthermore, the signal from the user arrives via many different paths which have different strengths.

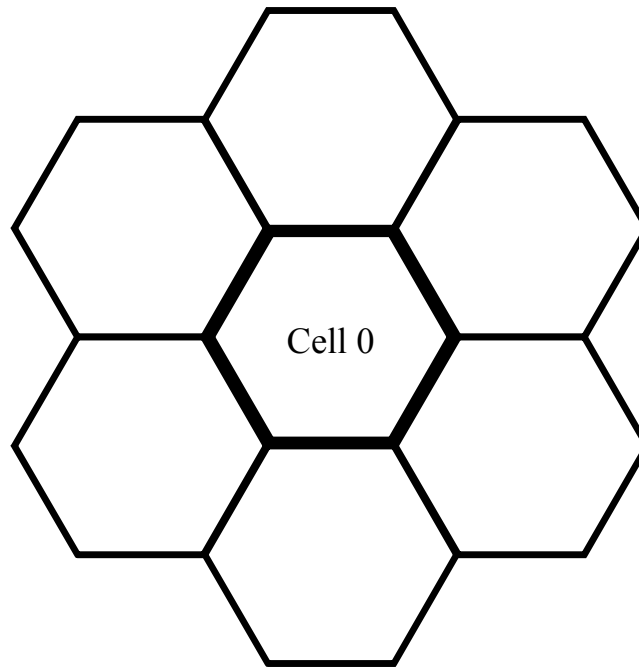


Figure 3.2. Seven-Cell Cluster Cellular System.

#### A. BUILDING THE DS-CDMA REVERSE SIGNAL

In our model, a basic seven-cell cluster cellular system will be used as shown in Figure 3.2. It is assumed that each cell has a hexagonal shape which represents the radio coverage area of each base station. Hexagons are used because a specific geographic area is covered with the fewest number of cells if they are hexagonal without leaving gaps or overlapping regions as circular cells do. It is also assumed that the base station antennas are positioned at the centers of the cells. The central hexagon which is named the 0 cell is our focus.

In each cell, there are  $K$  mobile users which are active during our analysis. Thus, there will be  $K$  mobile users in the center cell 0 and a total of  $6 \cdot K$  users in all the six

adjacent cells. The central base station receives the signals from the specific user of interest which is named user one (desired signal) but also signals from the other  $K - 1$  users of cell 0 which is called intracell interference, and from the  $6 \cdot K$  users of the adjacent cells which constitute the intercell or co-channel interference. All of the aforementioned signals are spread spectrum signals.

### 1. DS-CDMA Spreading and Despreading

As previously stated, all the received signals are spread spectrum signals. When a BPSK signal is spread by a factor of  $N$ , the main lobe of the power spectral density is spread by a factor  $N$  and the magnitude of the PSD is reduced by a factor of  $N$  also. Now a direct sequence spread spectrum signal is easily despreading when the demodulator at our base station knows the chipping signal (PN sequence).

When the DS signal is despreading after the multiplication with the chipping signal  $c(t)$ , the BPSK signal can be demodulated by a BPSK receiver. The baseband spreading and despreading for one data bit from user one which is spread by a factor of  $N=8$  is depicted in Figure 3.3.

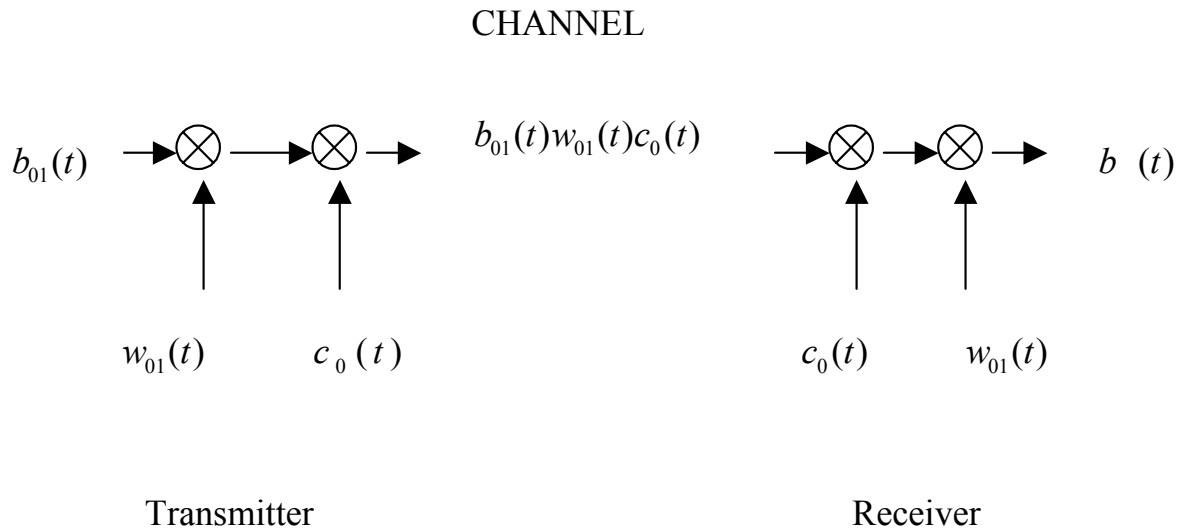


Figure 3.3. Baseband Spreading and Despreading for One Data Bit from User One by a Factor of  $N=8$ .

In our analysis, it is assumed that the transmitter mobile user 1 of center cell 0, and the receiver base station of the center cell are perfectly synchronized which means that the two PN sequences are at the exact same point in their pattern. Now, assume that user 1 of the center cell transmits one information bit  $b_{01} = 1$ , and is spread by a factor of 8 by the Walsh function  $w_{01} = (01010101)$  and the PN sequence of the center cell  $c_0 = (10111011)$  for this bit interval. Table 3.1 shows the result.

$b_{01}$	1 1 1 1 1 1 1 1
$w_{01}$	0 1 0 1 0 1 0 1
$b_{01} \oplus w_{01}$	1 0 1 0 1 0 1 0
$c_0$	1 0 1 1 1 0 1 1
$b_{01} \oplus w_{01} \oplus c_0$	0 0 0 1 0 0 0 1

Table 3.1. Spreading of Information Bit  $b_{01}$  of the Desired Cell.

Now at the base station of cell 0, the received signal is multiplied by the Walsh function  $w_{01}$  and PN sequence  $c_0$  in order to extract the information bit  $b_{01}$ .

$b_{01} \oplus w_{01} \oplus c_0$	0 0 0 1 0 0 0 1
$c_0$	1 0 1 1 1 0 1 1
$b_{01} \oplus w_{01} \oplus c_0 \oplus c_0$	1 0 1 0 1 0 1 0
$w_{01}$	0 1 0 1 0 1 0 1
$b_{01} \oplus w_{01} \oplus w_{01} = b_{01}$	1 1 1 1 1 1 1 1

Table 3.2. Extracting Information Bit  $b_{01}$  from the Received Spreaded Signal.

Now, for another user  $ij$  of an adjacent cell  $i$  with a Walsh function  $w_{ij}(t)$ , the transmitted signal would be  $b_{ij}(t)w_{ij}(t)c_i(t)$  and the received signal at base station 0 would be  $b_{ij}(t + \tau_{ij})w_{ij}(t + \tau_{ij})c_i(t + \tau_{ij})$  where  $\tau_{ij}$  is a time delay due to the lack of

synchronization of the adjacent cell user with our base station. Thus, the output would remain spread

$$b_{ij}(t + \tau_{ij})c_i(t + \tau_{ij})w_{ij}(t + \tau_{ij})c_0(t)w_1(t) = b_{ij}(t + \tau_{ij})c_{ij}(t + \tau_{ij})c_{01}(t) = b'_{ij}(t)c'_{ij}(t)c_{01}(t) \quad (3.1)$$

where  $c'_{ij}(t)$  is a new PN sequence which is different from  $c_{ij}(t)$ .

Now for another user  $j$  of cell 0 using the same Walsh code  $w_1(t)$ , the signal would be received as:

$$b_{0j}(t + \tau_{0j})c_0(t + \tau_{0j})w_{01}(t + \tau_{0j}) = b_{0j}(t + \tau_{0j})c_{01}(t + \tau_{0j}) = b_{0j}(t)c'_{01}(t) \quad (3.2)$$

Thus, the output would be  $b'_{0j}(t)c'_{01}(t)c_{01}(t)$  which is a spread or an even more spread signal.

## 2. The Transmitted Signal

Every user in our system transmits information BPSK signal  $b_{ij}(t)$  which is unique after it becomes DS-CDMA and is amplified to the proper power level. For convenience, it will be assumed that each user in a cell uses a different Walsh code  $w_{ij}(t)$

$$s_{ij}(t) = \sqrt{2P_{t_{ij}}} b_{ij}(t)w_{ij}(t)c_i(t) \cos(2\pi f_c t) \quad (3.3)$$

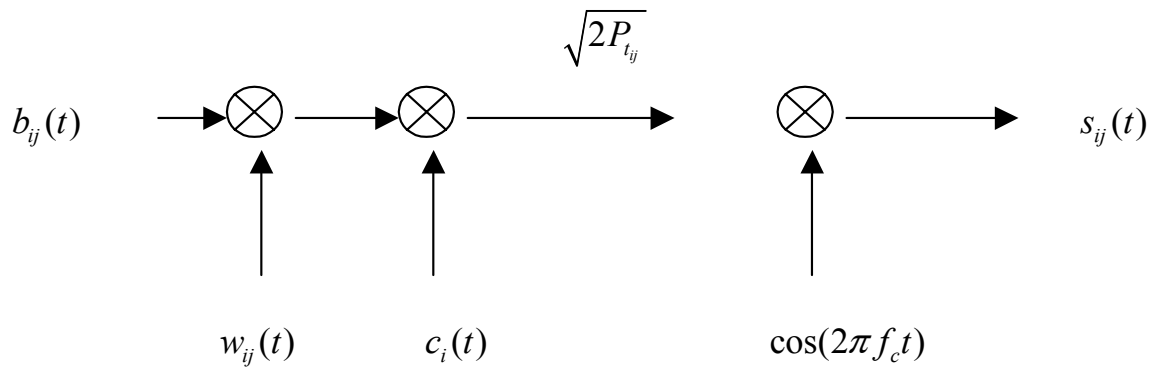


Figure 3.4. The Transmitted Signal.

where

$i$  = the number of the cell that user is in

$j$  = the number of Walsh code the user uses

$P_{t_{ij}}$  = the average transmitted power of the  $ij$  user

$b_{ij}(t)$  = the BPSK information signal of the  $ij$  user

$w_{ij}(t)$  = the Walsh function of the  $j$  user of the  $i$  cell

$c_i(t)$  = the PN spreading signal for the  $i$  cell

$f_c$  = the carrier frequency of the user

Now once each signal enters the channel, it is affected by reflection, scattering and diffraction. Reflection occurs from the several buildings and large walls that are between the user and the base station or from the earth, scattering from the street signs or the foliage and diffraction from the sharp objects that are in the signal's propagation path. Thus, the signals are attenuated due to path loss and are subject to fading and shadowing.

### 3. Free Space Propagation

Generally, in communication systems when there is a clear line-of-sight path between the receiver and the transmitter, and  $P_t$  is the transmission power and  $G_t$  and  $G_r$  are the transmitter's and receiver's antenna gains, then the received power  $P_r$  will be given by the formula

$$P_r(d) = \frac{P_t G_t G_r \lambda^2}{(4\pi)^2 d^2} \quad (3.4)$$

where  $d$  is the separation distance in meters between the transmitter and the receiver,  $\lambda$  is the wavelength  $\lambda = \frac{c}{f_c}$  (where  $c$  is the speed of light in meters/sec and  $f_c$  is the carrier frequency in Hz). It is assumed that there are no hardware losses. The difference in dB between the transmitted power  $P_t$  and the received power  $P_r$  is called path loss.

$$PL(\text{dB}) = 10 \log \left( \frac{P_t}{P_r} \right) = -10 \log \frac{\lambda^2 G_r G_t}{(4\pi)^2 d^2} \quad (3.5)$$

For unit gains  $G_r = G_t = 1$ , the path loss is given by:

$$PL(\text{dB}) = -10 \log \left[ \frac{\lambda^2}{(4\pi)^2 d^2} \right] = -20 \log \frac{\lambda}{4\pi d} \quad (3.6)$$

Usually large-scale propagation models calculate the received power  $P_r(d_0)$  at a relatively small distance  $d_0$  (reference point) and then calculate the received power at the desired distance  $d$ ,  $P_r(d)$  as follows

$$P_r(d) = P_r(d_0) \left( \frac{d_0}{d} \right)^2 \quad (3.7)$$

where  $d \geq d_0 \geq d_f$  and  $d_f$  is the Fraunhofer distance ( $d_f = \frac{2D^2}{\lambda}$ , where  $D$  is the largest dimension of the antenna).

In practice, a clear line of sight between the transmitter and receiver hardly exists and the average path loss is a function of distance  $d$

$$\overline{PL}(d) \propto \left( \frac{d}{d_0} \right)^n \quad (3.8)$$

where  $n$  is the path loss exponent. The path loss exponent depends on the type of environment in which the signal propagates. Table 3.3 is taken from [2].

<b>Environment</b>	<b>Path Loss Exponent</b>
Free Space	2
Urban area cellular radio	2.7-3.5
Shadowed urban cellular radio	3-5
In building line of sight	1.6-1.8
Obstructed in buildings	4-6
Obstructed in factories	2-3

Table 3.3. Values of the Path Loss Exponent for Various Types of Environment.

The average path loss in dB is given by:

$$\overline{PL}(\text{dB}) = \overline{PL}(d_0) + 10n \log\left(\frac{d}{d_0}\right) \quad (3.9)$$

In our analysis, it will be assumed that the path loss exponent  $n$  is equal to 4 ( $n = 4$ ).

## B. NAKAGAMI FADING CHANNEL

In this analysis, it is assumed that the reverse channel is a frequency-selective one and that the multi-path fading signal is characterized by the Nakagami- $m$  probability density function (pdf). The Nakagami- $m$  probability density function is given by

$$f_R(r) = \begin{cases} \frac{2}{\Gamma(m)} \cdot \left(\frac{m}{\Omega}\right) \cdot r^{2m-1} \exp\left(\frac{-m \cdot r^2}{\Omega}\right) & r \geq 0 \\ 0 & \text{elsewhere} \end{cases} \quad (3.10)$$

where  $\Omega$  is given by  $\Omega = E(R^2)$ ,  $E(\cdot)$  denotes the expected value, and  $\Gamma(m)$  is the gamma function given by:

$$\Gamma(m) = \int_0^{\infty} x^{m-1} \cdot \exp(-x) dx, m > 0 \quad (3.11)$$

The parameter  $m$  is given by:

$$m = \frac{\Omega^2}{\text{var}(r^2)} = \frac{\Omega^2}{E[(R^2 - \Omega)^2]} \geq \frac{1}{2} \quad (3.12)$$

The Nakagami- $m$  distribution includes both the Rayleigh distribution and the one-sided Gaussian distribution for  $m = 1$  and  $m = \frac{1}{2}$  respectively. As  $m$  increases and goes to infinity, the channel becomes non-fading. Nakagami- $m$  is a two-parameter distribution ( $m, \Omega$ ) and so it is more flexible and accurate than any other distribution.

In our analysis, various values for  $m = \frac{1}{2}, \frac{3}{4}, 1, 1.5, 2$  are used and it is assumed that  $\Omega$  is normalized,  $\Omega = 1$ .

## 1. Small Scale Fading due to Multiple Paths

In urban and suburban environments, the height of the mobile antenna is usually much lower than the height of the buildings that are between it and the base station. Thus, since there is no single line-of-sight path between the user and the base station, the amplitude of the radio signal fluctuates rapidly over a short period of time. This phenomenon is called fading and is caused because more than one copy of the transmitted signal travels along different paths and arrives at the base station at slightly different times after several reflections on various objects.

Some of the multipath copies may have been reflected off of moving objects, such as cars, trains or people, which causes a shift in the received signal frequency which is called the Doppler shift. A Doppler shift is also caused when the mobile user is moving relative to the base station during the communication period (conversation time). The base station receiver combines all the multipath components in order to extract the information bit from the transmitted signal.

## 2. Log-Normal Shadowing

The model in Equation (3.9) does not take into account that the path losses of two signals that arrive at the base station antenna from two different mobile users, who are at the same distance  $d$  from the receiver but in different directions, might be very different. This difference from the average value is due to different obstacles and conditions that exist over each path.

Generally, the path loss at a distance  $d$  is lognormally distributed

$$PL(d) = \overline{PL}(d) + X = \overline{PL}(d_0) + 10n \log\left(\frac{d}{d_0}\right) + X \quad (3.13)$$

where  $X$  is a zero-mean Gaussian distributed random variable  $N(0, \sigma_{dB})$  with standard deviation  $\sigma_{dB}$ , and  $\overline{PL}(d)$  is the average path loss due to distance  $d$ .



Since the shadowed path loss is a sum of a deterministic value  $\overline{PL}(d)$  and a zero-mean Gaussian distributed random variable,  $PL(d)$  is a Gaussian random variable with mean  $\overline{PL}(d)$  and a standard deviation  $\sigma_{dB}$ ,  $PL(d) \sim N(\overline{PL}, \sigma_{dB})$ .

$$PL = \overline{PL} + X$$

Now to convert from dB to a ratio:

$$\begin{aligned} PL &= 10 \log L \\ \overline{PL} &= 10 \log \overline{L} \\ X &= 10 \log X \end{aligned} \tag{3.14}$$

where  $X$  is a lognormal random variable  $X \sim \Lambda(0, \hat{\lambda} \sigma_{dB})$  where  $\hat{\lambda} = \ln 10 / 10$  as derived and  $L = \overline{L} X$ .

### 3. Power Control and Power Control Error

One of the goals of our DS-CDMA system is to adjust each mobile user's transmitter so that the received signal-to-interference ratio is the minimum possible. Any increase in mobile power raises the interference in our system which decreases the probability that weaker signals will be received and demodulated correctly.

If no power control is applied, the received power from a mobile user, which is very close to our base station, might be up to 80 dB stronger than the power received from far away subscribers. This is called the near-far problem.

The base station antenna combats the near-far and fading problems with the use of power control, which ensures that every signal from all the users within its coverage area is received with the same power. In order to achieve this, the base station measures the signal level of each user and then transmits back a power change command.

In our system, each base station in the seven cells uses power control over the users of its coverage area so, unfortunately, it will receive co-channel interference from those not under its power control. In our analysis, it is assumed that every base station wants to receive all the users of its cell with the same power  $P$ . Since there is a power control error, the actual received power would be  $P_{actual} = P + X_1$  where  $X_1$  is a zero-

mean Gaussian distributed random variable with a standard deviation  $\sigma_{1dB}$ ,  $X_1 \sim N(0, \sigma_{1dB})$ . Thus, the actual received power would be a random variable with mean  $P$  and standard deviation  $\sigma_{1dB}$ .

In order to convert from dB to ratio

$$\begin{aligned} P_{actual} &= 10 \log P_{actual} \\ P &= 10 \log P \\ X_1 &= 10 \log X_1 \end{aligned} \tag{3.15}$$

and  $P_{actual} = PX_1$  where  $X_1$  is a lognormal random variable  $X_1 \sim \Lambda(0, \tilde{\lambda}\sigma_{1dB})$  and  $\tilde{\lambda} = \ln 10/10$ .

### C. NAKAGAMI-LOGNORMAL CHANNEL MODEL

The aforementioned effects will be combined to develop the Nakagami-lognormal channel model. The Nakagami-lognormal channel model is a slow-flat-Nakagami fading channel with lognormal power control error for the users of the center cell 0 and a combination of lognormal power control error and shadowing for all the other users of the six adjacent cells.

#### 1. The Reverse Signal $S_0(t)$

The complex envelope of the reverse signal from user 1 is as follows

$$\tilde{S}_0(t) = \sqrt{2P_{t01}} b_{01}(t) w_{01}(t) c_0(t) = \sqrt{2P_{t01}} b_{01}(t) c_{01}(t) \tag{3.16}$$

where  $c_{01}(t)$  is the PN spreading signal for user one and is the product of the PN signal of the center cell  $c_0(t)$  and the Walsh function for user one is  $w_{01}(t)$  ( $c_{01}(t) = w_{01}(t)c_0(t)$ ).

The complex envelope  $\tilde{S}_o(t)$  is affected by small-scale fading as modeled by the Nakagami random variable as  $R \cdot \tilde{S}_0(t)$ . The signal is also affected by the large-scale path loss and the lognormal shadowing. Thus, Figure 3.5 applies.

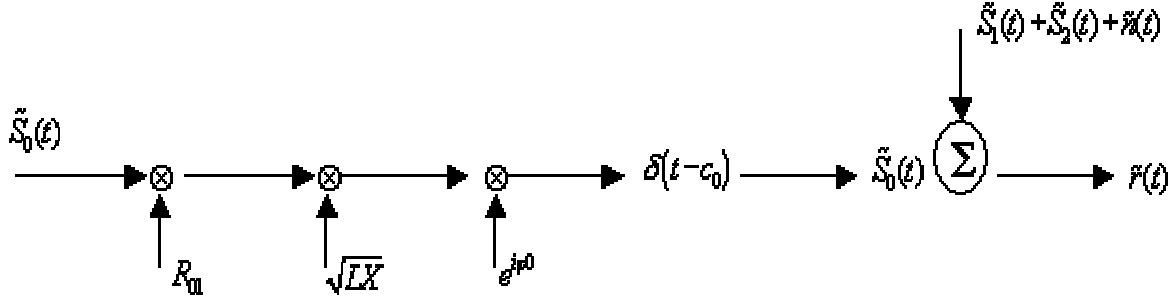


Figure 3.5. The Reverse Signal.

In Figure 3.5,  $\varphi_0$  and  $\tau_0$  are the phase and time delay between the transmitter (user one) and the base station receiver, which for our analysis will be set to zero,  $\tilde{S}_1(t)$  is the intracell interference,  $\tilde{S}_2(t)$  is the intercell interference and  $\tilde{n}(t)$  is the additive Gaussian noise. Thus, since each base station applies power control to all the users of its region, the signal received by the center cell antenna from user one (user 1) would be

$$\begin{aligned} \tilde{S}_0(t) &= \tilde{S}_0(t - t_0) \text{Re}^{j\varphi_0} \sqrt{X_1} = R_{01} \sqrt{2PX_1} b_{01}(t - t_0) c_{01}(t - t_0) e^{j\varphi_0} = \\ &= R_{01} \sqrt{2PX_{1_{01}}} b_{01}(t) c_{01}(t) = R_{01} \sqrt{P_{01}} b_{01}(t) c_{01}(t) \end{aligned} \quad (3.17)$$

Since  $t_0 = \varphi_0 = 0$  and  $X_1$  is the lognormal power control error for user one and  $P$  is the desired power

$$s_0(t) = \text{Re}\{\tilde{S}_0(t) e^{j2\pi f_c t}\} = R_{01} \sqrt{2P_{01}} b_{01}(t) c_{01}(t) \cos(2\pi f_c t) \quad (3.18)$$

where  $\text{Re}\{\cdot\}$  denotes the real part.

## 2. Intracell Interference

The base station antenna receives not only the desired signal from user one of the center cell but also  $K - 1$  similar signals  $s_{0k}$  from the other users of the same cell. Thus, the total interference from the center cell users would be

$$s_1(t) = \sum_{k=2}^K R_{0k} \sqrt{2P_{0k}} b_{0k}(t + \tau_k) w_{0k}(t + \tau_k) c_0(t + \tau_k) \cos(2\pi f_c t + \varphi_k) \quad (3.19)$$

where  $P_{0k} = PX_k$  and  $X_k$  is the lognormal power control error for user  $k$  and where

$K$  = the number of active users in the center cell

$0k$  = the mobile user  $k$  in the center cell 0

$R_{0k}$  = Nakagami fading random variable of the  $k$  user of the center cell 0

$P_{0k}$  = Lognormal random variable representing the average power received from the  $k$  user

$c_0(t)$  = PN spreading signal for the center cell

$w_{0k}(t)$  = Walsh function for the  $k$  user

$f_c$  = the carrier frequency of the signal

$\tau_k$  = the time delay from user  $k$ , relative to the delay from user one

$\varphi_k$  = the phase delay from user  $k$ , relative to the phase delay from user one

$b_{0k}$  = the information signal for the  $k$  user of cell 0

Now the product of the Walsh function  $w_{0k}(t)$  and the PN spreading signal  $c_0(t)$  is a new PN sequence  $c_{0k}(t)$  since it is received at a different time and phase delay for each user  $c_{0k}(t + \tau_k) = c'_{0k}(t)$ . Thus, the received spreading signals are totally different and not orthogonal to each other. So, in the reverse channel, the use of the Walsh code is for spreading and orthogonality only for the several signals that the same user may transmit and not for orthogonality between users. In our case, it is assumed that each user transmits only one signal ( $w_{0k}(t)$  function) and that there is a coherent detection for the desired user. Thus

$$s_1(t) = \text{Re}\left\{\tilde{S}_1(t)e^{i2\pi f_c t}\right\} = \sum_{k=2}^K R_{0k} \sqrt{2P_{0k}} b_{0k}(t + \tau_k) c_{0k}(t + \tau_k) \cos(2\pi f_c t + \varphi_k) \quad (3.20)$$

### 3. Co-Channel or Intercell Interference

As the base station of cell 0 receives  $K$  different signals from the  $K$  users of its coverage region, it receives  $6 \cdot K$  signals from the active mobile users of the six adjacent cells, where equal numbers of users in each adjacent cell with the number of users in the center cell is assumed.

Now according to [7] the power of every user  $ij$  in the adjacent cells is multiplied by a factor  $\lambda_{ij}$

$$\lambda_{ij} = \left( \frac{r_i}{r_0} \right)^n 10^{(\xi_0 - \xi_i/10)} \quad (3.21)$$

This factor  $\lambda_{ij}$  depends on the distances of the user  $ij$  from its cell base station  $r_i$  and from the central base station  $r_0$  (Figure 3.5). Now in (3.21),  $n$  is the path loss exponent for the urban environment,  $\xi_0$  is the factor due to the shadowing for the distance  $r_0$  ( $0, \sigma_0$ ) with standard deviation  $\sigma_0$  and  $\xi_i$  is due to the power control error that is done by the adjacent cell  $i$  to the user  $ij$  and has a standard deviation  $\sigma_i$ .

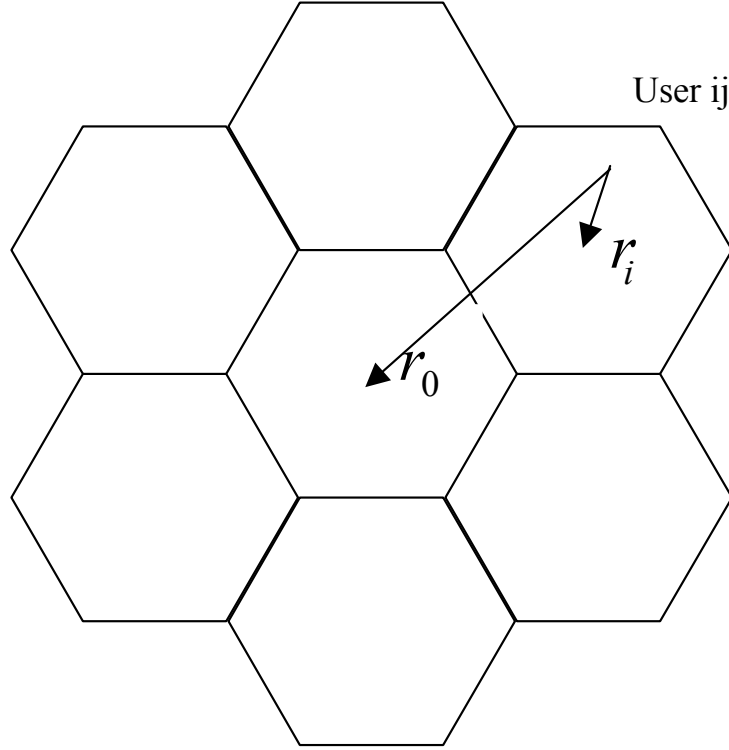


Figure 3.5. Mobile User  $ij$  in Adjacent Cell  $i$ .

Thus, the intercell interference  $s_2(t)$  would be:

$$\begin{aligned}
 s_2(t) &= \sum_{i=1}^6 \sum_{j=1}^K R_{ij} \sqrt{2P\lambda_{ij}} b_{ij}(t + \tau_{ij}) w_{ij}(t + \tau_{ij}) c_i(t + \tau_{ij}) \cos(2\pi f_c t + \varphi_{ij}) \\
 &= \sum_{i=1}^6 \sum_{j=1}^K R_{ij} \sqrt{2P_{ij}} b_{ij}(t + \tau_{ij}) c_{ij}(t + \tau_{ij}) \cos(2\pi f_c t + \varphi_{ij}) \quad (3.22)
 \end{aligned}$$

with

$i$  = the adjacent cells  $i = 1, 2, \dots, 6$

$ij$  = mobile user  $j$  of adjacent cell  $i$

$K$  = the number of active users in each adjacent cell

$R_{ij}$  = the Nakagami fading random variable for the signal from the  $ij$  user

$P_{ij}$  = Lognormal random variable representing the average power received from the  $ij$  user  $P_{ij} = P\lambda_{ij}$

$\lambda_{ij}$  = the factor that the power of user  $ij$  is multiplied by

$b_{ij}(t)$  = the information signal for the  $j$  user of adjacent cell  $i$

$w_{ij}(t)$  = Walsh function for the  $j$  user of adjacent cell  $i$

$c_i(t)$  = the PN spreading signal for the adjacent cell  $i$

$f_c$  = the carrier frequency of the signal

$\tau_{ij}$  = the time delay for the signal of  $ij$  user relative to the delay for user one of the center cell

$\varphi_{ij}$  = the phase delay for the signal of  $ij$  user relative to the delay for user one of the center cell

$c_{ij}(t)$  = the new PN spreading sequence for user  $ij$

#### 4. The Received Signal $r(t)$

Now the signal that the central base station antenna receives is the sum of the reverse signal from user one, the same cell interference  $S_1(t)$ , the other-cell interference  $S_2(t)$  and the Additive White Gaussian Noise (AWGN),  $n(t)$

$$\begin{aligned}
 r(t) &= s_0(t) + s_1(t) + s_2(t) + n(t) \\
 &= R_{01}\sqrt{2P_{01}}b_{01}(t)c_{01}(t)\cos(2\pi f_c t) \\
 &\quad + \sum_{k=2}^K R_{0k}\sqrt{2P_{0k}}b_{0k}(t)c_{0k}(t)\cos(2\pi f_c t + \varphi_k) \\
 &\quad + \sum_{i=1}^6 \sum_{j=1}^K \sqrt{2P_{ij}}b_{ij}(t + \tau_{ij})c_{ij}(t + \tau_{ij})\cos(2\pi f_c t + \varphi_{ij}) + n(t)
 \end{aligned} \tag{3.23}$$

#### **D. SUMMARY**

In Chapter III, a Nakagami-lognormal reverse channel model was developed. For the users of the center cell, the model includes the effects of lognormal power control error and the small-scale propagation effects of our slow-flat Nakagmi fading channel. For the active mobile users of the six adjacent cells, the situation is more complicated. The signal from a mobile user in the adjacent cell  $i$  is affected by the power control error of the  $i$  cell base station and also from the lognormal shadowing for the distance  $r_0$  of this user from the center cell's base station.

It can also be concluded that the received signal from the base station 0, contains the signal from the mobile user one of the center cell,  $K - 1$  signals from all the other active mobile users of the center cell (intracell interference)  $6 \cdot K$  signals from the mobile users in the six adjacent cells (co-channel interference) and also Additive White Gaussian Noise. In Chapter IV, the signal-to-noise plus interference ratio (SNIR) and the bit error rate (BER) will be developed.



THIS PAGE INTENTIONALLY LEFT BLANK

### APPENDIX III. LOGNORMAL RANDOM VARIABLE

The probability density function (pdf) of a Gaussian random variable  $X$  in dB represented by the variable  $\chi$  is given by the following formula

$$f_x(\chi) = \frac{1}{\sqrt{2\pi}\sigma_{dB}} e^{-\frac{(\chi-m_{dB})^2}{2\sigma_{dB}^2}}, -\infty < \chi < +\infty \quad (3.24)$$

and  $\sigma_{dB} > 0$  where  $m_{dB}$  is the expected value or mean of  $X$  ( $E[X] = m_{dB}$ ) and  $\sigma_{dB}$  is its standard deviation ( $\sigma_{dB} = \text{Var}[X] = E[(X - m_{dB})^2]$ ).

A memoryless system is defined in Figure 3.6, where  $g(\square)$  operates on the input variable  $X$  to yield the output  $X$ .

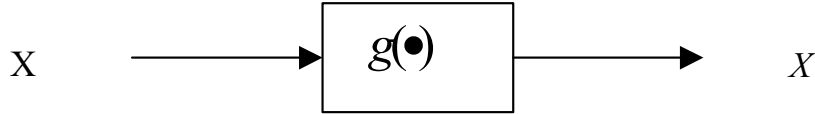


Figure 3.6. Memoryless System.

The operation and its inverse are  $X = g(X)$  and  $X = g^{-1}(X)$

The pdf of the output variable is:

$$f_x(x) = \frac{1}{\left| \frac{dx}{d\chi} \right|} f_x(\chi) / \chi \quad (3.25)$$

In order to transform the random variable from units of decibels to ratio using:

$$X = 10 \log X \rightarrow X = 10 \frac{X}{10} = g(X) \quad (3.26)$$

Thus, from Equations (3.25) and (3.26)

$$f_x(x) = \frac{1}{\left| \frac{dx}{d\chi} \right|} f_x(\chi) / \chi = \frac{1}{\frac{d10^{z/10}}{d\chi}} f_x(\chi) / \chi$$

$$\begin{aligned}
&= \frac{1}{\left| \frac{\ln 10}{10} \right| x} \frac{1}{\sqrt{2\pi}\sigma_{dB}} e^{-\frac{(10\log x - m_{dB})^2}{2\sigma_{dB}^2}} \\
&= \frac{1}{\hat{\lambda}x\sqrt{2\pi}\sigma_{dB}} e^{-\frac{(10\log x - m_{dB})^2}{2\sigma_{dB}^2}}
\end{aligned} \tag{3.27}$$

where  $\hat{\lambda} = \frac{\ln 10}{10}$ . So,

$$\begin{aligned}
f_x(x) &= \frac{1}{x\sqrt{2\pi}(\hat{\lambda}\sigma_{dB})} e^{-\frac{\hat{\lambda}^2(10\log x - m_{dB})^2}{\hat{\lambda}^2 2\sigma_{dB}^2}} = \frac{1}{x\sqrt{2\pi}(\hat{\lambda}\sigma_{dB})} e^{-\frac{\hat{\lambda}10\log x - \hat{\lambda}m_{dB}}{2(\hat{\lambda}\sigma_{dB})^2}} \\
&= \frac{1}{x\sqrt{2\pi}(\hat{\lambda}\sigma_{dB})} e^{-\frac{(\ln 10\log x - \hat{\lambda}m_{dB})^2}{2(\hat{\lambda}\sigma_{dB})^2}} = \frac{1}{x\sqrt{2\pi}\sigma} e^{-\frac{(\ln x - m)^2}{2\sigma^2}}
\end{aligned} \tag{3.28}$$

where  $m = \hat{\lambda}m_{dB}$  and  $\sigma = \hat{\lambda}\sigma_{dB}$ . Thus, the random variable  $X$  has a lognormal distribution  $X \sim \Lambda(m, \sigma) \equiv \Lambda(\hat{\lambda}m_{dB}, \sigma_{dB})$ .

The  $n$ th moment of  $X$  is given by:

$$E[X^n] = e^{nm + n^2 \frac{\sigma^2}{2}} \tag{3.29}$$

So, the expected value or mean is given by:

$$\begin{aligned}
E[X] &= e^{m + \sigma^2/2} \\
E[X^2] &= e^{2m + 2\sigma^2}
\end{aligned} \tag{3.30}$$

Thus,

$$\text{Var}[X] = E[X^2] - (E[X])^2 = e^{2m + 2\sigma^2} \left( e^{m + \sigma^2/2} \right)^2 = e^{2m + 2\sigma^2} e^{2m + \sigma^2} = e^{2m + \sigma^2} (e^{\sigma^2} - 1) \tag{3.31}$$

and the median of  $X$  is given by  $M_{ed}(X) = e^m$ .

## IV. DS-CDMA PERFORMANCE ANALYSIS

In Chapter III, the Nakagami-lognormal channel model was designed and the signal that the base station antenna of the center cell receives was presented.

In this chapter, the Signal-to-Noise plus Interference Ratio for the uncoded signal will be examined and then shown that with the aid of Forward Error Correction (FEC) coding, the Probability of Bit Error can be decreased.

As mentioned previously, a seven-cell cluster with the user of interest (user 1) in the center cell will be used. Each cell has  $K$  users. The users that are in the center cell are uniformly distributed in the small circle with radius  $R=1$  while the users of the adjacent cells are uniformly distributed in the area of the ring between  $R$  and  $3R$ .

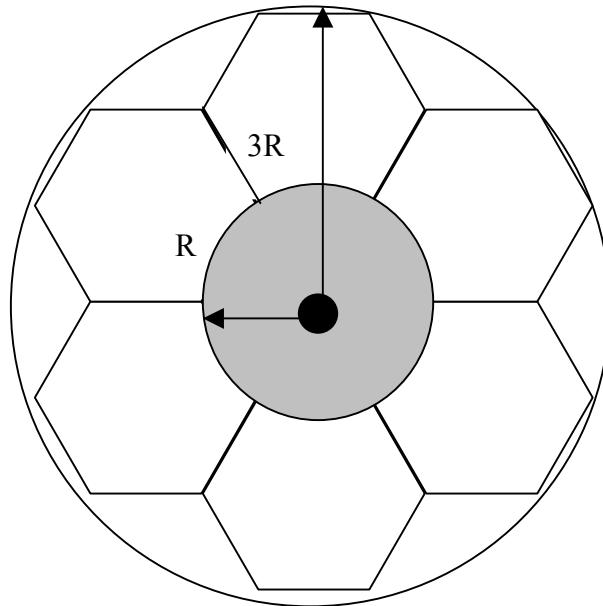


Figure 4.1. Seven-Cell Cluster Cellular System.

## A. PERFORMANCE OF THE BASIC SYSTEM

The base station receiver must take one bit at a time of the received signal  $r(t)$  in order to extract the information signal from mobile user one of the center cell. Thus, it multiplies the received signal with the PN spreading sequence of user one  $c_{01}(t)$  in order to despread the data of user one and it is also synchronized with the mobile user one. A block diagram of the base station is shown in Figure 4.2

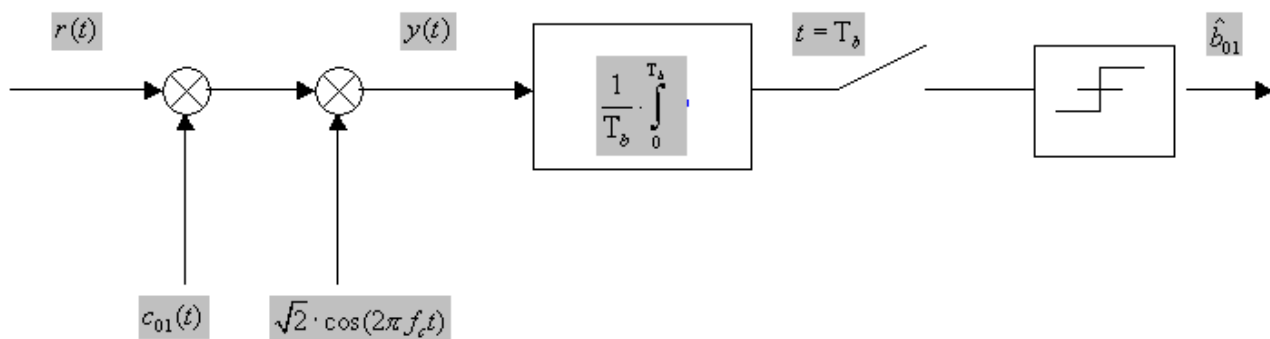


Figure 4.2. Base Station Receiver.

### 1. The Demodulated Signal $y(t)$

As mentioned previously, the received signal is multiplied with  $\sqrt{2} \cdot \cos(2\pi f_c t)$  and the PN spreading sequence  $c_{01}(t)$

$$\begin{aligned}
 y(t) &= r(t) \cdot \sqrt{2} \cdot \cos(2\pi f_c t) \cdot c_{01}(t) \\
 &= [s_0(t) + s_1(t) + s_2(t) + n(t)] \cdot \sqrt{2} \cdot \cos(2\pi f_c t) \cdot c_{01}(t) \\
 &= I_1(t) + \gamma_1(t) + \gamma_2(t) + n_1(t)
 \end{aligned} \tag{4.1}$$

where the first term  $I_1(t)$  contains the desired information  $b_{01}(t)$ , the second term  $\gamma_1(t)$  contains the intra-cell interference, the third term  $\gamma_2(t)$  contains the inter-cell interference and finally the fourth term  $n_1(t)$  is the noise component.

These four components are described in detail:

(1) The desired component  $I_1(t)$  :

$$\begin{aligned}
I_1(t) &= s_0(t) \cdot c_{01}(t) \cdot \sqrt{2} \cdot \cos(2\pi f_c t) \\
&= R_{01} \cdot \sqrt{2 \cdot P_{01}} \cdot b_{01}(t) \cdot c_{01}(t) \cdot \cos(2\pi f_c t) \cdot c_{01}(t) \cdot \sqrt{2} \cdot \cos(2\pi f_c t) \\
&= R_{01} \cdot \sqrt{2 \cdot P_{01}} \cdot \sqrt{2} \cdot b_{01}(t) \cdot (c_{01}(t) \cdot c_{01}(t)) \cdot (\cos(2\pi f_c t) \cdot \cos(2\pi f_c t)) \\
&= R_{01} \cdot 2 \cdot \sqrt{P_{01}} \cdot b_{01}(t) \cdot \left( \frac{1 + \cos(4\pi f_c t)}{2} \right) \\
&= R_{01} \cdot \sqrt{P_{01}} \cdot b_{01}(t) \cdot (1 + \cos(4\pi f_c t)) \tag{4.2}
\end{aligned}$$

since  $c_{01}(t) \cdot c_{01}(t) = 1$  .

(2) The intra-cell interference component  $\gamma_1(t)$  :

$$\begin{aligned}
\gamma_1(t) &= s_1(t) \cdot c_{01}(t) \cdot \sqrt{2} \cdot \cos(2\pi f_c t) \\
&= \left( \sum_{k=2}^K R_{0k} \cdot \sqrt{2 \cdot P_{0k}} \cdot b_{0k}(t + \tau_k) \cdot c_{0k}(t + \tau_k) \cdot \cos(2\pi f_c t + \varphi_k) \right) \cdot c_{01}(t) \cdot \sqrt{2} \cdot \cos(2\pi f_c t) \\
&= \sum_{k=2}^K R_{0k} \cdot \sqrt{2 \cdot P_{0k}} \cdot \sqrt{2} \cdot b_{0k}(t + \tau_k) \cdot (c_{0k}(t + \tau_k) \cdot c_{01}(t)) \cdot (\cos(2\pi f_c t + \varphi_k) \cdot \cos(2\pi f_c t)) \\
&= \sum_{k=2}^K R_{0k} \cdot 2 \cdot \sqrt{P_{0k}} \cdot b_{0k}(t + \tau_k) \cdot c''_{0k}(t) \cdot \left( \frac{\cos(4\pi f_c t + \varphi_k) + \cos(\varphi_k)}{2} \right) \\
&= \sum_{k=2}^K R_{0k} \cdot \sqrt{P_{0k}} \cdot b_{0k}(t + \tau_k) \cdot c''_{0k}(t) \cdot (\cos(4\pi f_c t + \varphi_k) + \cos(\varphi_k)) \tag{4.3}
\end{aligned}$$

where  $c''_{0k}(t) = c_{0k}(t + \tau_k) \cdot c_{01}(t)$  is a new PN sequence and so  $\gamma_1(t)$  is still spread.

(3) The inter-cell interference component  $\gamma_2(t)$  :

$$\gamma_2(t) = s_2(t) \cdot c_{01}(t) \cdot \sqrt{2} \cdot \cos(2\pi f_c t)$$

$$\begin{aligned}
&= \left( \sum_{i=1}^6 \sum_{j=1}^K R_{ij} \cdot \sqrt{2 \cdot P_{ij}} \cdot b_{ij}(t + \tau_{ij}) \cdot c_{ij}(t + \tau_{ij}) \cdot \cos(2\pi f_c t + \varphi_{ij}) \right) \cdot c_{01}(t) \cdot \sqrt{2} \cdot \cos(2\pi f_c t) \\
&= \sum_{i=1}^6 \sum_{j=1}^K R_{ij} \cdot \sqrt{2} \cdot \sqrt{2 \cdot P_{ij}} \cdot b_{ij}(t + \tau_{ij}) \cdot (c_{ij}(t + \tau_{ij}) \cdot c_{01}(t)) \cdot (\cos(2\pi f_c t + \varphi_{ij}) \cdot \cos(2\pi f_c t)) \\
&= \sum_{i=1}^6 \sum_{j=1}^K R_{ij} \cdot 2 \cdot \sqrt{P_{ij}} \cdot b_{ij}(t + \tau_{ij}) \cdot c_{ij}''(t) \cdot \left( \frac{\cos(4\pi f_c t + \varphi_{ij}) + \cos(\varphi_{ij})}{2} \right) \\
&= \sum_{i=1}^6 \sum_{j=1}^K R_{ij} \cdot \sqrt{P_{ij}} \cdot b_{ij}(t + \tau_{ij}) \cdot c_{ij}''(t) \cdot (\cos(4\pi f_c t + \varphi_{ij}) + \cos(\varphi_{ij})) \tag{4.4}
\end{aligned}$$

where  $c_{ij}''(t) = c_{ij}(t + \tau_{ij}) \cdot c_{01}(t)$  is a new PN sequence and so  $\gamma_2(t)$  is still spread like  $\gamma_1(t)$ .

(4) The noise component  $n_1(t)$  :

$$n_1(t) = n(t) \cdot c_{01}(t) \cdot \sqrt{2} \cdot \cos(2\pi f_c t) \tag{4.5}$$

## 2. The Decision Statistic $Y$

The decision statistic  $Y$  determines if the bit  $b_{01}(t)$  for  $t \in (0, T_b)$  is a logical one or a logical zero.  $Y$  is the output of the integrator where the input is already found in  $y(t)$  :

$$\begin{aligned}
Y &= \frac{1}{T_b} \cdot \int_0^{T_b} y(t) dt \\
&= \frac{1}{T_b} \cdot \int_0^{T_b} (I_1(t) + \gamma_1(t) + \gamma_2(t) + n_1(t)) dt \\
&= \frac{1}{T_b} \cdot \int_0^{T_b} I_1(t) dt + \frac{1}{T_b} \cdot \int_0^{T_b} \gamma_1(t) dt + \frac{1}{T_b} \cdot \int_0^{T_b} \gamma_2(t) dt + \frac{1}{T_b} \cdot \int_0^{T_b} n_1(t) dt \tag{4.6}
\end{aligned}$$

Now, the Nakagami fading random variable  $R_{01} = r$  will be fixed and the lognormal random variable  $P_{01}$  for the received power:

$$\begin{aligned}
Y_{r,p} &= \left[ \frac{1}{T_b} \cdot \int_0^{T_b} y(t) dt \right]_{r,p} \\
&= \left[ \frac{1}{T_b} \cdot \int_0^{T_b} I_1(t) dt + \frac{1}{T_b} \cdot \int_0^{T_b} \gamma_1(t) dt + \frac{1}{T_b} \cdot \int_0^{T_b} \gamma_2(t) dt + \frac{1}{T_b} \cdot \int_0^{T_b} n_1(t) dt \right]_{r,p} \\
&= \bar{Y} + \zeta_1 + \zeta_2 + n
\end{aligned} \tag{4.7}$$

The desired information bit is contained in  $\bar{Y}$  :

$$\begin{aligned}
\bar{Y} &= \frac{1}{T_b} \cdot \int_0^{T_b} I_1(t) dt \\
&= \frac{1}{T_b} \cdot \int_0^{T_b} r \cdot \sqrt{p} \cdot b_{01}(t) \cdot (1 + \cos(4\pi f_c t)) dt \\
&= r \cdot \sqrt{p} \cdot b_{01} \cdot \left( \frac{1}{T_b} \cdot \int_0^{T_b} (1 + \cos(4\pi f_c t)) dt \right) \\
&= r \cdot \sqrt{p} \cdot b_{01}
\end{aligned} \tag{4.8}$$

where  $b_{01}(t)$  is a constant  $b_{01} = \pm 1$  during the period of a bit and the term with the  $\cos(4\pi f_c t)$  is neglected due to the integration which is 0.

The intra-cell interference is contained in the term  $\zeta_1(t)$  :

$$\begin{aligned}
\zeta_1(t) &= \frac{1}{T_b} \cdot \int_0^{T_b} \sum_{k=2}^K R_{0k} \cdot \sqrt{P_{0k}} \cdot b_{0k}(t + \tau_k) \cdot c_{0k}''(t) \cdot (\cos(4\pi f_c t + \varphi_k) + \cos(\varphi_k)) dt \\
&= \frac{1}{T_b} \cdot \int_0^{T_b} \sum_{k=2}^K R_{0k} \cdot \sqrt{P_{0k}} \cdot b_{0k}(t + \tau_k) \cdot c_{0k}''(t) \cdot \cos(\varphi_k) dt
\end{aligned} \tag{4.9}$$

where the term which contained the  $\cos(4\pi f_c t + \varphi_k)$  was neglected.

The inter-cell interference is contained in the term  $\zeta_2(t)$



$$\begin{aligned}
\zeta_2(t) &= \frac{1}{T_b} \cdot \int_0^{T_b} \sum_{i=1}^6 \sum_{j=1}^K R_{ij} \cdot \sqrt{P_{ij}} \cdot b_{ij}(t + \tau_{ij}) \cdot c_{ij}''(t) \cdot (\cos(4\pi f_c t + \varphi_{ij}) + \cos(\varphi_{ij})) dt \\
&= \frac{1}{T_b} \cdot \int_0^{T_b} \sum_{i=1}^6 \sum_{j=1}^K R_{ij} \cdot \sqrt{P_{ij}} \cdot b_{ij}(t + \tau_{ij}) \cdot c_{ij}''(t) \cdot \cos(\varphi_{ij}) dt
\end{aligned} \tag{4.10}$$

where the term which contained the  $\cos(4\pi f_c t + \varphi_{ij})$  was neglected.

Finally, the additive noise is contained in the term  $n$  :

$$\begin{aligned}
n &= \frac{1}{T_b} \cdot \int_0^{T_b} n_1(t) dt \\
&= \frac{1}{T_b} \cdot \int_0^{T_b} n(t) \cdot c_{01}(t) \cdot \sqrt{2} \cdot \cos(2\pi f_c t) dt
\end{aligned} \tag{4.11}$$

Now the intra-cell interference, the inter-cell interference and the noise terms are combined into one single term  $\xi$  :

$$\begin{aligned}
Y_{r,p} &= \bar{Y} + \zeta_1 + \zeta_2 + n \\
&= \bar{Y} + \xi
\end{aligned} \tag{4.12}$$

Now  $Y_{r,p}$  is a Gaussian random variable  $\mathbf{y}$  whose expected value is given by  $E\{\mathbf{y}\} = \bar{Y}$  and the variance is the sum of the variances of the intra-cell interference term, the inter-cell interference term and the noise term:

$$\text{Var}\{\mathbf{y}\} = \text{Var}\{\xi\} = \text{Var}\{\zeta_1\} + \text{Var}\{\zeta_2\} + \text{Var}\{n\} = \sigma_\xi^2 \tag{4.13}$$

This approximation is possible because the intra-cell interference term  $\zeta_1$ , the inter-cell interference term  $\zeta_2$  and the additive white Gaussian noise term  $n$  are modeled as independent zero-mean Gaussian random variables.

### 3. Signal-to-Noise plus Interference Ratio

The Signal-to-Noise plus Interference Ratio is defined as follows:

$$SNIR_{r,p} = \frac{\bar{Y}^2}{\sigma_\xi^2} \quad (4.14)$$

Now the intra-cell interference term  $\zeta_1$  is a zero-mean random variable so its variance is as follows:

$$\text{Var}\{\zeta_1\} = E\{\zeta_1^2\} - [E\{\zeta_1\}]^2 = E\{\zeta_1^2\} = \frac{1}{3 \cdot N} \cdot \sum_{k=2}^K E\{R_{0k}^2\} \cdot E\{P_{0k}\} \quad (4.15)$$

The inter-cell interference term  $\zeta_2$  is also a zero-mean random variable so its variance is given by:

$$\text{Var}\{\zeta_2\} = E\{\zeta_2^2\} = \frac{1}{3 \cdot N} \cdot \sum_{i=1}^6 \sum_{j=1}^K E\{R_{ij}^2\} \cdot E\{P_{ij}\} \quad (4.16)$$

The variance of  $\zeta_2$  which is the most complicated is calculated in Appendix IV.A and the variance of  $\zeta_1$  can be derived with the same manner.

Now the variance of the noise component is calculated in Appendix IV.B and is given by:

$$\text{Var}\{n\} = \frac{N_0}{2 \cdot T} \quad (4.17)$$

Thus,

$$\bar{Y}^2 = (r \cdot \sqrt{p} \cdot b_{01})^2 = r^2 \cdot p \cdot b_{01}^2 = r^2 \cdot p \quad (4.18)$$

and

$$\begin{aligned} \sigma_\xi^2 &= \text{Var}\{\xi\} = \text{Var}\{\zeta_1\} + \text{Var}\{\zeta_2\} + \text{Var}\{n\} \\ &= \frac{1}{3 \cdot N} \cdot \sum_{k=2}^K E\{R_{0k}^2\} \cdot E\{P_{0k}\} + \frac{1}{3 \cdot N} \cdot \sum_{i=1}^6 \sum_{j=1}^K E\{R_{ij}^2\} \cdot E\{P_{ij}\} + \frac{N_0}{2 \cdot T} \end{aligned} \quad (4.19)$$

Thus, the Signal-to-Noise plus Interference Ratio is given by:

$$SNIR_{r,p} = \frac{\bar{Y}^2}{\sigma_{\xi}^2} = \frac{r^2 \cdot p}{\frac{1}{3 \cdot N} \cdot \sum_{k=2}^K E\{R_{0k}^2\} \cdot E\{P_{0k}\} + \frac{1}{3 \cdot N} \cdot \sum_{i=1}^6 \sum_{j=1}^K E\{R_{ij}^2\} \cdot E\{P_{ij}\} + \frac{N_0}{2 \cdot T}} \quad (4.20)$$

## B. CONVOLUTIONAL ENCODING

As is known, the performance of a communication system can be improved by using error control coding. There are two major error control strategies: automatic repeat request and forward error correction coding (FEC) [6, 7, 8].

In our case, FEC will be used with convolutional coding. Our encoder is an  $(n, k)$  encoder which means that for every  $k$  information bits,  $n$  coded bits are produced where  $n > k$ .

The new coded bit will have duration  $T_{cc}$  and the following equality must be satisfied:  $nT_{cc} = kT$  (where  $T$  is the duration of the uncoded bit).

The new coded bit rate is:  $R_{cc} = \frac{1}{T_{cc}}$  where  $T_{cc} = \frac{k}{n}T = r_{cc}T$  and  $r_{cc} = \frac{k}{n}$  is the code rate. Thus,  $\frac{1}{r_{cc}}$  coded bits are generated for every data bit. The coded bit rate

$R_{cc} = \frac{R_b}{r_{cc}}$  is higher than the uncoded rate. For the same transmission power for coded and uncoded bits

$$\begin{aligned} P &= E_b R_b = E_{cc} R_{cc} \\ E_{cc} &= \frac{R_b}{R_{cc}} E_b = r_{cc} E_b \end{aligned} \quad (4.21)$$

where  $E_{cc}$  is the average energy for a coded bit, which means that the average energy per coded bit is less than that of an uncoded bit and so the addition of coding increases the probability of a coded bit error or the demodulated BER is increased. However, when the demodulated symbols are sent to the error control decoder, some of them are corrected which improves the reliability of the demodulated data. Thus, a good code solution will lead to an improvement in performance over our initial uncoded system.

Now, the convolutional encoder uses  $k$  shift registers and  $n$  modulo-2 adders. At least one of the  $k$  shift registers must have  $v-1$  stages where the parameter  $v$  is called constraint length of the convolutional encoder and depicts the number of data bit shifts over which a single bit can influence the encoder output.

In our case, a Viterbi algorithm with soft-decision decoding will be used with a rate  $r_{cc} = \frac{1}{2}$  and  $v=3$ . The output of our demodulator  $Y$  will be the input to the decoder.

If the two paths are considered in the trellis of the rate  $\frac{1}{2}$  convolutional code that begins from the same state A, after three transitions, they merge again at point  $\Gamma$  (Figure 4.3). The two information sequences will be 000 and 100 and the transmitted sequences 00 00 00 and 11 01 11.

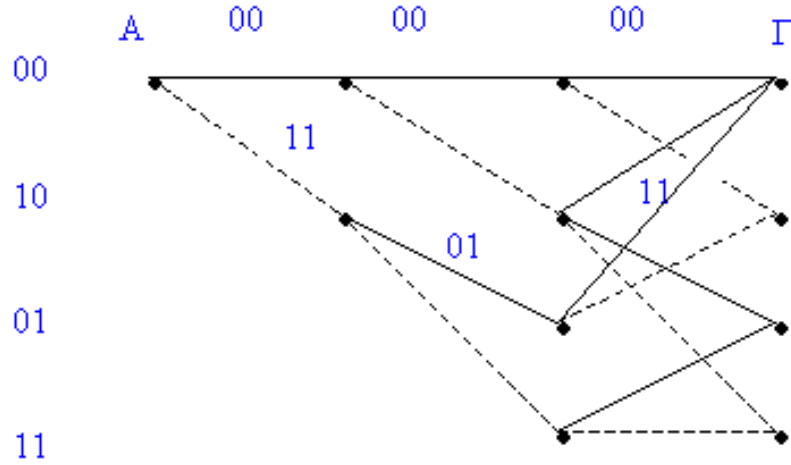


Figure 4.3. Trellis Diagram.

Now assume that the entire zero sequence was transmitted.

$$y_{jm} \Big|_{r_{01jm}, P_{01jm}} = \bar{Y}_{jm} + \xi_{jm}^c$$

$$E\{y_{jm}\} = \bar{Y}_{jm}^c = r_{jm} \sqrt{P_{01jm}}, t = T_{cc}$$

$$\xi_{jm}^c = \zeta_{1jm}^c + \zeta_{2jm}^c + n_{jm}^c$$

$$\begin{aligned} \text{Var}\{y_{jm}\} = \text{Var}\{\xi_{jm}^c\} &= \sigma_{\xi_{jm}^c}^2 = \frac{1}{3N} \sum_{k=2}^K E\{R_{0k}^2\} E\{P_{0k}\} \\ &+ \frac{1}{3N} \sum_{i=1}^6 \sum_{j=1}^K E\{R_{ij}^2\} E\{P_{ij}\} + \frac{N_0}{2T_{cc}} \end{aligned} \quad (4.22)$$

The Viterbi soft-decision decoder branch and path metrics are developed using  $B$  branches per path and  $n$  coded bits per branch. Each transmitted coded bit is viewed as a logically coded bit, denoted  $c_{jm}^{(i)} \in \{0,1\}$ , rather than a voltage  $b_{jm}^c \in \{\pm 1\}$ , such that  $b_{jm}^c = 1 - 2c_{jm}^{(i)}$ , where  $j$  indicates the branch ( $j = 1, 2, 3$ ) and  $m$  the bit of that branch ( $m = 1, 2$ ) and  $i$  is the number of the path. For our situation, the first path is denoted as the  $i = 0$  path and the second part as the  $i = 1$  path.

The Viterbi algorithm branch metrics are calculated after Proakis  $\mu_j^{(i)} = \sum_m^h (1 - 2c_{jm}^{(i)})$  and are summed over  $B$  branches to form path metrics.

$$CM^{(i)} = \sum_{j=1}^B \mu_j^{(i)} = \sum_{j=1}^B \sum_{m=1}^n y_{jm} (1 - 2c_{jm}^{(i)}) \quad (4.23)$$

So, for the all-zero path or  $i = 0$ :

$$CM^{(0)} = \sum_{j=1}^B \sum_{m=1}^n y_{jm} (1 - 2c_{jm}^{(0)}) = \sum_{j=1}^B \sum_{m=1}^n y_{jm} (1 - 0) = \sum_{j=1}^B \sum_{m=1}^n y_{jm} \quad (4.24)$$

Now for another path,  $i = 1$ :

$$CM^{(1)} = \sum_{j=1}^B \sum_{m=1}^n y_{jm} (1 - 2c_{jm}^{(1)}) \quad (4.25)$$

where  $c_{jm}^{(1)} = 1$  if there is an error. If  $d$  bits are equal to 1, then the two paths will differ in these  $d$  positions (in our example  $d = 5$ ). The probability of error for every path that

differs in  $d$  positions from the all zero path will be found. If  $CM^{(0)}$  is greater than  $CM^{(1)}$  at point  $\Gamma$  where they merge, then  $CM^{(0)}$  will continue to be greater than  $CM^{(1)}$  in any path that stems from node  $\Gamma$ . Thus, our decoder will discard the incorrect path.

First event error probability is the probability that a different from the all zero path (correct path) has a greater metric than the all zero at a specific node. In this occasion, the decoder will wrongly discard the all zero path ( $i = 0$ ) in favor of the incorrect path ( $i = 1$ ).

$$\begin{aligned}
P_2(d) \Big|_{r_{01jm}, P_{01jm}} &= P_r \{ CM^{(1)} \geq CM^{(0)} \} = P_r \{ CM^{(1)} - CM^{(0)} \geq 0 \} \\
&= P_r \left\{ -2 \sum_{j=1}^B \sum_{m=1}^n y_{jm} (c_{jm}^{(1)} - c_{jm}^{(0)}) \geq 0 \right\} = P_r \left\{ -2 \sum_{j=1}^B \sum_{m=1}^n y_{jm} c_{jm}^{(1)} \geq 0 \right\} \\
&= P_r \left\{ \sum_{\ell=1}^d y'_\ell \leq 0 \right\}
\end{aligned} \tag{4.26}$$

where the index  $\ell$  runs over the  $d$  bits where the two paths differ ( $c_{jm}^{(1)} = 1$ )

$$y_\ell = \sum_{\ell=1}^d y'_\ell \tag{4.27}$$

where  $y_\ell$  is the sum of  $d$  independent identically distributed Gaussian random variables  $y'_\ell$ . So  $y_\ell$  is a Gaussian random variable with expected value (mean)

$$E\{y_\ell\} = \sum_{\ell=1}^d E\{y'_\ell\} = \sum_{\ell=1}^d r_\ell \sqrt{P_{01\ell}} = \sum_{\ell=1}^d r_\ell \sqrt{x_\ell P} \tag{4.28}$$

where  $x_\ell$  is our lognormal random variable of power control error  $x_\ell \sim \Lambda(0, \lambda \sigma_{dB})$ .

The variance of the Gaussian random variable  $y_\ell$  is defined by:

$$\begin{aligned}
\sigma_{y_\ell}^2 &= \text{Var}\{y_\ell\} = \sum_{\ell=1}^d \text{Var}\{y'_\ell\} \\
&= \sum_{\ell=1}^d \left\{ \frac{1}{3N} \sum_{k=2}^K E\{R_{0k}^2\} E\{P_{0k}\} + \frac{1}{3N} \sum_{i=1}^6 \sum_{j=1}^k E\{R_{ij}^2\} E\{P_{ij}\} + \frac{N_0}{2T_{cc}} \right\}
\end{aligned} \tag{4.29}$$

So,

$$\begin{aligned}
P_2(d) \Big|_{r_\ell, P_{k\ell}} &= P_r \{y_\ell \leq 0\} = Q \left( \sqrt{\frac{\bar{y}_\ell^2}{\sigma_{y_\ell^2}}} \right) = \\
&= Q \left( \frac{\sum_{\ell=1}^d r_{01_\ell}^2 x_\ell p}{\sqrt{\frac{1}{3N} \sum_{k=2}^K E\{R_{0k}^2\} E\{P_{0k}\} + \frac{1}{3N} \sum_{i=1}^6 \sum_{j=1}^K E\{R_{ij}^2\} E\{P'_{ij}\} + \frac{N_0}{2T_{cc}}}}} \right) = \\
&= Q \left( \frac{\sum_{\ell=1}^d r_\ell^2 x_\ell p}{\sqrt{\frac{1}{3N} \sum_{k=2}^K E\{R_{0k}^2\} E\{P_{0k}\} + \frac{1}{3N} \sum_{i=1}^6 \sum_{j=1}^K E\{R_{ij}^2\} E\{P'_{ij}\} + \frac{N_0}{2T_{cc}}}}} \right) \\
&= Q \left( \sqrt{\frac{\sum_{\ell=1}^d r_\ell^2 x_\ell p}{a}} \right) = Q \left( \sqrt{\frac{Z_d}{a}} \right) = P_2(d) \Big|_{z_d}
\end{aligned}$$

where:

$$\begin{aligned}
a &= \frac{1}{3N} \sum_{k=2}^K E\{R_{0k}^2\} PE\{X_{0k}\} + \frac{1}{3N} \sum_{i=1}^6 \sum_{j=1}^K E\{R_{ij}^2\} PE\{\lambda_{ij}\} + \frac{N_0}{2T_{cc}} \\
a &= \frac{1}{3N} \exp\left(\frac{\tilde{\lambda}^2 \sigma_{dB}^2}{2}\right) \sum_{k=2}^K P + \frac{1}{3N} \sum_{i=1}^6 \sum_{j=1}^K PE\{\lambda_{ij}\} + \frac{N_0}{2T_{cc}}
\end{aligned}$$

and thus:

$$P_2(d) \Big|_{r_\ell, P_{k\ell}} = Q \left( \frac{\sum_{\ell=1}^d r_\ell^2 x_\ell}{\sqrt{\frac{1}{3N} \exp\left(\frac{\tilde{\lambda}^2 \sigma_{dB}^2}{2}\right) (K-1) + \frac{1}{3N} \sum_{i=1}^6 \sum_{j=1}^K E\{\lambda_{ij}\} + \frac{N_0}{2E_c}}} \right) \quad (4.30)$$

where  $E_c = \binom{k}{n} E_b$  is the coded bit energy and  $E\{R_{0k}^2\} = E\{R_{ij}^2\} = 1$ .

The first-event error probability for a single path with distance  $d$  from the all zero path ( $i = 0$ ) has been derived. In fact, there are many possible paths with different distances that merge with the all zero path at out node  $\Gamma$ . By summing all the  $P_2(d)$ , an upper bound on the first-event error probability can be estimated

$$P_e \leq \sum_{d=d_{free}}^{\infty} a_d P_2(d) \quad (4.31)$$

where  $a_d$  is the number of paths with distance  $d$  from the  $i = 0$  path that merge with the all zero path at our node  $\Gamma$  for the first time.

A more useful measure is the upper bound of the probability of bit error  $P_b$  (with FEC). This again is given by summing over all  $d$ , the product of the total number of incorrectly decoded information bits  $\beta_d$  for the incorrect path at node  $\Gamma$  and the pairwise error probability  $P_2(d)$ , which for  $k = 1$  is given by the formula

$$P_b < \sum_{d=d_{free}}^{\infty} \beta_d \cdot P_2(d) \quad (4.32)$$

and for  $k > 1$ :

$$P_b < \frac{1}{k} \sum_{d=d_{free}}^{\infty} \beta_d \cdot P_2(d) \quad (4.33)$$

The values of  $a_d$  and  $\beta_d$  can be calculated. In our analysis, in order to calculate the upper bound on the probability of bit error  $P_b$ , not all of the terms of the summation

will be used, but only the first five:  $P_b < \frac{1}{k} \sum_{d=d_{free}}^{d_{free}+4} \beta_d \cdot P_2(d)$ . For a code rate  $\frac{1}{2}$

convolutional code with a constraint length  $v=8$ ,  $d_{free} = 10$ , and so the first five terms

will be  $d = d_{free}, d_{free+1}, d_{free+2}, d_{free+3}, d_{free+4} = 10, 11, 12, 13, 14$

$$P_b < \beta_{10} P_2(10) + \beta_{11} P_2(11) + \beta_{12} P_2(12) + \beta_{13} P_2(13) + \beta_{14} P_2(14) \quad (4.34)$$

where  $\beta_{10} = 2$ ,  $\beta_{11} = 22$ ,  $\beta_{12} = 60$ ,  $\beta_{13} = 148$  and  $\beta_{14} = 340$ .



### C. BIT ERROR ANALYSIS OF DS-CDMA

In this section, the performance of the reverse channel of our cellular communication system will be examined when some factors such as the power control error, the lognormal shadowing for the adjacent cells and the Nakagami-fading variable  $m$  are varied. All the following Figures were produced by using matlab codes.

In Figures 4.4 and 4.5, the probability of bit error for 20 users per cell for lognormal shadowing  $\sigma = 7$  and  $\sigma = 9$  respectively can be seen as well as for  $m = 1$  in which the power control error lognormal parameter  $\sigma_{1dB}$  is varied.

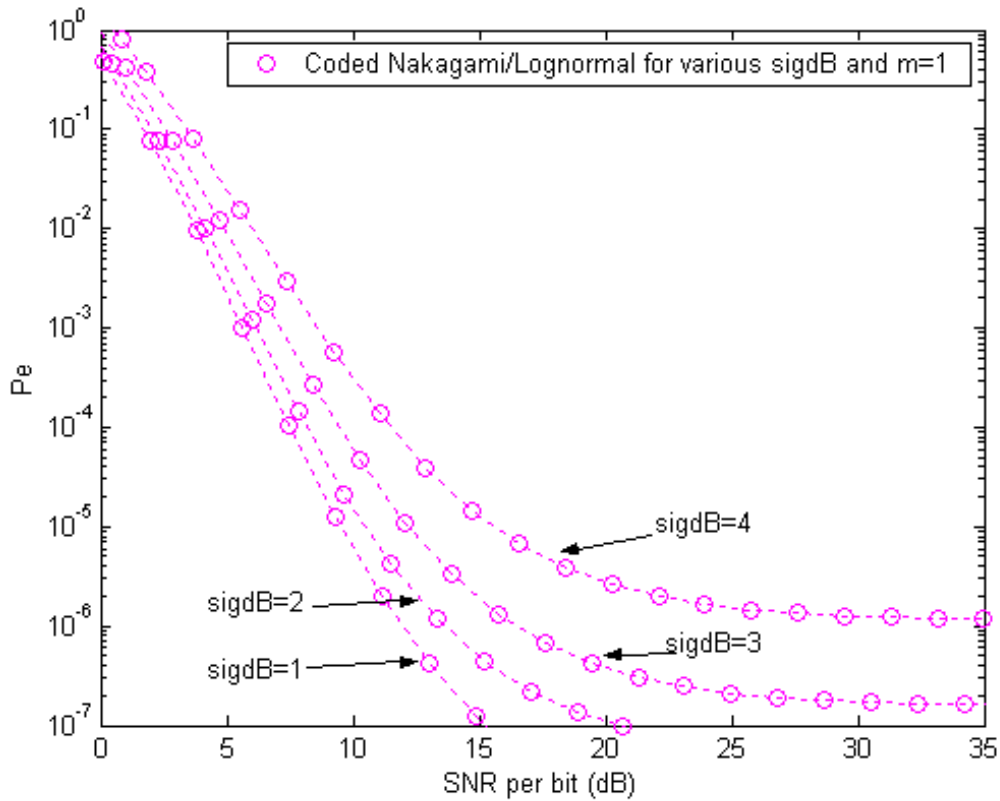


Figure 4.4. Coded Nakagami for Lognormal Shadowing  $\sigma = 7$  and Power Control Error  $\sigma_{1dB} = 1, 2, 3, 4$  for  $m = 1$  and 20 Users per Cell.

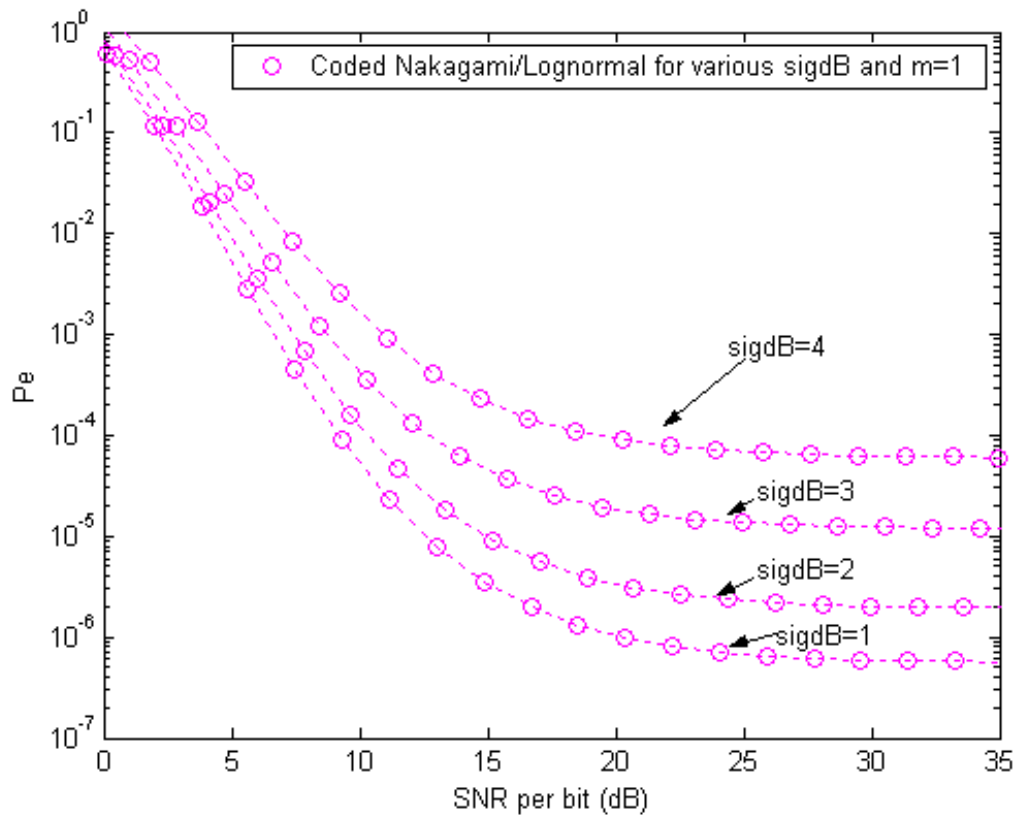


Figure 4.5. Coded Nakagami for Lognormal Shadowing  $\sigma = 9$  and Power Control Error  $\sigma_{1dB} = 1, 2, 3, 4$  for  $m = 1$  and 20 Users per Cell.

From both figures it can be seen that when the lognormal parameter of power control error increases the probability of bit error also increases. When comparing the two figures, it can be determined that when the lognormal shadowing parameter is greater the probability of bit error is also greater.

In Figures 4.6 and 4.7, the probability of bit error for 20 users per cell for lognormal shadowing  $\sigma = 7$  and  $\sigma = 9$  respectively can be seen and for the power control error lognormal parameter  $\sigma_{1dB} = 4$  in which the Nakagami-fading parameter  $m$  is varied.

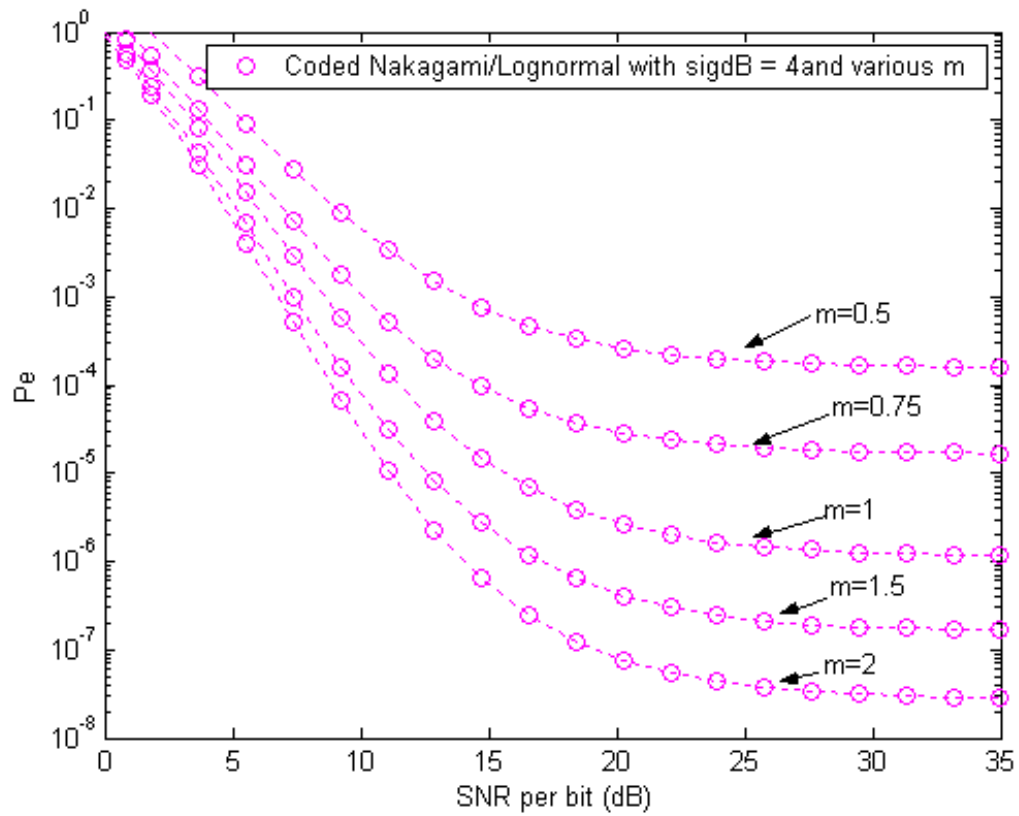


Figure 4.6. Coded Nakagami for Lognormal Shadowing  $\sigma = 7$  and Power Control Error  $\sigma_{dB} = 4$  for  $m = 0.5, 0.75, 1, 1.5, 2$  and 20 Users per Cell.

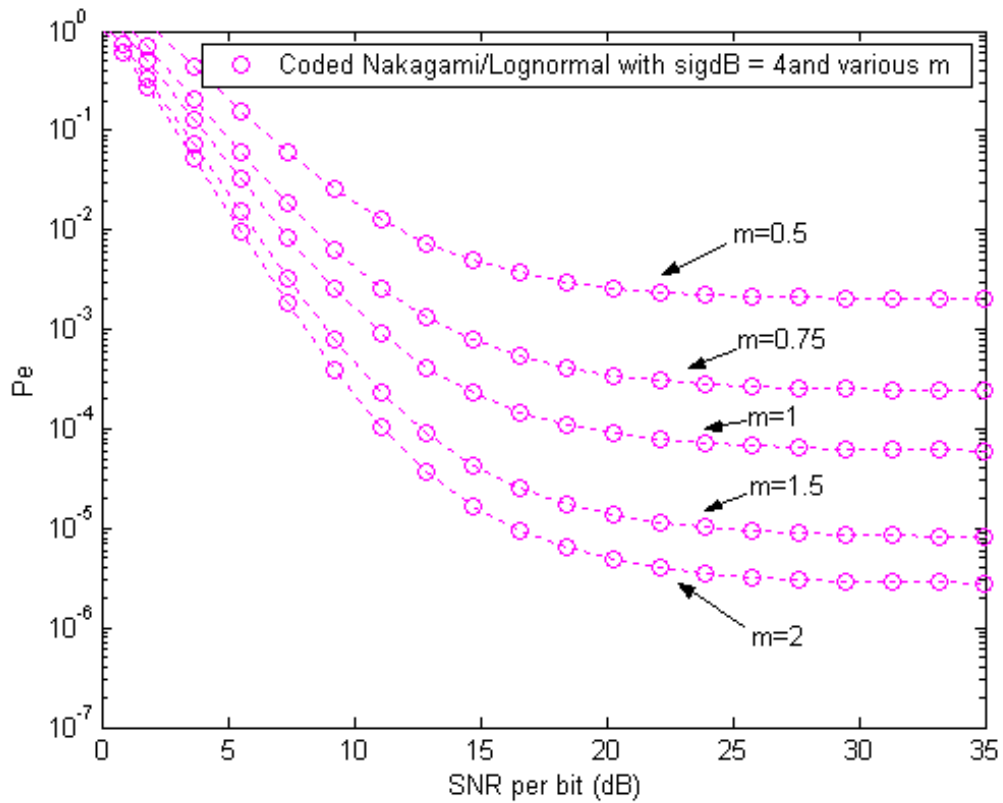


Figure 4.7. Coded Nakagami for Lognormal Shadowing  $\sigma = 9$  and Power Control Error  $\sigma_{dB} = 4$  for  $m=0.5, 0.75, 1, 1.5, 2$  and 20 Users per Cell.

From Figures 4.6 and 4.7, it can be observed that when the Nakagami-fading parameter  $m$  increases the probability of bit error decreases.

The performance of our system can also be considered in terms of the number of the users per cell that can be supported at a given SNR per bit.

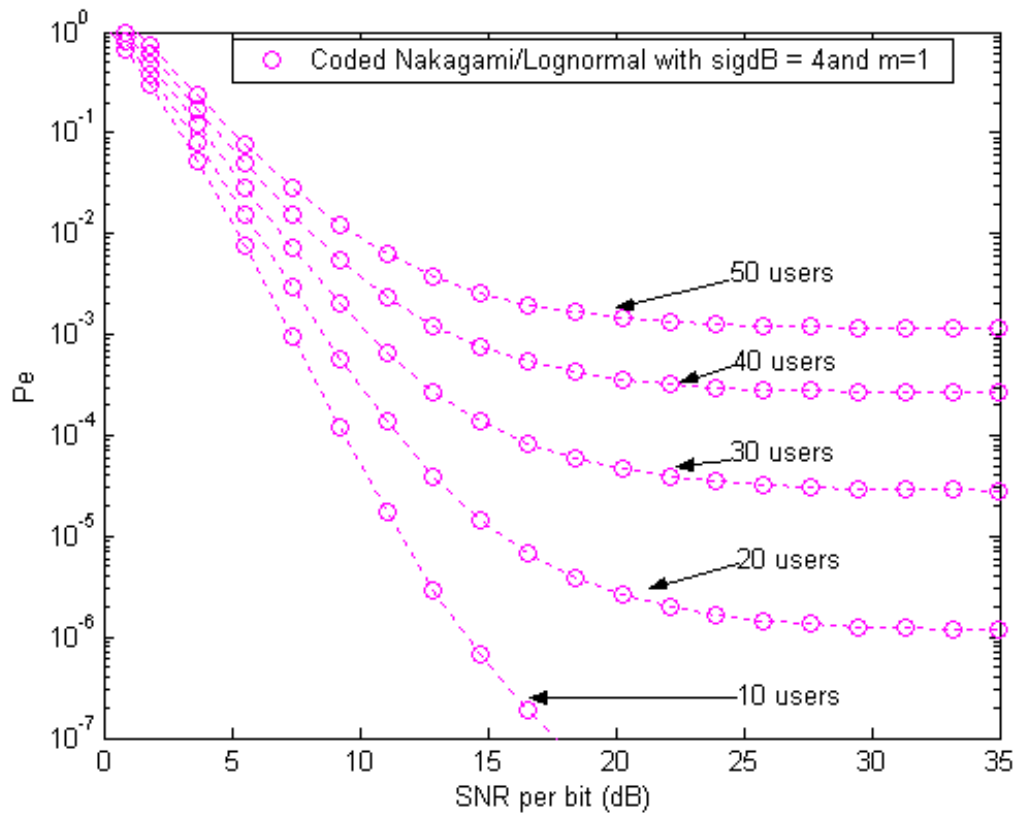


Figure 4.8. Coded Nakagami for Lognormal Shadowing  $\sigma = 7$  and Power Control Error  $\sigma_{1dB} = 4$  for  $m = 1$ .

From Figure 4.8, it can be observed that as the inter-cell and the intra-cell interference increase so does the probability of bit error.

## APPENDIX IV-A. CALCULATION OF THE VARIANCE OF THE INTERCELL INTERFERENCE

The variance of the intercell interference term  $\zeta_2$  will be calculated according to [1].

$$\begin{aligned}\zeta_2 &= \frac{1}{T} \int_0^T \sum_{i=1}^6 \sum_{j=1}^K R_{ij} \sqrt{P'_{ij}} b_{ij}(t + \tau_{ij}) c_{ij}(t + \tau_{ij}) c_{01}(t) \cos(\varphi_{ij}) dt \\ \zeta_2 &= \sum_{i=1}^6 \sum_{j=1}^K \frac{1}{T} \int_0^T R_{ij} \sqrt{P'_{ij}} b_{ij}(t + \tau_{ij}) c_{ij}(t + \tau_{ij}) c_{01}(t) \cos(\varphi_{ij}) dt\end{aligned}\quad (4.35)$$

Now,  $I_{ij} = \frac{1}{T} R_{ij} \sqrt{P'_{ij}} \cos(\varphi_{ij}) \int_0^T a_{ij}(t + \tau_{ij}) c_{01}(t) dt$

where  $a_{ij}(t + \tau_{ij}) = b_{ij}(t + \tau_{ij}) \cdot c_{ij}(t + \tau_{ij})$  and  $c_{01}(t)$  are PN signals.

$$\begin{aligned}E\{I_{ij}^2\} &= E\left\{\left(\frac{1}{T} R_{ij} \sqrt{P'_{ij}} \cos(\varphi_{ij}) \int_0^T a_{ij}(t + \tau_{ij}) c_{01}(t) dt\right)^2\right\} = \\ &= E\left\{\frac{1}{T^2} R_{ij}^2 P'_{ij} \cos^2(\varphi_{ij}) \left(\int_0^T a_{ij}(t + \tau_{ij}) c_{01}(t) dt\right) \left(\int_0^T a_{ij}(\lambda + \tau_{ij}) c_{01}(\lambda) d\lambda\right)\right\} \\ &= \frac{1}{T^2} E\{R_{ij}^2\} E\{P'_{ij}\} E\{\cos^2(\varphi_{ij})\} E\left\{\int_0^T \int_0^T a_{ij}(t + \tau_{ij}) a_{ij}(\lambda + \tau_{ij}) c_{01}(t) c_{01}(\lambda) d\lambda\right\} \quad (4.36) \\ &= \frac{1}{T^2} E\{R_{ij}^2\} E\{P'_{ij}\} \frac{1}{2} \int_0^T \int_0^T E\left\{\underbrace{a_{ij}(t + \tau_{ij}) a_{ij}(\lambda + \tau_{ij})}_{\beta(t-\lambda)}\right\} E\left\{\underbrace{c_{01}(t) c_{01}(\lambda)}_{\beta(t-\lambda)}\right\} dt d\lambda \\ &= \frac{E\{R_{ij}^2\} E\{P'_{ij}\}}{2T^2} \int_0^T \int_0^T \beta^2(t - \lambda) dt d\lambda\end{aligned}$$

where  $\beta(u)$  is the autocorrelation function of a PN signal

$$\beta(u) = \begin{cases} 1 - \frac{|u|}{T}, & |u| \leq T \\ 0, & \text{otherwise} \end{cases} \quad (4.37)$$

It is also assumed that  $E\{\cos^2(\varphi_{ij})\} = \frac{1}{2}$  because  $\varphi_{ij}$  is uniformly distributed in  $[0, 2\pi]$ .

Changing the variables:

$$\begin{aligned} u = t - \lambda & & u + v = 2t \\ \text{and} & & \\ v = t + \lambda & & u - v = -2\lambda \end{aligned} \tag{4.38}$$

so  $t = \frac{1}{2}(u + v)$  and  $\lambda = \frac{1}{2}(v - u)$ .

$$J_{t\lambda} = \det \begin{pmatrix} \frac{\partial t}{\partial u} & \frac{\partial t}{\partial v} \\ \frac{\partial \lambda}{\partial u} & \frac{\partial \lambda}{\partial v} \end{pmatrix} = \det \begin{pmatrix} \frac{1}{2} & \frac{1}{2} \\ \frac{1}{2} & -\frac{1}{2} \end{pmatrix} = \frac{1}{2} \tag{4.39}$$

Now since  $u = t - \lambda$  and  $t \in (0, T)$  and  $\lambda \in (0, T)$ ,  $-T < u < T$  and  $|u| < v < 2T - |u|$  as shown in Figure 4.9.

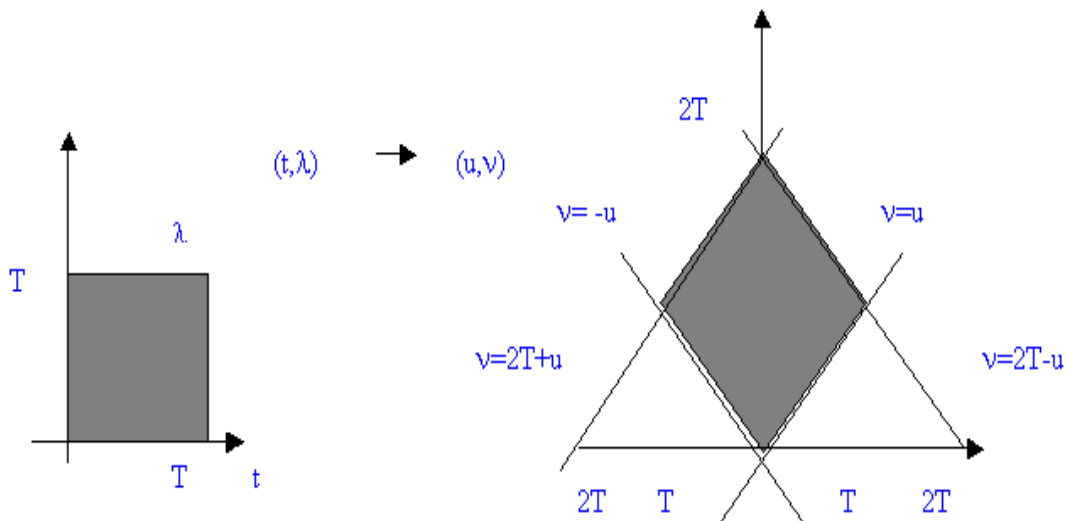


Figure 4.9. Transformation of the Limits of Integration.

$$\begin{aligned}
E\{I_{ij}^2\} &= \frac{E}{2T^2} \{R_{ij}^2\} E\{P'_{ij}\} \int_{-T}^T \int_{|\mu|}^{2T-|\mu|} \beta^2(u) J_{t\lambda} dv du \\
&= \frac{E\{R_{ij}^2\} E\{P'_{ij}\}}{2T^2} \int_0^T \int_u^{2T-u} \beta^2(u) dv du = \frac{E\{R_{ij}^2\} E\{P'_{ij}\}}{2T^2} \int_0^T \beta^2(u) (2T-u-u) du \\
&= \frac{E\{R_{ij}^2\} E\{P'_{ij}\}}{2T^2} \int_0^{T/N} \left(1 - \frac{Nu}{T}\right)^2 (2T-2u) du \\
&= \frac{E\{R_{ij}^2\} E\{P'_{ij}\}}{2T^2} \int_0^{T/N} \left(1 - \frac{N^2 u^2}{T^2} - \frac{2Nu}{T}\right)^2 (2T-2u) du \\
&= \frac{E\{R_{ij}^2\} E\{P'_{ij}\}}{2T^2} \int_0^{T/N} \left(2T-2u + 2\frac{N^2 u^2}{T} - 2\frac{N^2 u^3}{T^2} - 4Nu + 4\frac{Nu^2}{T}\right) du \\
&= \frac{E\{R_{ij}^2\} E\{P'_{ij}\}}{2T^2} 2 \left[ Tu - \frac{u^2}{2} + \frac{N^2 u^3}{3T} - \frac{N^2 u^4}{4T^2} - Nu^2 + \frac{2Nu^3}{3T} \right]_0^{T/N} \\
&= \frac{E\{R_{ij}^2\} E\{P'_{ij}\}}{T^2} \left[ \frac{T^2}{N} - \frac{T^2}{2N^2} + \frac{N^2 T^3}{3TN^3} - \frac{N^2 T^4}{4T^2 N^4} - \frac{NT^2}{N^2} + \frac{2}{3} \frac{N}{T} \frac{T^3}{N^3} \right] \\
&= \frac{E\{R_{ij}^2\} E\{P'_{ij}\}}{T^2} \left[ \frac{T^2}{N} - \frac{T^2}{2N^2} + \frac{T^2}{3N} - \frac{T^2}{4N^2} - \frac{T^2}{N} + \frac{2}{3} \frac{T^3}{N^2} \right] \\
&= \frac{E\{R_{ij}^2\} E\{P'_{ij}\}}{T^2} \left[ \frac{T^2}{3N} - \frac{T^2}{12N^2} \right] \\
&\approx \frac{E\{R_{ij}^2\} E\{P'_{ij}\}}{T^2} \frac{T^2}{3N} = \frac{E\{R_{ij}^2\} E\{P'_{ij}\}}{3N} \tag{4.40}
\end{aligned}$$

for  $N \gg 1$  (in our case  $N = 128$ ).

So:

$$\text{Var}\{\zeta_2\} = E\{\zeta_2^2\} = E\left\{ \left[ \sum_{i=1}^6 \sum_{j=1}^K I_{ij} \right]^2 \right\} = \sum_{i=1}^6 \sum_{j=1}^K E\{I_{ij}^2\} = \frac{1}{3N} \sum_{i=1}^6 \sum_{j=1}^K E\{R_{ij}^2\} E\{P'_{ij}\} \tag{4.41}$$

in the same manner the variance is found for intracell interference:

$$\text{Var}\{\zeta_1\} = E\{\zeta_1^2\} = \frac{1}{3N} \sum_{k=2}^K E\{R_{0k}^2\} E\{P_{0k}\} \tag{4.42}$$



THIS PAGE INTENTIONALLY LEFT BLANK

## APPENDIX IV-B. CALCULATION OF THE VARIANCE OF THE NOISE COMPONENT

The following analyses are based on [4].

The signal  $n'(t) = c_{01}(t)n(t)$  where  $c_{01}(t)$  and  $n(t)$  are modeled as independent random processes, which are wide sense stationary, has the following autocorrelation function:

$$\begin{aligned} R_{n'(t)} &= E[n'(t)n'(t+\tau)] = E[c_{01}(t)n(t)c_{01}(t+\tau)n(t+\tau)] = E[c_{01}(t)c_{01}(t+\tau)]E[n(t)n(t+\tau)] \\ &= R_{c_{01}}(\tau)R_n(\tau) \end{aligned} \quad (4.43)$$

Thus, the power spectral density of  $n'(t)$  is:

$$S_{n'} = F\{R_{n'(t)}\} = F\{R_{c_{01}}(\tau) \cdot R_n(\tau)\} = S_{c_{01}}(f) * S_n(f) \quad (4.44)$$

where \* is the symbol of the convolution operation. Now since  $n(t)$  is Additive White Gaussian Noise it has a PSD of  $S_n(f) = N_0/2$  and the spreading PN sequence has a PSD of:

$$S_{c_{01}}(f) = T_c \sin^2(f T) \quad (4.45)$$

So,

$$\begin{aligned} S_{n'}(f) &= S_{c_{01}}(f) * S_n(f) = \int_{-\infty}^{\infty} S_{c_{01}}(f-u)S_n(u)du \\ &= \int_{-\infty}^{\infty} S_{c_{01}}(u)S_n(f-u)du = \frac{T_c N_0}{2} \int_{-\infty}^{\infty} \sin^2(u T_c) du \end{aligned} \quad (4.46)$$

With the substitutions  $x = \pi u T_c$  and  $dx = \pi T_c du$ :

$$S_{n'}(f) = \frac{T_c N_0}{2} \pi T_c \int_{-\infty}^{\infty} \left(\frac{\sin x}{x}\right)^2 dx = \frac{N_0}{2\pi} \int_{-\infty}^{\infty} \left(\frac{\sin x}{x}\right)^2 dx = \frac{N_0}{2\pi} \pi = \frac{N_0}{2} \quad (4.47)$$

Thus, the PSD of  $n'$  is equal to the PSD of  $n(t)$  so the nature and the characteristics of the AWGN are unaffected by despreading which means that  $n'(t)$  is also a zero mean AWGN.

When multiplying  $n'$  by  $\sqrt{2} \cos(2\pi f_c t)$ ,  $n_1(t) = n' \sqrt{2} \cos(2\pi f_c t)$  where  $n_1(t)$  is also AWGN because the characteristics of AWGN are unchanged by the frequency translations. Now, the PSD of  $n_1(t)$  is as follows:

$$S_{n_1}(f) = \frac{1}{4} (\sqrt{2})^2 \left( \frac{N_0}{2} + \frac{N_0}{2} \right) = \frac{1}{4} 2N_0 = \frac{N_0}{2} \quad (4.48)$$

Now the PSD at the output of the integrator with the transfer function  $H(f)$  is

$$S_{out}(f) = S_{in}(f) |H(f)|^2 :$$

$$S_n(f) = S_{n_1}(f) \left| \frac{\sin(\pi fT)}{\pi fT} \right|^2 = \frac{N_0}{2} \left| \frac{\sin(\pi fT)}{\pi fT} \right|^2 \quad (4.49)$$

Thus, the variance or the noise power at the integrator output would be as follows:

$$\sigma^2 = \int_{-\infty}^{\infty} S_n(f) df = \frac{N_0}{2} \int_{-\infty}^{\infty} \left| \frac{\sin(\pi fT)}{\pi fT} \right|^2 df = \frac{N_0}{2\pi T} \int_{-\infty}^{\infty} \left[ \frac{\sin(x)}{x} \right]^2 dx = \frac{N_0}{2\pi T} \pi = \frac{N_0}{2T} \quad (4.50)$$

## APPENDIX IV-C. PROBABILITY OF BIT ERROR

There will be a bit error when a bit one is transmitted and our decision statistic  $y$  is less than zero ( $y < 0$ ), or when a bit zero is transmitted and our decision statistic  $y$  is greater than zero ( $y > 0$ ). Generally, the probability of transmitting a zero is equal to the probability of transmitting a one.

$$P_r(1) = P_r(0) = \frac{1}{2} \quad (4.51)$$

Thus, the probability of bit error is given by:

$$\begin{aligned} P_b &= P_r(\text{error}|1)P_r(1) + P_r(\text{error}|0)P_r(0) \\ &= \frac{1}{2} [P_r(\text{error}|1)] + P_r(\text{error}|0) = \frac{1}{2} [P_r(y < 0|1) + P_r(y > 0|0)] \end{aligned} \quad (4.52)$$

Now, from symmetry:

$$P_r(y < 0|1) = P_r(y > 0|0) \quad (4.53)$$

So,  $P_b = P_r(y < 0|1) = P_r(y > 0|0)$ . Now:

$$P_b = P_r(y > 0|0) = \int_0^{\infty} f_y(y|0) dy = \frac{1}{\sqrt{2\pi}\sigma_\zeta} \int_0^{\infty} \exp\left[-\frac{(y + \bar{Y})^2}{2\sigma_\zeta^2}\right] dy \quad (4.54)$$

Now defining  $\mu = \frac{y + \bar{Y}}{2\sigma_\zeta}$ :

$$\begin{aligned} P_b &= \frac{1}{\sqrt{2\pi}} \int_{\bar{Y}/\sigma_\zeta}^{\infty} \exp(-\phi^2/2) d\phi = Q\left(-\frac{\bar{Y}}{\sigma_\zeta}\right) = Q\left(\frac{\bar{Y}}{\sigma_\zeta}\right) \\ P_b &= Q\left(\sqrt{\frac{\bar{Y}^2}{\sigma_\zeta^2}}\right) \text{ or } P_b = \frac{1}{2} \text{erfc}\left(\sqrt{\frac{\bar{Y}^2}{2\sigma_\zeta^2}}\right) \text{ or } P_b = Q(\sqrt{SNIR}) \end{aligned} \quad (4.55)$$

THIS PAGE INTENTIONALLY LEFT BLANK

#### APPENDIX IV-D. PLOTS OF THE PERFORMANCE OF THE SYSTEM FOR VARIOUS USERS AND PARAMETERS

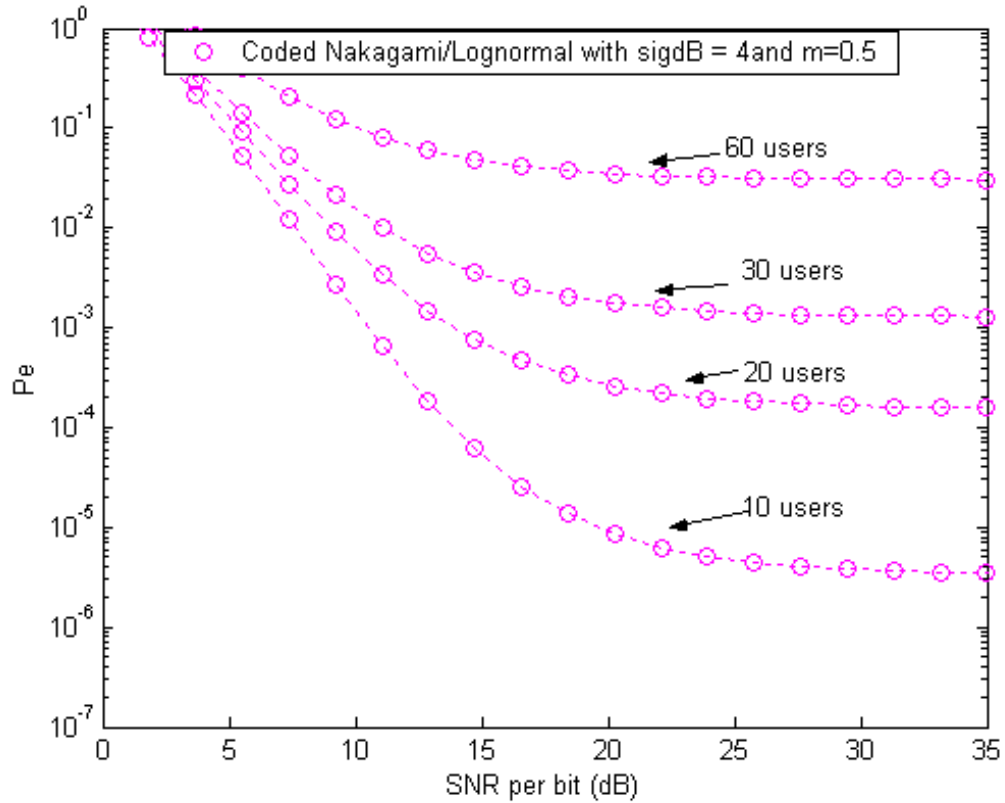


Figure 4.10. Coded Nakagami for Lognormal Shadowing  $\sigma = 7$  and Power Control Error  $\sigma_{dB} = 4$  for  $m = 0.5$ .

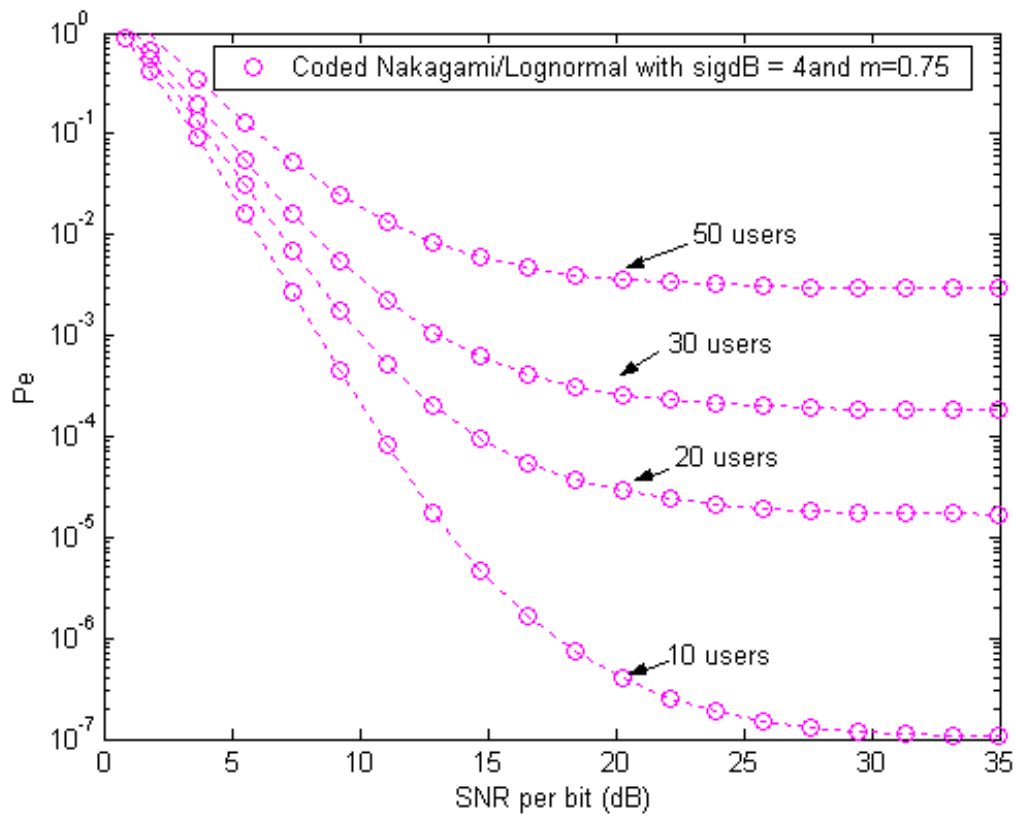


Figure 4.11. Coded Nakagami for Lognormal Shadowing  $\sigma = 7$  and Power Control Error  $\sigma_{dB} = 4$  for  $m = 0.75$ .

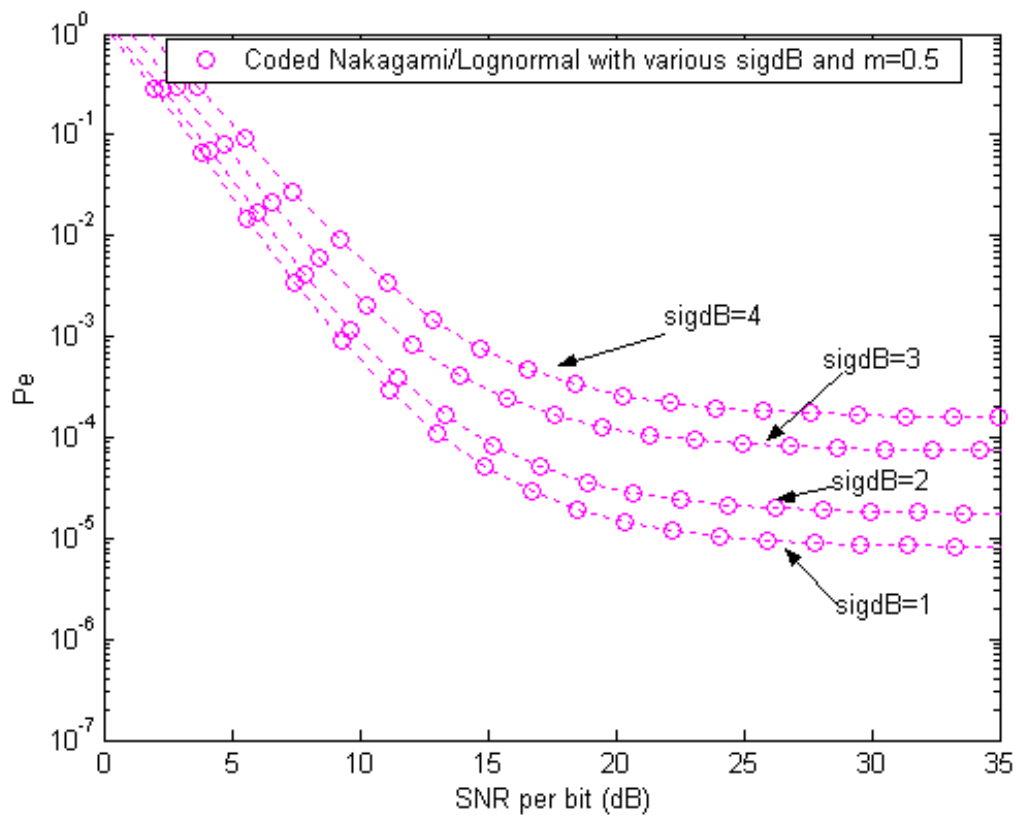


Figure 4.12. Coded Nakagami for Lognormal Shadowing  $\sigma = 7$  and Power Control Error  $\sigma_{1dB} = 1, 2, 3, 4$  for  $m = 0.5$  and 20 Users per Cell.



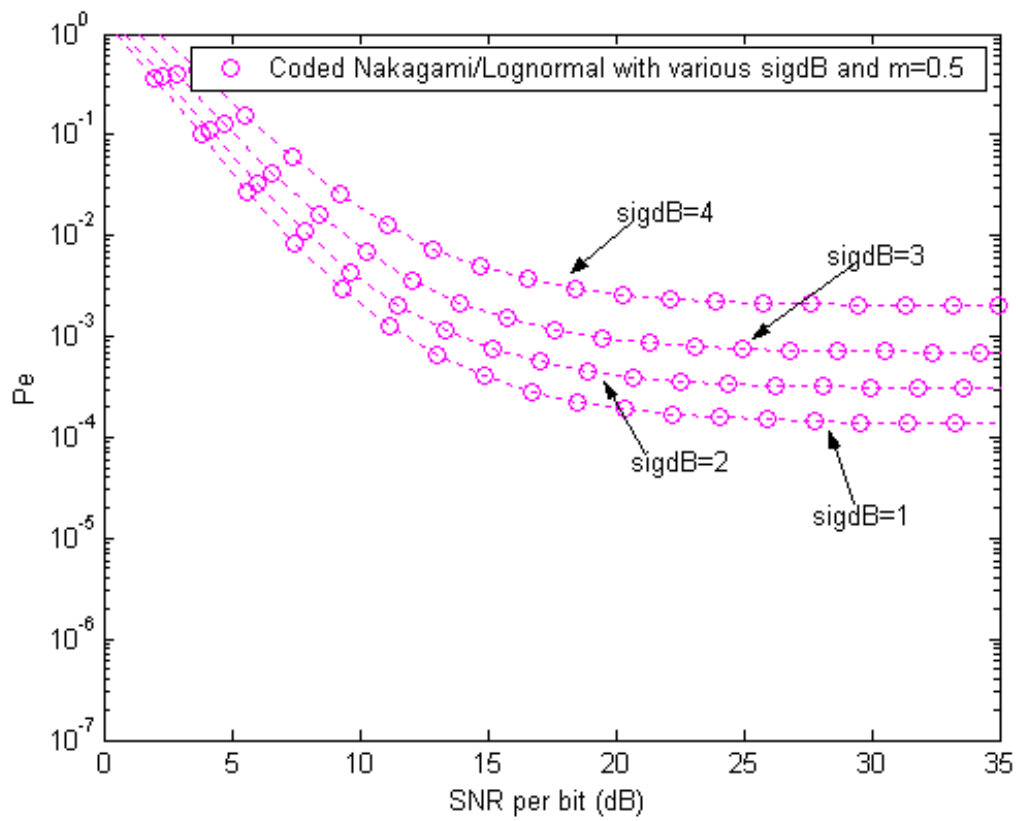


Figure 4.13. Coded Nakagami for Lognormal Shadowing  $\sigma = 9$  and Power Control Error  $\sigma_{1dB} = 1, 2, 3, 4$  for  $m = 0.5$  and 20 Users per Cell.

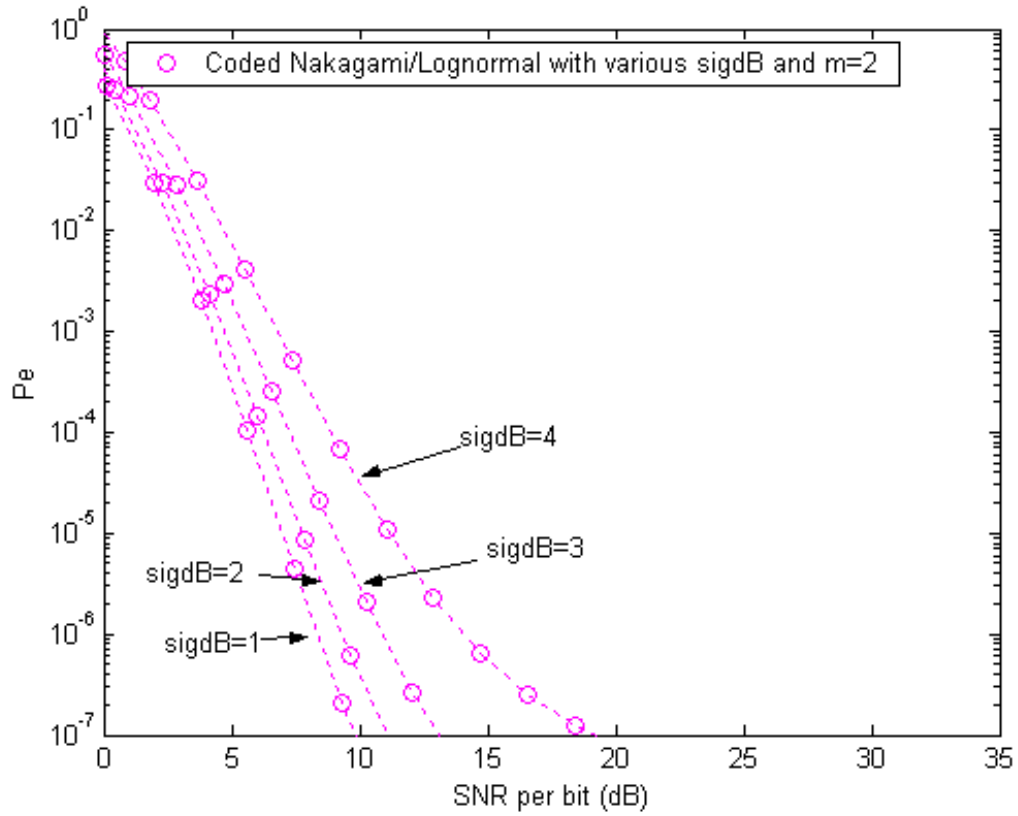


Figure 4.14. Coded Nakagami for Lognormal Shadowing  $\sigma = 7$  and Power Control Error  $\sigma_{1dB} = 1, 2, 3, 4$  for  $m = 2$  and 20 Users per Cell.

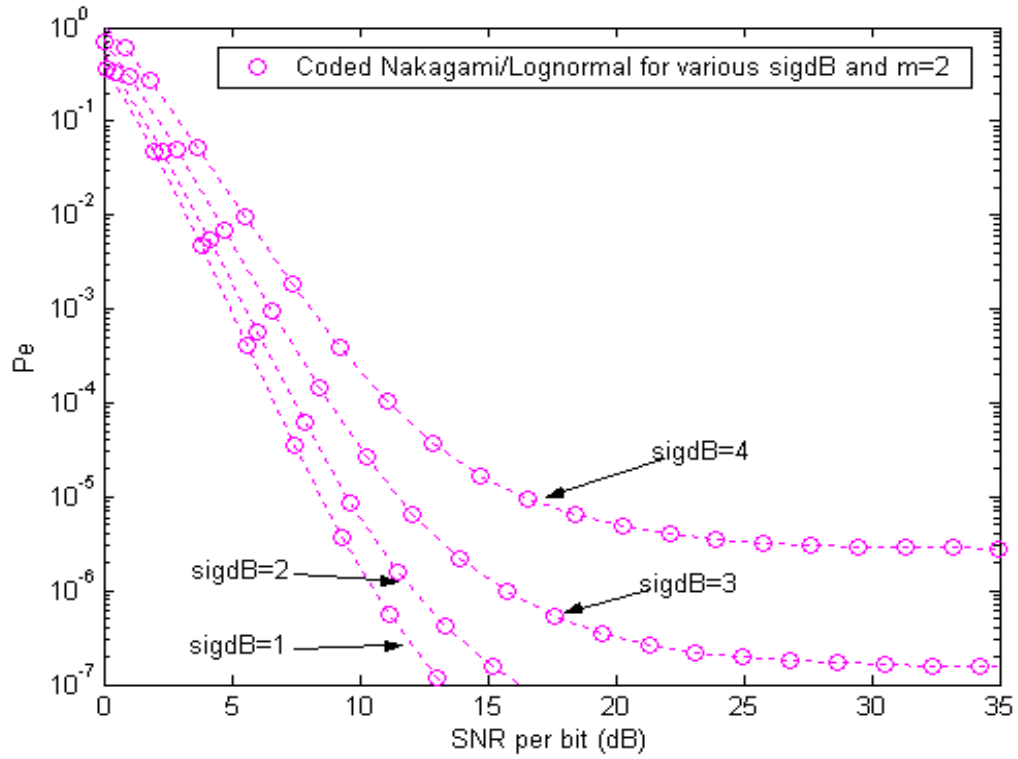


Figure 4.15. Coded Nakagami for Lognormal Shadowing  $\sigma = 9$  and Power Control Error  $\sigma_{1dB} = 1, 2, 3, 4$  for  $m = 2$  and 20 Users per Cell.

## V. VARIOUS TECHNIQUES TO IMPROVE THE PERFORMANCE OF OUR SYSTEM

In Chapter IV, an upper bound for the Probability of Bit Error for the reverse channel of a DS-CDMA cellular communication system was developed and the effects of the variation of several factors were seen such as the Lognormal Power Control Error, Lognormal shadowing and of the variable  $m$  of the Nakagami-fading channel.

In Chapter V, the idea of the Rake Receiver and the technique of Sectoring in order to achieve better performance for our system and maximize the number of subscribers (users) to be served in a specific geographic region will be introduced.

### A. RAKE RECEIVER

As seen in Chapter II, Spread Spectrum communications systems provide very good resistance to multipath fading since the delayed versions of a PN signal have very low correlation with the PN sequence itself.

A Spread Spectrum communication system can further improve its performance by the implementation of a Rake receiver at the base station of each cell [6],[9].

A Rake receiver has the ability to detect and combine the  $L$  strongest resolvable components of the signal in order to extract the information desired. It is actually a combination of  $L$  correlators whose outputs are properly weighted to provide a better estimation of the desired signal. In our case, assume  $L = 3$ , which means that our Rake receiver has 3 fingers and is depicted in Figure 5.1.

Usually the strongest multipath component of the signal arrives first at our receiver because the faster it arrives the fewer reflections it has and so, normally, the less attenuation it gets. The first correlator is synchronized to it. The second strongest multipath component arrives after  $\tau_1$  seconds, which is a very small amount of time, and the second correlator is synchronized to it. Finally, the third strongest component arrives after  $\tau_2$  seconds, from the first component, and the third correlator is synchronized to it. Now each correlator has very low correlation with the multipath components that are not synchronized with it.

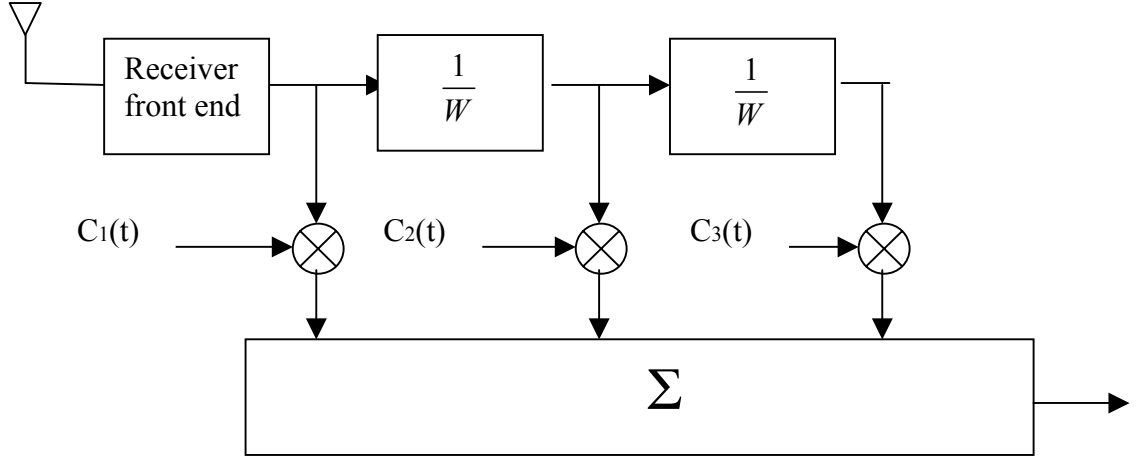


Figure 5.1. Typical Rake Receiver for  $L=3$ .

Now, if the output of any of the three correlators is corrupted by fading, which means that it has a very low signal to noise ratio (SNR), then it should be assigned to a proper small weighting factor to eliminate its effect.

Thus, for a Rake receiver at our base station from (4.30), the new First Event Error Probability would be

$$P_2(d) = Q \left( \sqrt{\frac{\sum_{n=1}^L \sum_{\ell=1}^d r_{\ell n}^2 x_{\ell n} P}{\frac{1}{3N} \sum_{n=1}^L \sum_{k=2}^K E\{R_{0kn}^2\} E\{P_{0kn}\} + SI + \frac{1}{3N} \sum_{n=1}^L \sum_{i=1}^6 \sum_{j=1}^K E\{R_{ijn}^2\} E\{P'_{ij}\} + \frac{N_0}{2}}} \right)$$

where the term  $SI$  in the denominator is called Self Interference and is due to the Rake fingers according to [10]

$$SI = \frac{1}{2N} \sum_{n=1}^L \sum_{n'=1, n' \neq n}^L E\{R_{01n'n}^2\} E\{P_{01n'n}\}$$

where  $n'$  is the number of the path of the desired signal.

The improvement in the performance of our system is obvious in Figure 5.2 for 30 users per cell and for a Rayleigh -fading channel ( $m=1$ ).

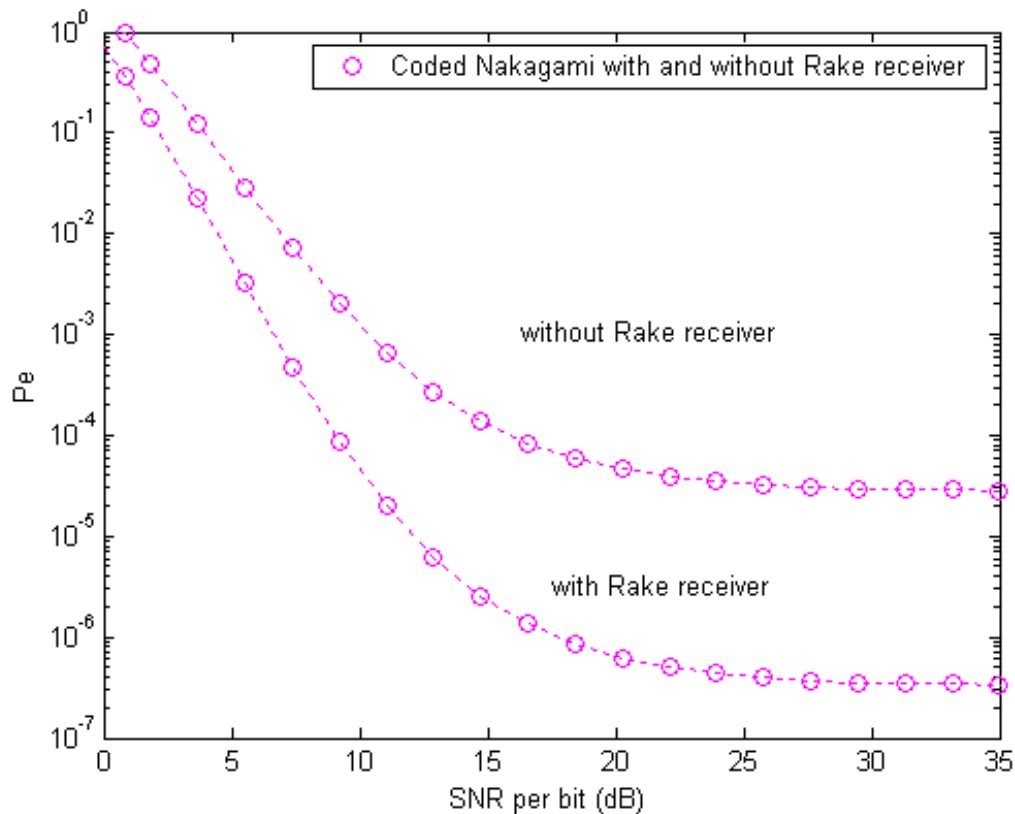


Figure 5.2. Coded Nakagami with and without Rake Receiver for 30 Users per Cell and for Lognormal Shadowing  $\sigma = 7$  and Power Control Error  $\sigma_{1dB} = 4$  and  $m = 1$ .

## B. SECTORING

As the demand for wireless and mobile communications service increases rapidly, especially in urban environments, the number of users that must be supported per unit coverage area increases as well. When the number of users increases, both the intra-cell and inter-cell interference increases, and so the performance of the DS-CDMA system, which is multiple access interference limited, degrades. In order for a communication link to be effective the probability of bit error must be less than 0.001.

A technique called sectoring [2], which implements directional antennas at the base stations instead of at omni-directional stations, is often used today in order to receive only a fraction of the existing interference.

A hexagonal cell is normally partitioned into three ( $120^\circ$ ) or six ( $60^\circ$ ) sectors by using three or six directional antennas respectively as shown in Figures 5.3 and 5.4.

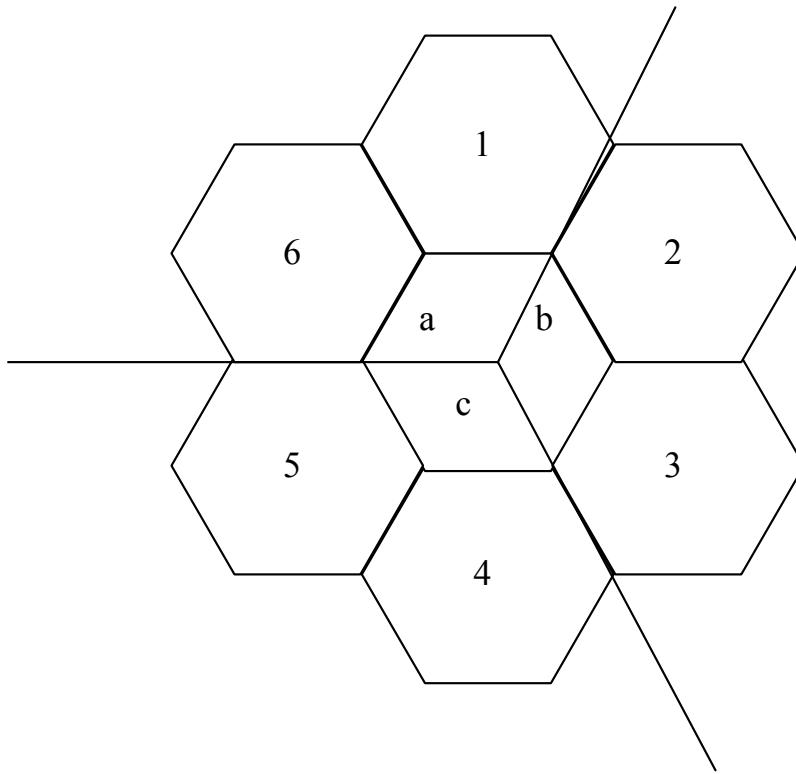


Figure 5.3.  $120^\circ$  Sectoring.

As seen in Figure 5.3, for  $120^\circ$  sectoring, the directional antenna in sector “a” of the center cell’s base station will receive intra-cell interference from the mobile users that are in sector “a”, and co-channel interference from the mobile users in cells one and six.

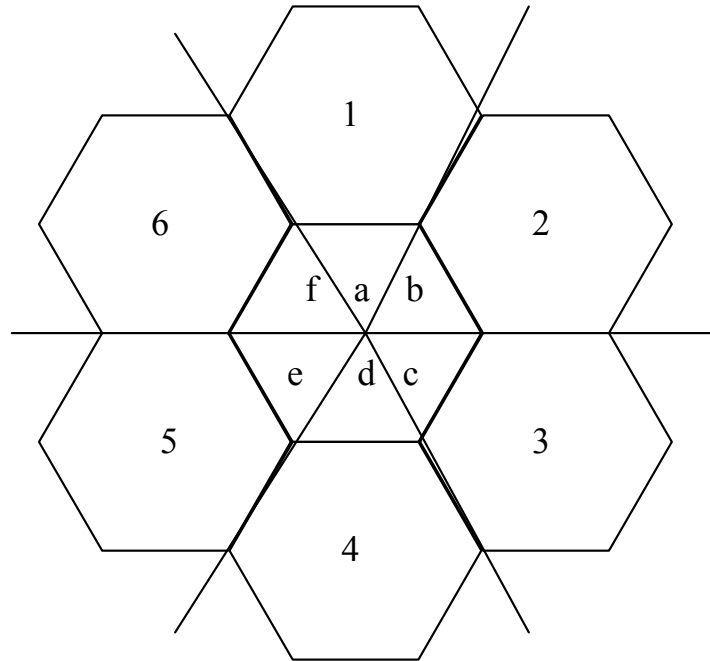


Figure 5.4. 60° Sectoring.

From Figure 5.4, for 60° sectoring, the directional antenna in sector “a” of the center cell’s base station will receive intra-cell interference from the mobile users that are in the now smaller sector “a”, and co-channel interference only from the mobile users in cell one.

Now, assuming that the users in the center cell are equally distributed and that each cell has the same number of active users, the total interference is reduced to 1/3 for 120° and to 1/6 for 60° of the initial value without sectoring.

The main drawbacks of using sectoring are that there is an increased number of sectoring antennas at each base station and an increased number of hand-offs. The first is the more serious because it means greater cost.

In Figure 5.5 the effects of sectoring (without Rake Receiver) in the performance of our communications system can be seen.



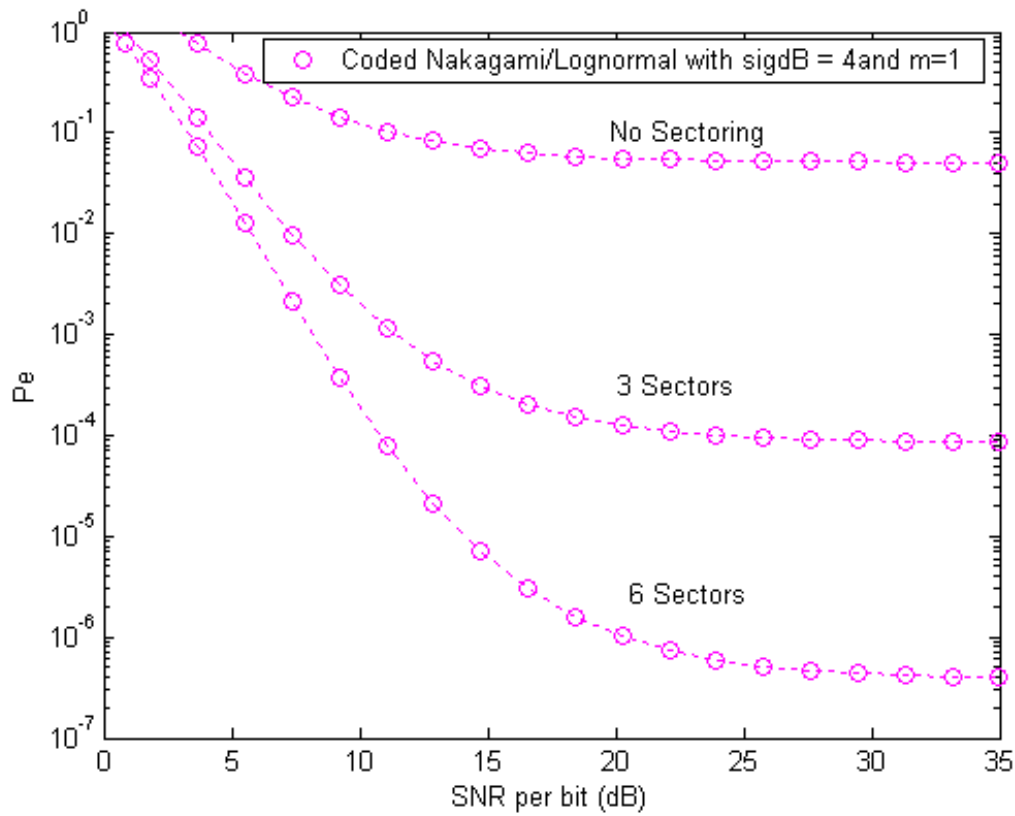


Figure 5.5. Coded Nakagami with and without Sectoring for 100 Users per Cell and for Lognormal Shadowing  $\sigma = 7$  and Power Control Error  $\sigma_{1dB} = 4$  and  $m = 1$ .

As can easily be seen, without sectoring, our system cannot perform adequately to serve up to 100 users per cell. For  $120^\circ$  (3 sectors per cell) the performance of our system would be just satisfactory while for  $60^\circ$  (6 sectors per cell) it would be very satisfactory.

## APPENDIX V. PLOTS OF THE PERFORMANCE OF THE SYSTEM WITH THE USE OF RAKE RECEIVER AND SECTORING

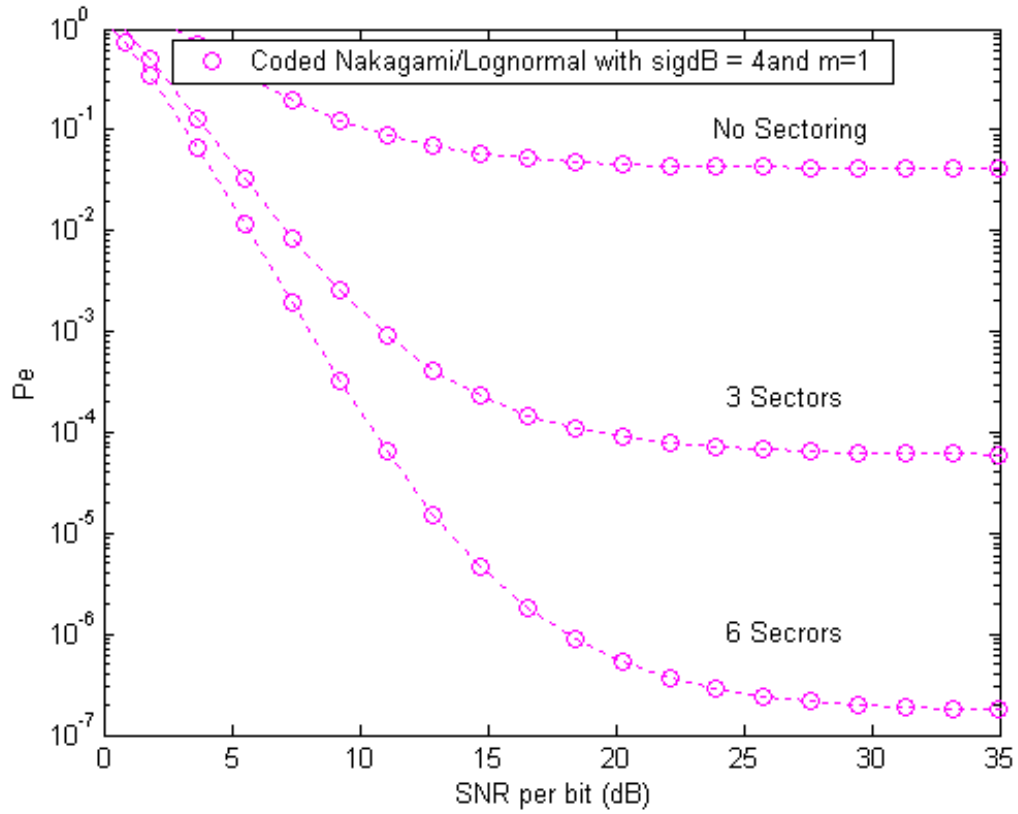


Figure 5.6. Coded Nakagami with and without Sectoring for 60 Users per Cell and for Lognormal Shadowing  $\sigma = 9$  and Power Control Error  $\sigma_{1dB} = 4$  and  $m = 1$ .

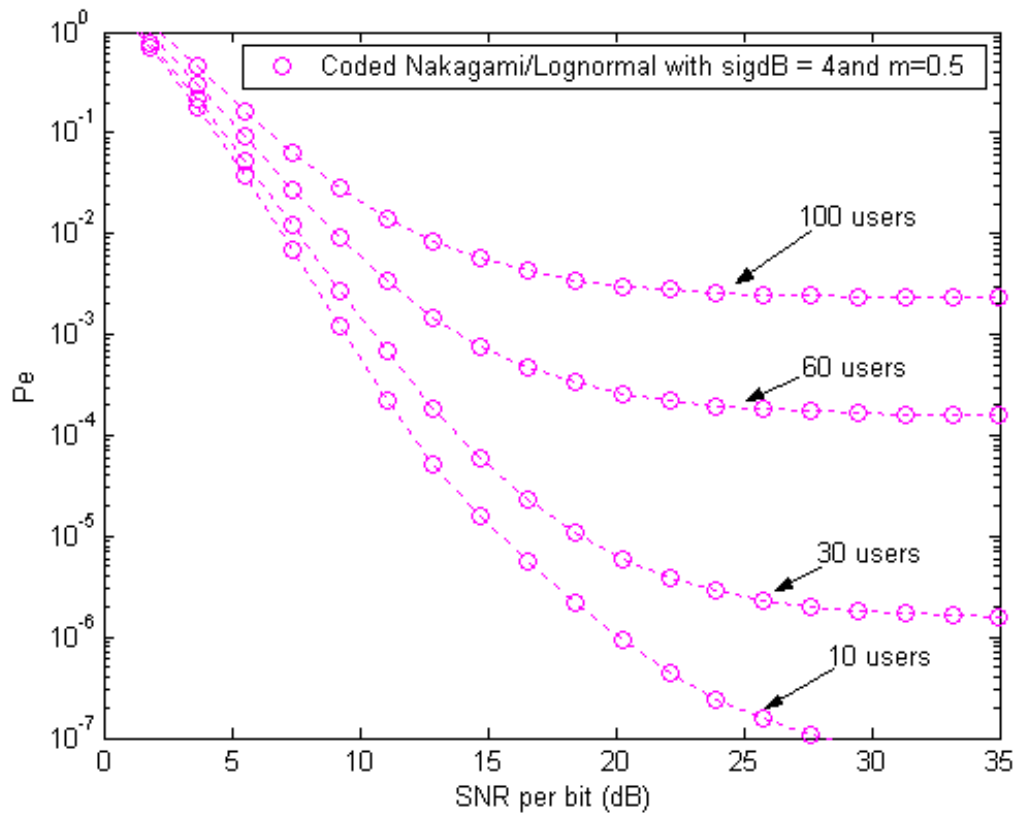


Figure 5.7. Coded Nakagami for Lognormal Shadowing  $\sigma = 7$  and Power Control Error  $\sigma_{dB} = 4$  for  $m=0.5$  and Various Users for  $120^\circ$  Sectoring.

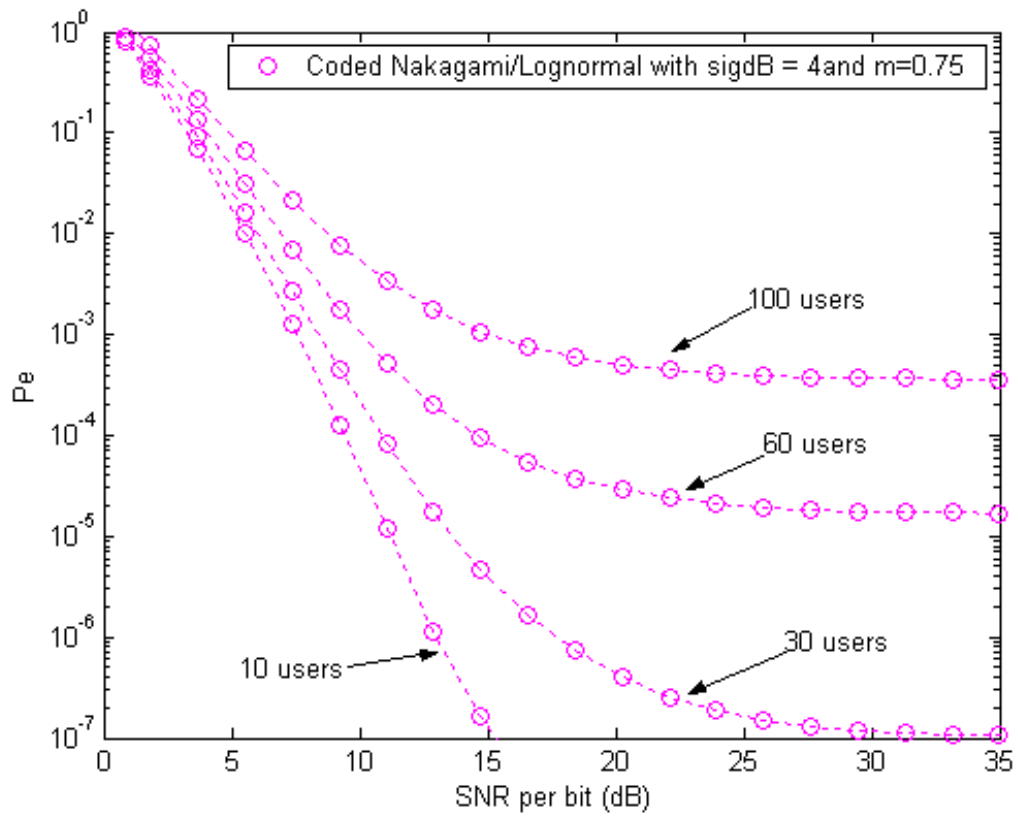


Figure 5.8. Coded Nakagami for Lognormal Shadowing  $\sigma = 7$  and Power Control Error  $\sigma_{1dB} = 4$  for  $m = 0.75$  and Various Users for  $120^\circ$  Sectoring.

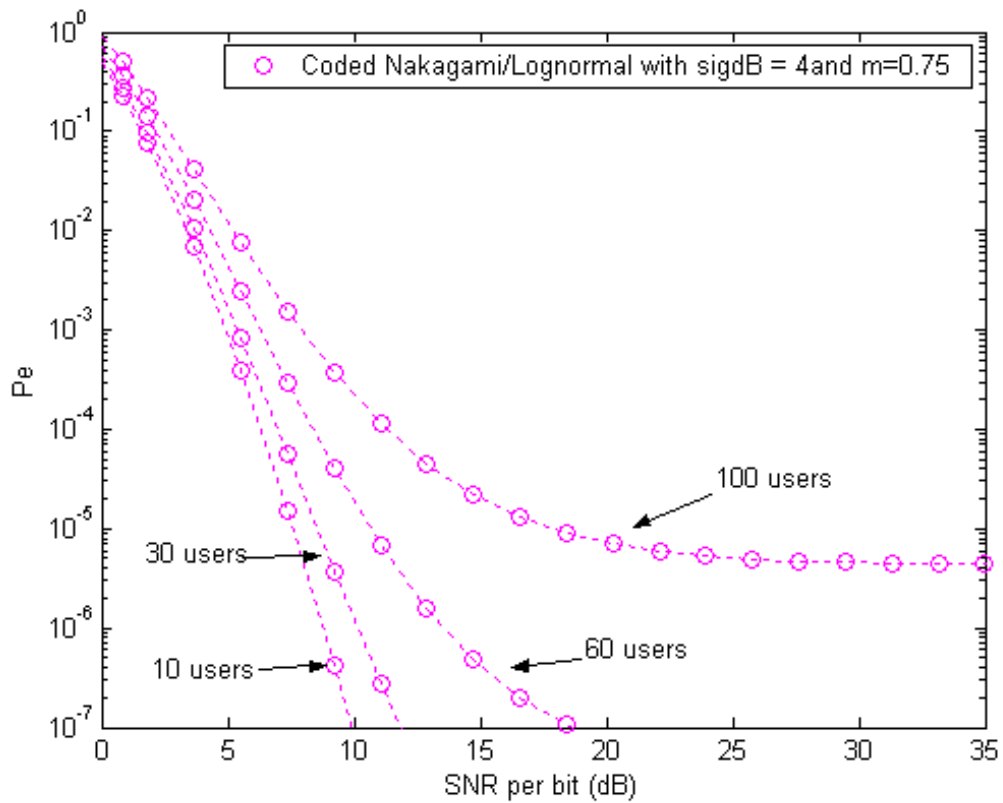


Figure 5.9. Coded Nakagami for Lognormal Shadowing  $\sigma = 7$  and Power Control Error  $\sigma_{1dB} = 4$  for  $m=0.75$  and Various Users for  $120^\circ$  Sectoring and Rake Receiver.

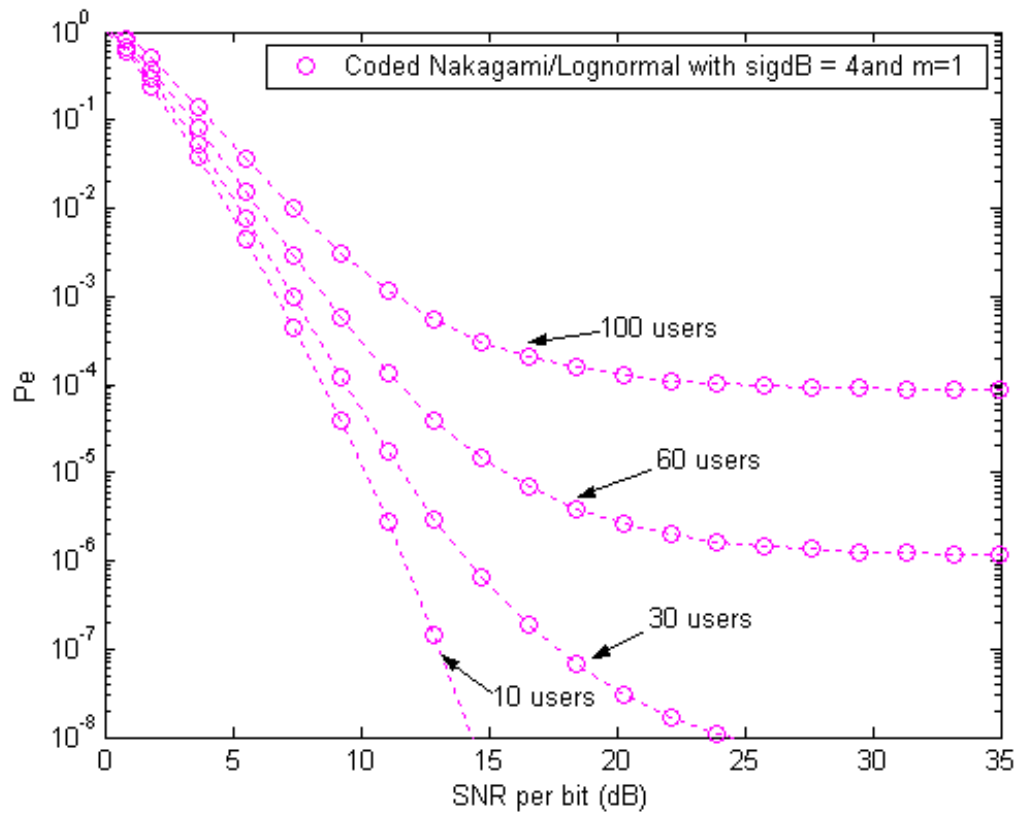


Figure 5.10. Coded Nakagami for Lognormal Shadowing  $\sigma = 7$  and Power Control Error  $\sigma_{1dB} = 4$  for  $m=1$  and Various Users for  $120^\circ$  Sectoring.

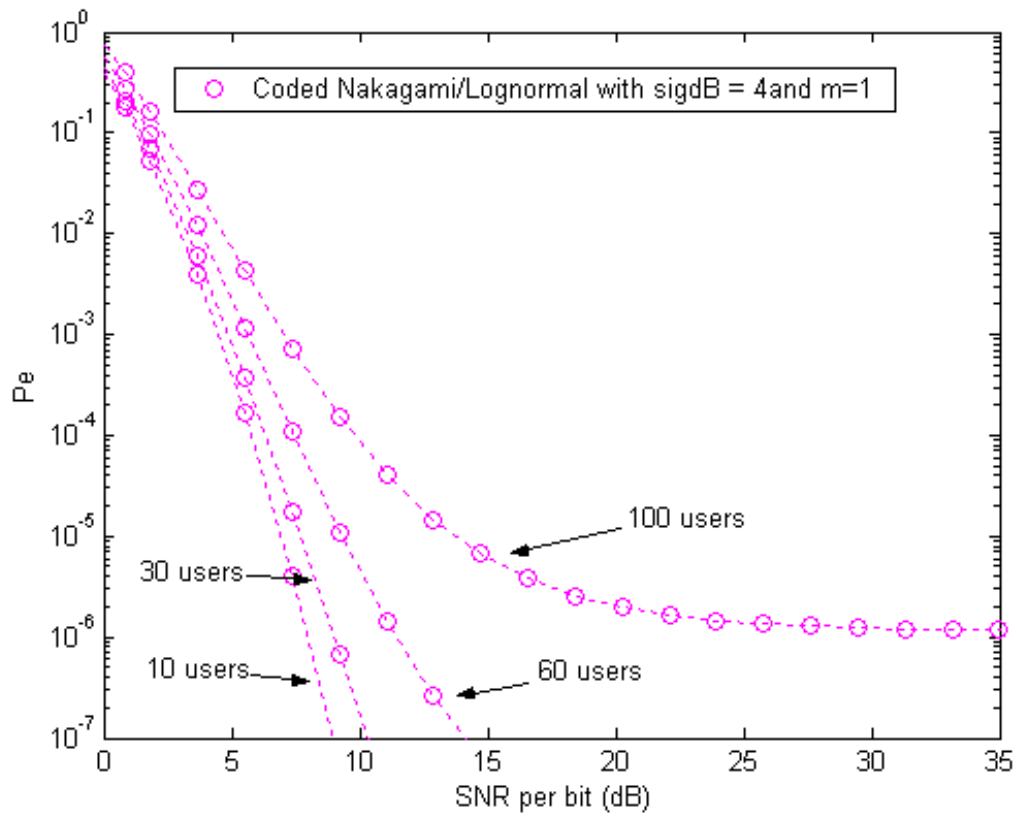


Figure 5.11. Coded Nakagami for Lognormal Shadowing  $\sigma = 7$  and Power Control Error  $\sigma_{1dB} = 4$  for  $m=1$  and Various Users for  $120^\circ$  Sectoring and Rake Receiver.

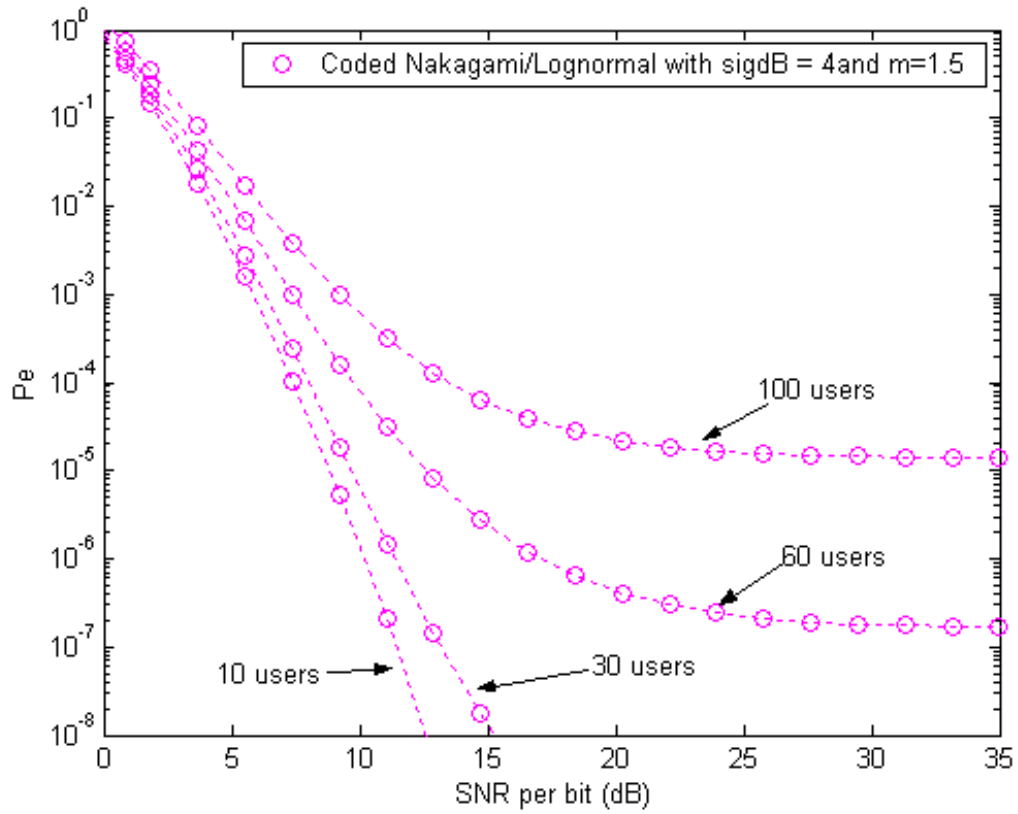


Figure 5.12. Coded Nakagami for Lognormal Shadowing  $\sigma = 7$  and Power Control Error  $\sigma_{dB} = 4$  for  $m=1.5$  and Various Users for  $120^\circ$  Sectoring.



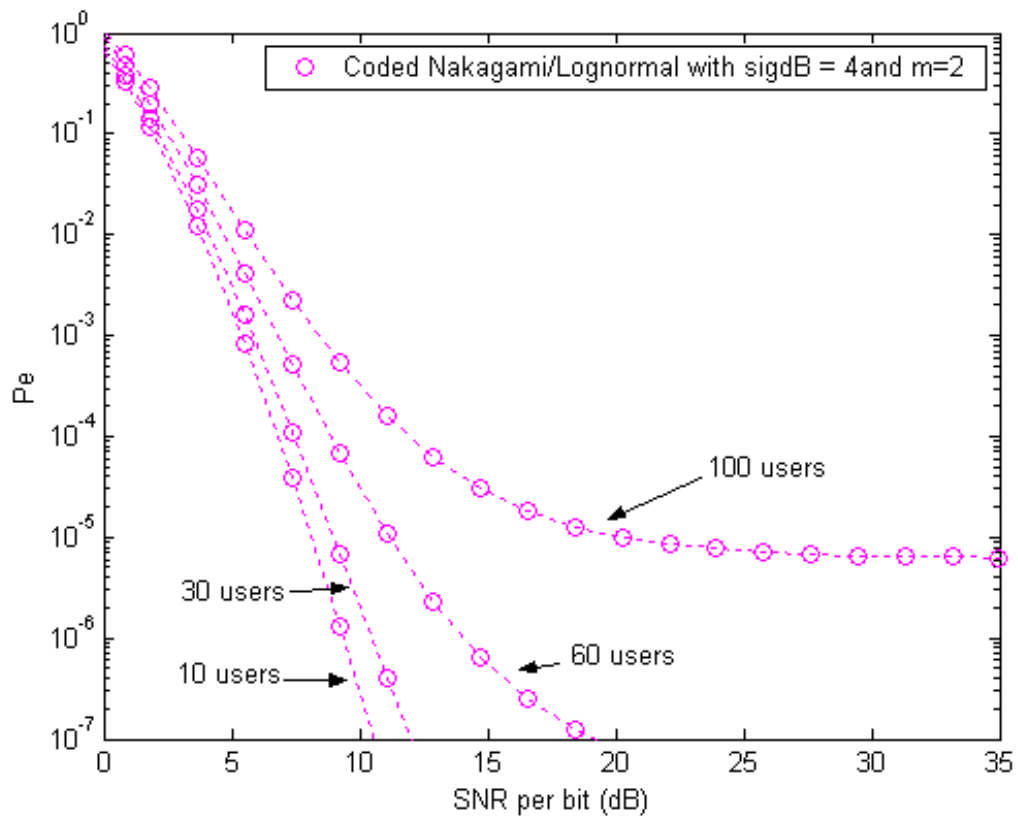


Figure 5.13. Coded Nakagami for Lognormal Shadowing  $\sigma = 7$  and Power Control Error  $\sigma_{1dB} = 4$  for  $m=2$  and Various Users for  $120^\circ$  Sectoring.

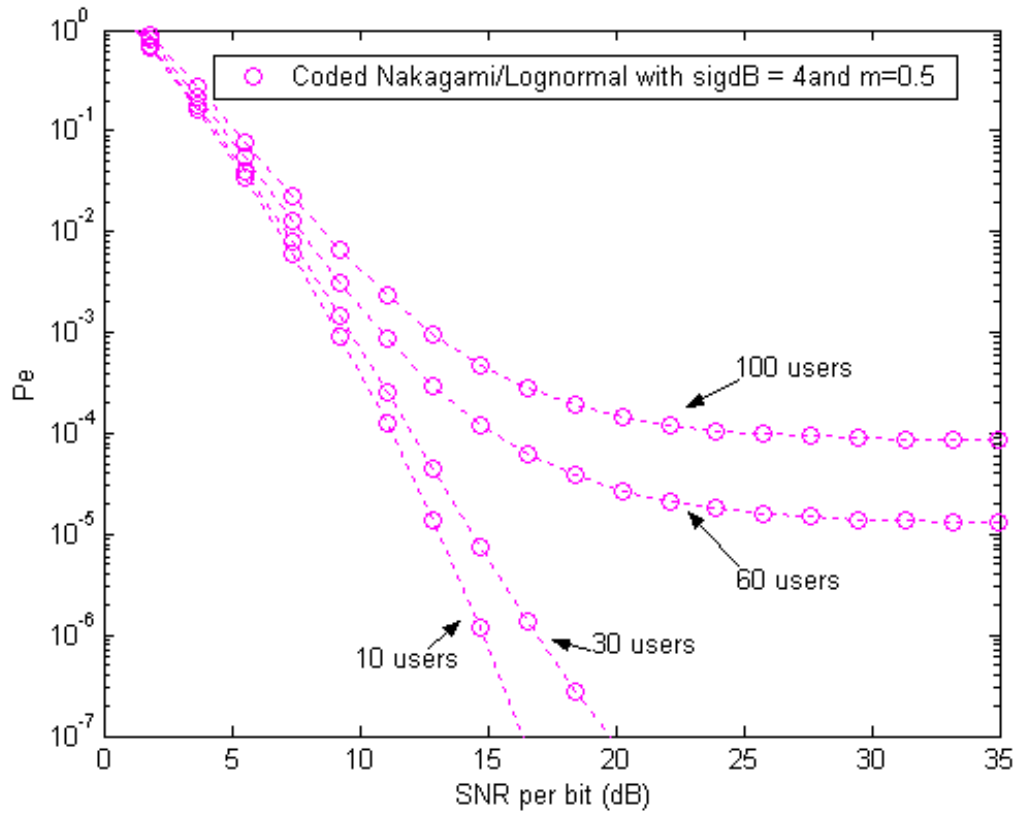


Figure 5.14. Coded Nakagami for Lognormal Shadowing  $\sigma = 7$  and Power Control Error  $\sigma_{1dB} = 4$  for  $m=0.5$  and Various Users for  $60^\circ$  Sectoring.

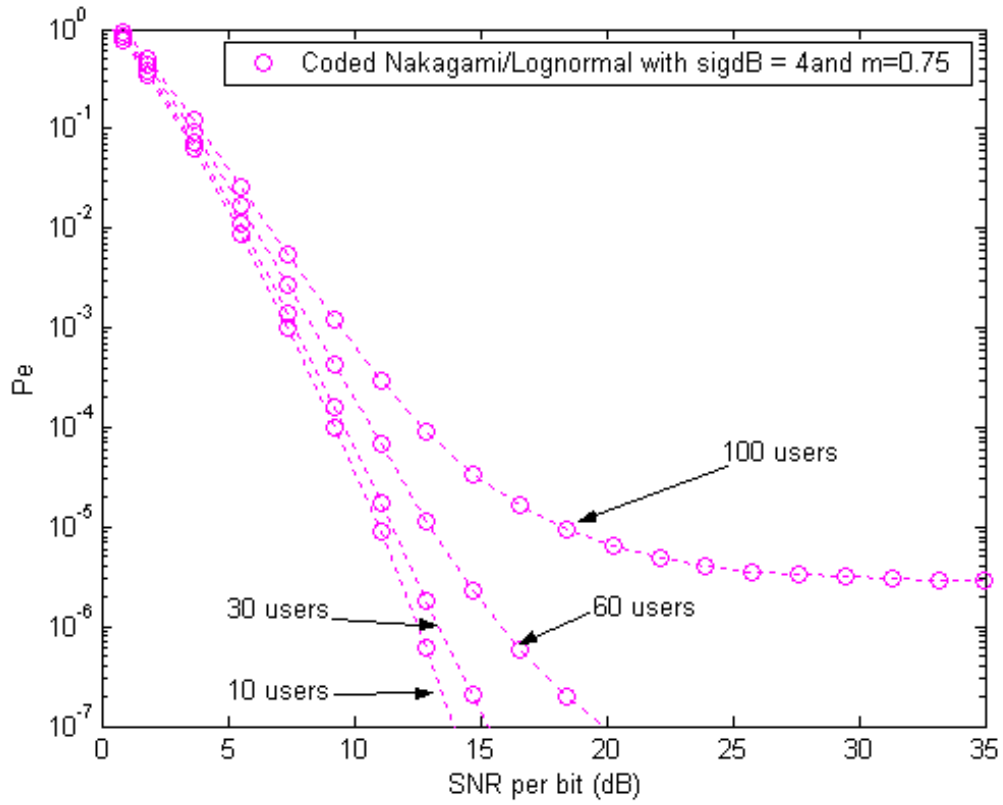


Figure 5.15. Coded Nakagami for Lognormal Shadowing  $\sigma = 7$  and Power Control Error  $\sigma_{dB} = 4$  for  $m = 0.75$  and Various Users for  $60^\circ$  Sectoring.

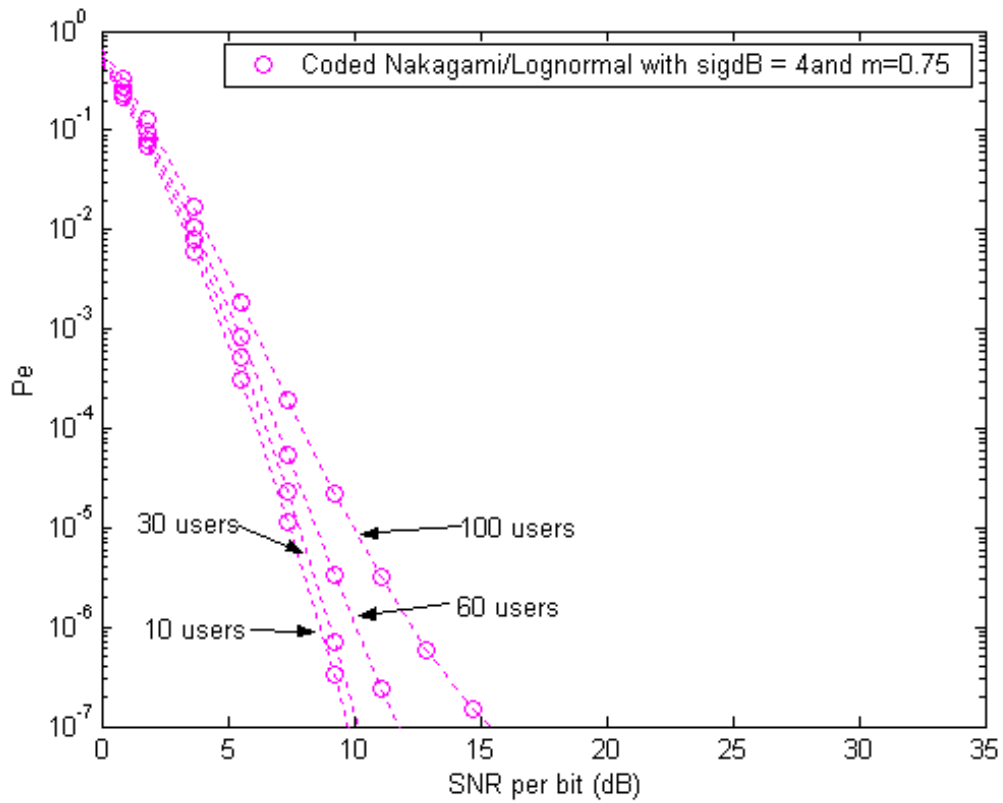


Figure 5.16. Coded Nakagami for Lognormal Shadowing  $\sigma = 7$  and Power Control Error  $\sigma_{dB} = 4$  for  $m=0.75$  and Various Users for  $60^\circ$  Sectoring and Rake Receiver.

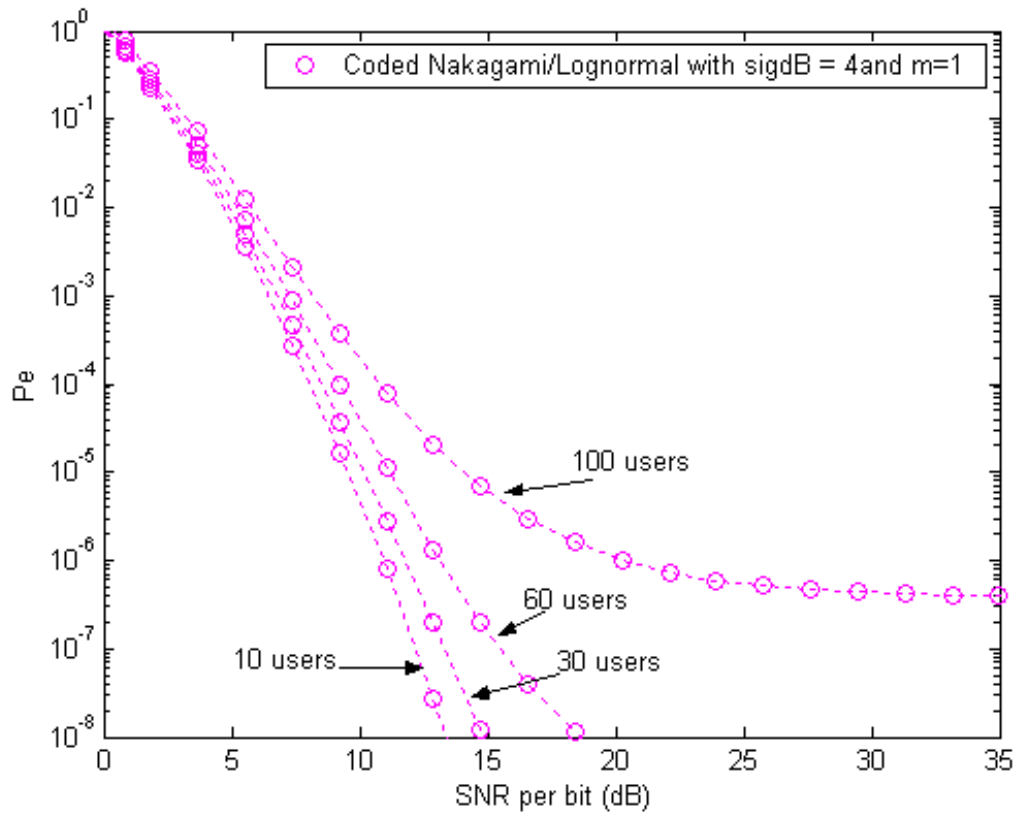


Figure 5.17. Coded Nakagami for Lognormal Shadowing  $\sigma = 7$  and Power Control Error  $\sigma_{dB} = 4$  for  $m=1$  and Various Users for  $60^\circ$  Sectoring.

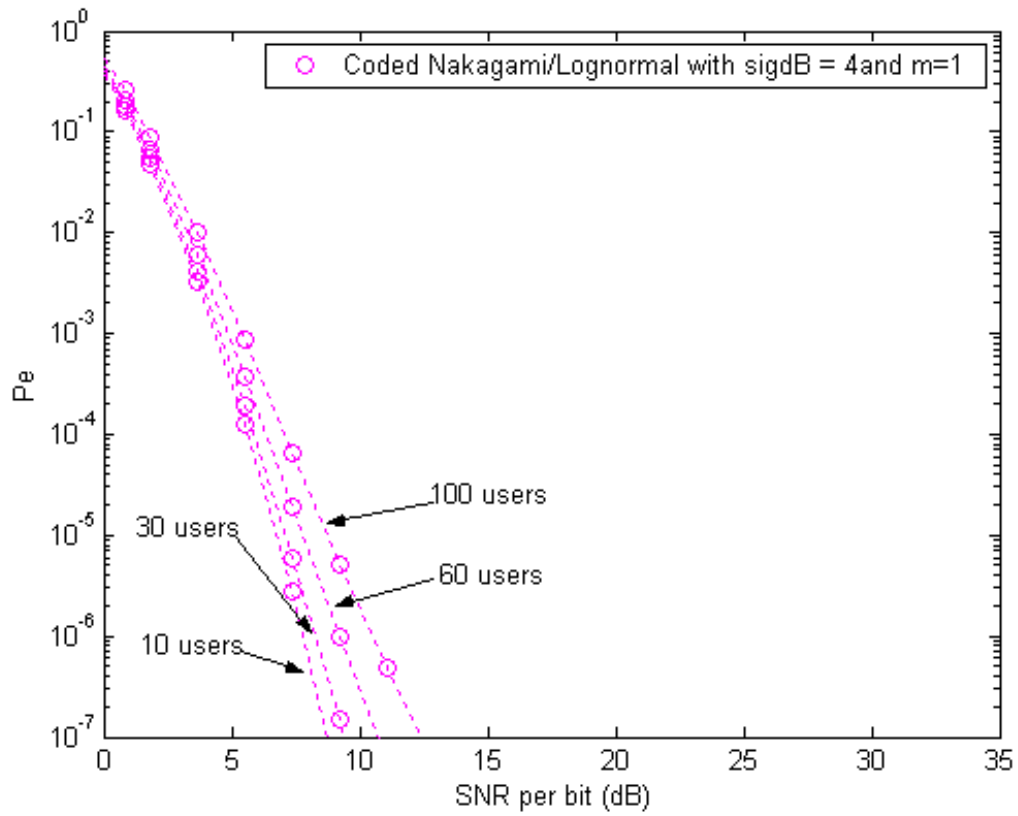


Figure 5.18. Coded Nakagami for Lognormal Shadowing  $\sigma = 7$  and Power Control Error  $\sigma_{dB} = 4$  for  $m=1$  and Various Users for  $60^\circ$  Sectoring with Rake Receiver.

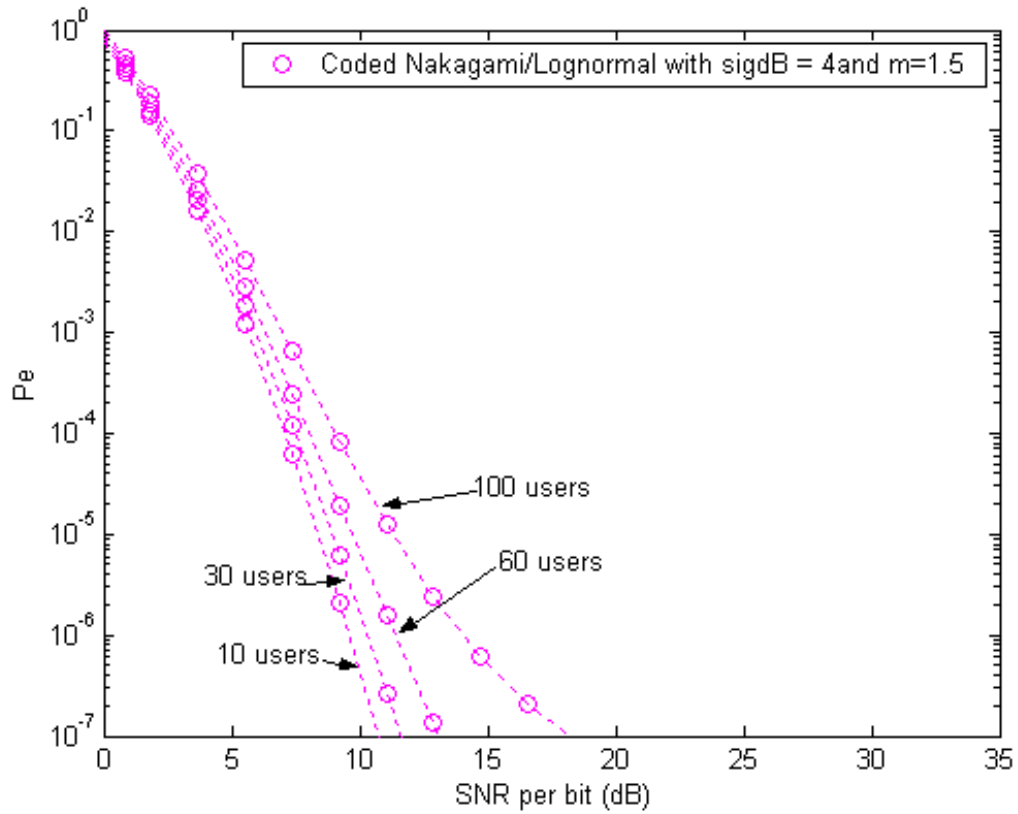


Figure 5.19. Coded Nakagami for Lognormal Shadowing  $\sigma = 7$  and Power Control Error  $\sigma_{dB} = 4$  for  $m = 1.5$  and Various Users for  $60^\circ$  Sectoring.

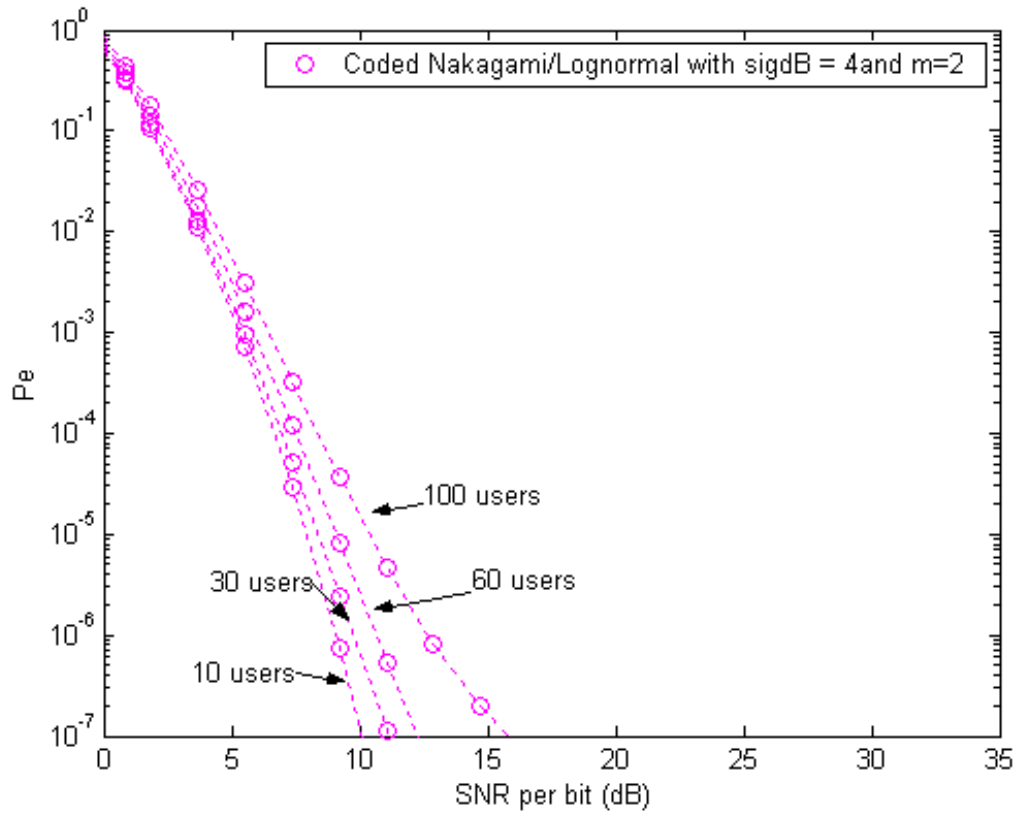


Figure 5.20. Coded Nakagami for Lognormal Shadowing  $\sigma = 7$  and Power Control Error  $\sigma_{dB} = 4$  for  $m=2$  and Various Users for  $60^\circ$  Sectoring.



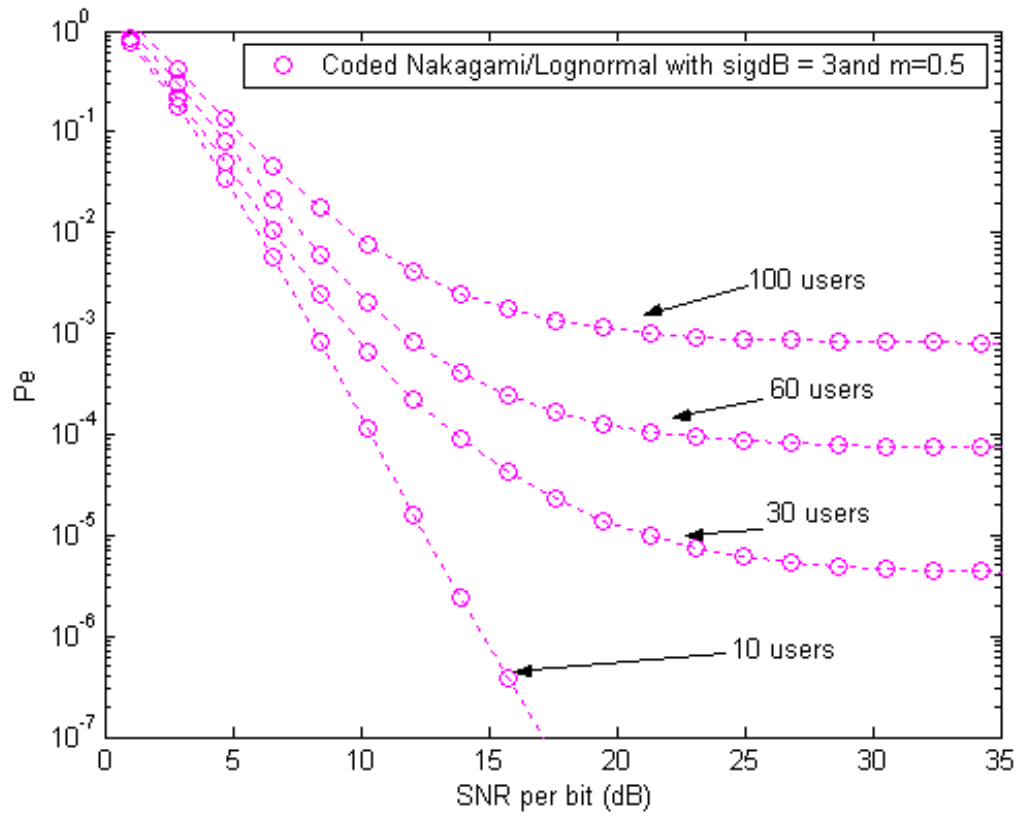


Figure 5.21. Coded Nakagami for Lognormal Shadowing  $\sigma = 7$  and Power Control Error  $\sigma_{dB} = 3$  for  $m = 0.5$  and Various Users for  $120^\circ$  Sectoring.

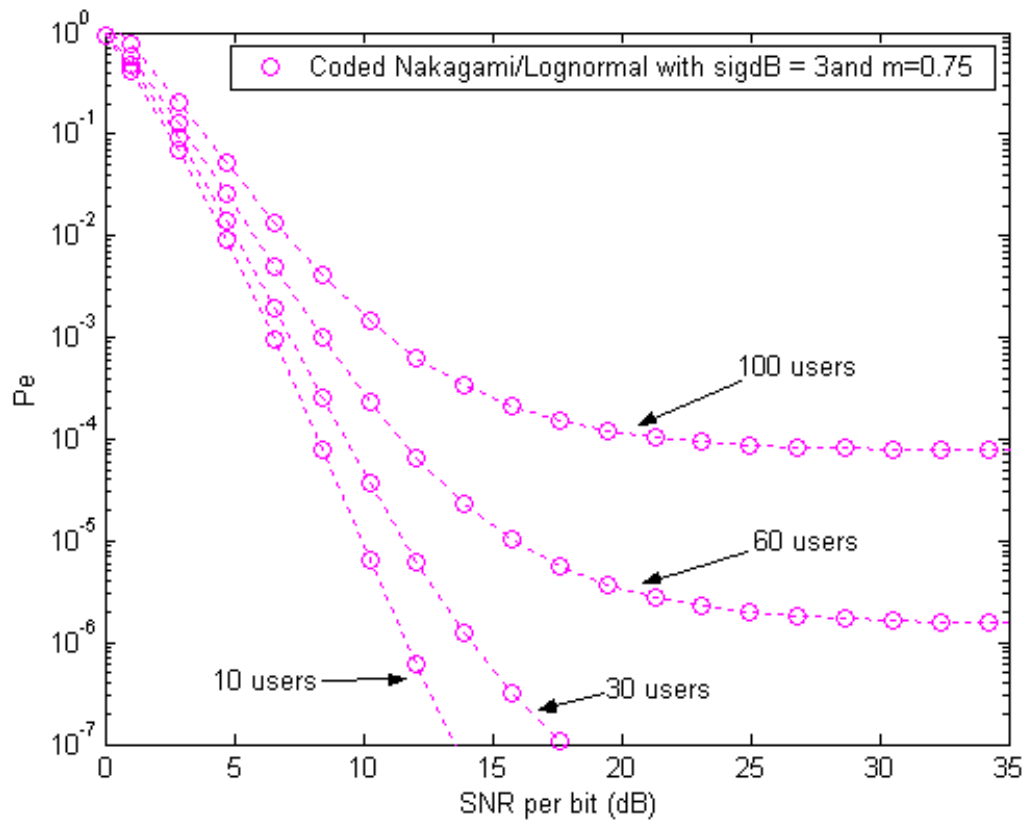


Figure 5.22. Coded Nakagami for Lognormal Shadowing  $\sigma = 7$  and Power Control Error  $\sigma_{dB} = 3$  for  $m=0.75$  and Various Users for  $120^\circ$  Sectoring.

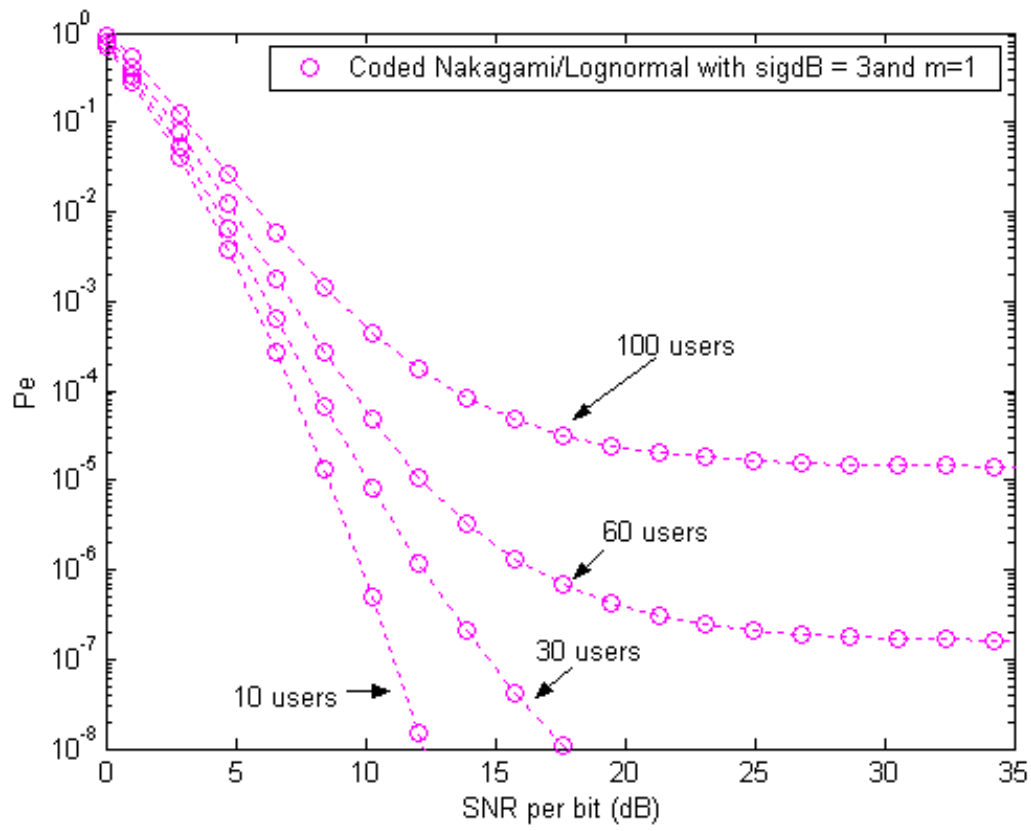


Figure 5.23. Coded Nakagami for Lognormal Shadowing  $\sigma = 7$  and Power Control Error  $\sigma_{1dB} = 3$  for  $m = 1$  and Various Users for  $120^\circ$  Sectoring.

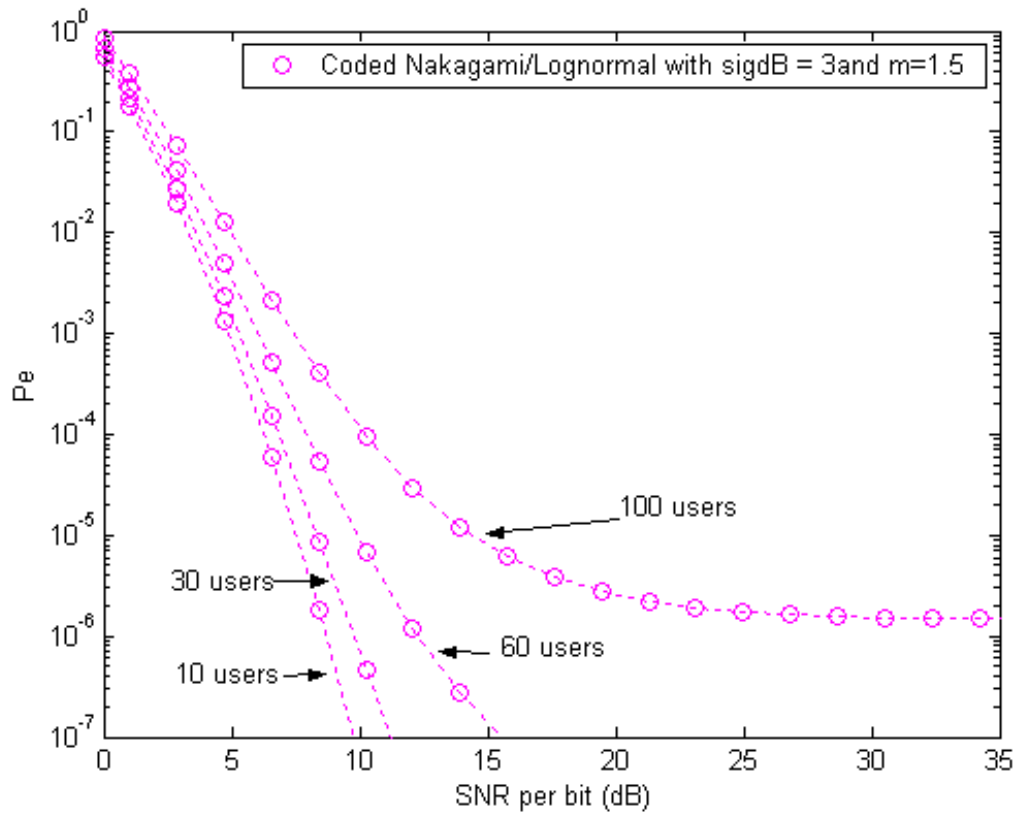


Figure 5.24. Coded Nakagami for Lognormal Shadowing  $\sigma = 7$  and Power Control Error  $\sigma_{dB} = 3$  for  $m=1.5$  and Various Users for  $120^\circ$  Sectoring.

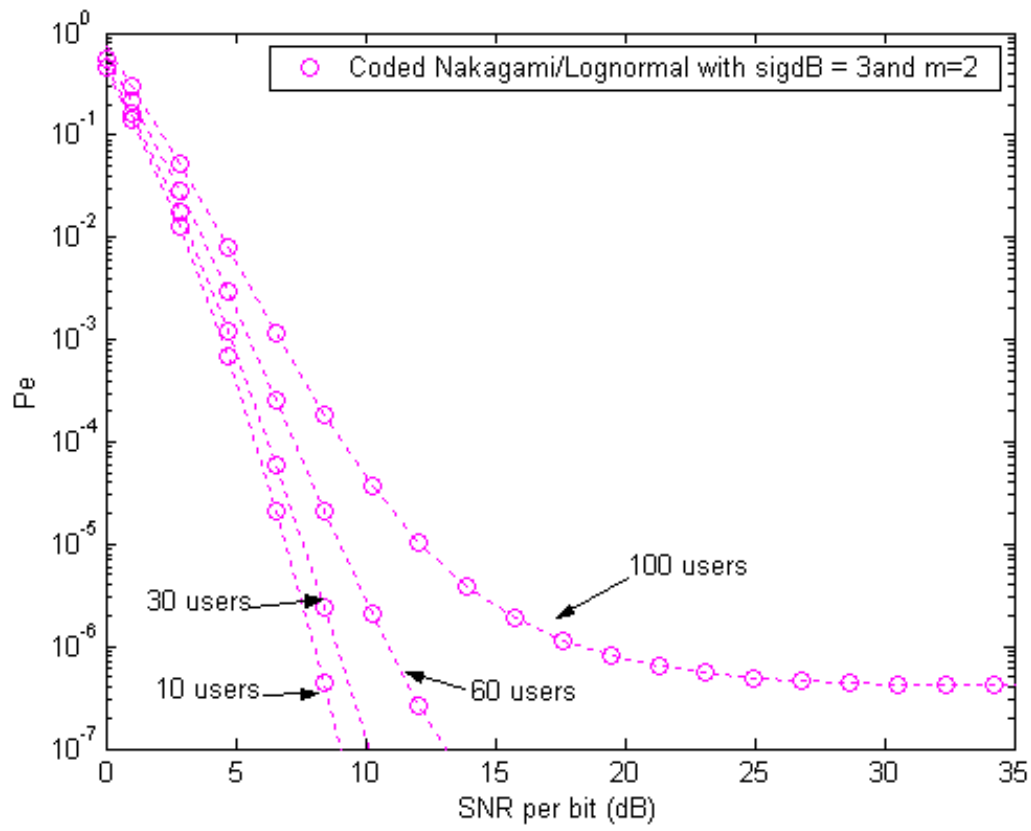


Figure 5.25. Coded Nakagami for Lognormal Shadowing  $\sigma = 7$  and Power Control Error  $\sigma_{dB} = 3$  for  $m=2$  and Various Users for  $120^\circ$  Sectoring.

## VI. JAMMING

In this chapter the effects of jamming on communications systems are examined. The following analysis is based on [4].

### A. PERFORMANCE OF BPSK IN BARRAGE NOISE JAMMING

Suppose someone, for any reason, wants to jam a simple BPSK signal by using a band limited noise-like signal  $n_I(t)$  with PSD  $S_{n_I}(f)$ . Thus, for a system where the only interference is the AWGN and  $n_I(t)$  which are independent random processes, the total noise power at the integrator output is:

$$\sigma^2 = \frac{N_0}{2T_b} + \sigma_I^2 = \frac{N_0}{2T_b} + \frac{1}{2} \int_{-\infty}^{\infty} [S_{n_I}(f - f_c) + S_{n_I}(f + f_c)] \left[ \frac{\sin(\pi f T_b)}{\pi f T_b} \right]^2 df \quad (6.1)$$

It is supposed that  $S_{n_I}(f)$  is  $\frac{N_I}{2}$  within the null-to-null bandwidth of the BPSK signal and zero elsewhere, so:

$$\sigma^2 = \frac{N_0}{2T_b} + \frac{1}{2} N_I \int_{-R_b}^{R_b} \left( \frac{\sin(\pi f T_b)}{\pi f T_b} \right)^2 df \Rightarrow \sigma^2 = \frac{N_0}{2T_b} + \frac{0.903 N_I}{2T_b} \quad (6.2)$$

Thus:

$$P_b = Q\left(\sqrt{\frac{\bar{Y}^2}{\sigma_I^2}}\right) = Q\left(\sqrt{\frac{\bar{Y}^2}{\frac{N_0}{2T_b} + \frac{0.903}{2T_b} N_I}}\right) = Q\left(\sqrt{\frac{2E_b}{N_0 + 0.903 N_I}}\right) \quad (6.3)$$

### B. PERFORMANCE OF DS SPREAD SPECTRUM SYSTEMS IN BARRAGE NOISE JAMMING

When a DS spread spectrum system is attacked by a band limited noise-like signal  $n_{I_{ss}}(t)$  then, as in the previous case, the total noise power at the integrator output is

$$\sigma^2 = \frac{N_0}{2T_b} + \sigma_{I_{ss}}^2 = \frac{N_0}{2T_b} + \frac{1}{2} \int_{-\infty}^{\infty} S_{n_{I_{ss}}}(f) \left( \frac{\sin(\pi f T_b)}{\pi f T_b} \right)^2 df \quad (6.4)$$

where  $S_{n_{iss}}(f)$  is PSD of the barrage noise signal at the integrator output.

Now, if the jammer's power is the same for the DS spread spectrum with the conventional's BPSK

$$P_I = P_{I_{ss}} \Rightarrow 2R_b N_I = 2R_{cc} N_{I_{ss}} \Rightarrow N_{I_{ss}} = N_I \frac{R_b}{R_{cc}} = N_I \frac{R_b}{NR_b} \Rightarrow N_{I_{ss}} = \frac{N_I}{N} \quad (6.5)$$

where  $N$  is the spreading factor. Now

$$n_i(t) = n'(t) \cdot c_{01}(t) \cdot \sqrt{2} \cdot \cos(2\pi f_c t)$$

The PSD of  $c_{01}(t) \cdot \sqrt{2} \cdot \cos(2\pi f_c t)$  is:

$$S(f) = \frac{1}{2} \cdot T_{cc} \cdot \left\{ \sin^2 c^2(T_{cc}(f - f_c)) + \sin^2 c^2(T_{cc}(f + f_c)) \right\} \quad (6.6)$$

Thus, the PSD at the integrator's input would be:

$$\begin{aligned} S_{n_{iss}}(f) &= \int_{-\infty}^{\infty} S_{n'_{iss}}(u) \cdot S(f - u) du \\ &= \frac{T_{cc} \cdot N_{I_{ss}}}{4} \cdot \int_{f_c - R_{cc}}^{f_c + R_{cc}} \left\{ \sin^2 c^2[T_{cc}(f - f_c - u)] + \sin^2 c^2[T_{cc}(f + f_c - u)] \right\} du \\ &\quad + \frac{T_{cc} \cdot N_{I_{ss}}}{4} \cdot \int_{-f_c - R_{cc}}^{-f_c + R_{cc}} \left\{ \sin^2 c^2[T_{cc}(f - f_c - u)] + \sin^2 c^2[T_{cc}(f + f_c - u)] \right\} du \end{aligned} \quad (6.7)$$

Now, with the substitutions  $v = (f - f_c - u) \cdot T_{cc}$  in the first and third terms and  $v = (f + f_c - u) \cdot T_{cc}$  in the second and fourth terms in the preceding equation:

$$\begin{aligned} S_{n_{iss}}(f) &= \frac{N_{I_{ss}}}{4} \cdot \int_{(f-2f_c-R_{cc})/R_{cc}}^{(f-2f_c+R_{cc})/R_{cc}} \sin^2 c^2 v dv + \frac{N_{I_{ss}}}{2} \cdot \int_{(f-R_{cc})/R_{cc}}^{(f+R_{cc})/R_{cc}} \sin^2 c^2 v dv + \frac{N_{I_{ss}}}{4} \cdot \int_{(f+2f_c-R_{cc})/R_{cc}}^{(f+2f_c+R_{cc})/R_{cc}} \sin^2 c^2 v dv \\ &= \frac{N_{I_{ss}}}{4} \cdot \int_{-2f_c/R_{cc}-(1-f/R_{cc})}^{-2f_c/R_{cc}+(1+f/R_{cc})} \sin^2 c^2 v dv + \frac{N_{I_{ss}}}{2} \cdot \int_{-(1-f/R_{cc})}^{(1+f/R_{cc})} \sin^2 c^2 v dv + \frac{N_{I_{ss}}}{4} \cdot \int_{2f_c/R_{cc}-(1-f/R_{cc})}^{2f_c/R_{cc}+(1+f/R_{cc})} \sin^2 c^2 v dv \end{aligned}$$

So for high carrier frequencies where  $f \gg R_{cc}$  and when  $R_{cc} \gg R_b$  only the second term of  $S_{n_{iss}}(f)$  is passing through the integrator without significant attenuation

$$\text{and so } S_{n_{iss}}(f) = \frac{N_{I_{ss}}}{2} \int_{-1+f/R_{cc}}^{1+f/R_{cc}} \sin c^2 v dv \quad (6.8)$$

Now for  $f = R_b$ :

$$S_{n_{iss}}(R_b) = \frac{N_{I_{ss}}}{2} \int_{-1+R_b/R_{cc}}^{1+R_b/R_{cc}} \sin c^2 v dv = \frac{N_{I_{ss}}}{2} \int_{-1+1/N}^{1+1/N} \sin c^2 v dv \quad (6.9)$$

In our case for  $N = 128$  and from Equation (6.9):

$$S_{n_{iss}}(R_b) = \frac{N_{I_{ss}}}{2} \int_{-1+1/128}^{1+1/128} \sin c^2 v dv \approx \frac{N_{I_{ss}}}{2} \int_{-1}^1 \sin c^2 v dv = \frac{0.903}{2} \cdot N_{I_{ss}} \quad (6.10)$$

For  $f = 0$ :

$$S_{n_{iss}}(0) = \frac{N_{I_{ss}}}{2} \int_{-1}^1 \sin c^2 v dv = \frac{0.903}{2} \cdot N_{I_{ss}} \quad (6.11)$$

From Equations (6.10) and (6.11), it can be seen that the PSD of the jammer at the integrator input has constant value equal to  $\frac{0.903}{2} \cdot N_{I_{ss}}$  for the entire bandwidth of the integrator and so:

$$\sigma^2 = \frac{N_0}{2T_b} + \frac{0.903}{2} \cdot N_{I_{ss}} \int_{-\infty}^{\infty} \left( \frac{\sin(\pi f T_b)}{\pi f T_b} \right)^2 df = \frac{N_0}{2T_b} + \frac{0.903}{2} \cdot \frac{N_{I_{ss}}}{T_b} \quad (6.12)$$

The probability of bit error for DS is:

$$P_b = Q\left(\sqrt{\frac{\bar{Y}^2}{\sigma^2}}\right) = Q\left(\sqrt{\frac{2\bar{Y}^2 T_b}{N_0 + 0.903 N_{I_{ss}}}}\right) = Q\left(\sqrt{\frac{2E_b}{N_0 + 0.903 N_{I_{ss}}}}\right) \Rightarrow$$

$$P_b = Q\left(\sqrt{\frac{2E_b}{N_0 + 0.903 \frac{N_I}{N}}}\right) \quad (6.13)$$



From Equations (6.3) and (6.13), it can be derived that the jammer's effect for the same power is N times smaller for the DS spread spectrum system.

The factor N is the direct sequence processing gain and is the effective increase in Signal to Noise Ratio when the effects of the thermal noise are negligible ( $\frac{N_I}{N} \gg N_0$ ).

### C. PERFORMANCE OF REVERSE CHANNEL OF A DS SPREAD SPECTRUM SYSTEM WITH FEC IN BARRAGE NOISE JAMMING

When the DS CDMA system is attacked by a band limited noise jamming signal  $n_{I_{ss}}(t)$ , the total noise power at the integrator output would be:

$$\begin{aligned} \sigma_{\zeta_{total}}^2 &= \text{Var}\{\zeta_1\} + \text{Var}\{\zeta_2\} + \text{Var}\{n\} + \text{Var}\{n_{I_{ss}}\} \\ &= \frac{1}{3 \cdot N} \cdot \sum_{k=2}^K E\{R_{0k}^2\} \cdot E\{P_{0k}\} + \frac{1}{3 \cdot N} \cdot \sum_{i=1}^6 \sum_{j=1}^K E\{R_{ij}^2\} \cdot E\{P_{ij}\} + \frac{N_0}{2 \cdot T_{cc}} + \frac{0.903}{2} \cdot \frac{N_{I_{ss}}}{T_{cc}} \end{aligned} \quad (6.14)$$

So the upper bound of the first event error probability is as follows

$$P_2(d) \Big|_{r_i, P_{kt}} = Q \left( \sqrt{\frac{\sum_{\ell=1}^d r_{\ell}^2 x_{\ell}}{\frac{1}{3N} \exp\left(\frac{\lambda^2 \sigma_{dB}^2}{2}\right) (K-1) + \frac{1}{3N} \sum_{i=1}^6 \sum_{j=1}^K E\{\lambda_{ij}\} + \frac{N_0}{2E_c} + \frac{0.903}{2} \cdot \frac{N_{I_{ss}}}{E_c}}} \right) \quad (6.15)$$

and for a specific value of  $\frac{E_c}{N_0} = 15\text{dB}$ , the effect of barrage noise jamming for users per

cell can be seen. The aforementioned value of  $\frac{E_c}{N_0}$  is chosen because, as seen from all the

previous figures, the probability of bit error achieves its best value at that value.

In Figure 6.1, the probability of error versus SNR for 100 users per cell and 120° sectoring for lognormal shadowing  $\sigma = 7$  power control error  $\sigma_{1dB} = 4$  and  $m = 1$  without jamming is shown while Figure 6.2 shows the probability of error versus Signal to Interference (Jamming) Ratio for 100 users per cell and 120° sectoring for lognormal

shadowing  $\sigma = 7$  power control error  $\sigma_{1dB} = 4$  and  $m=1$  and for a specific value of  $\frac{E_c}{N_0} = 15\text{dB}$ .

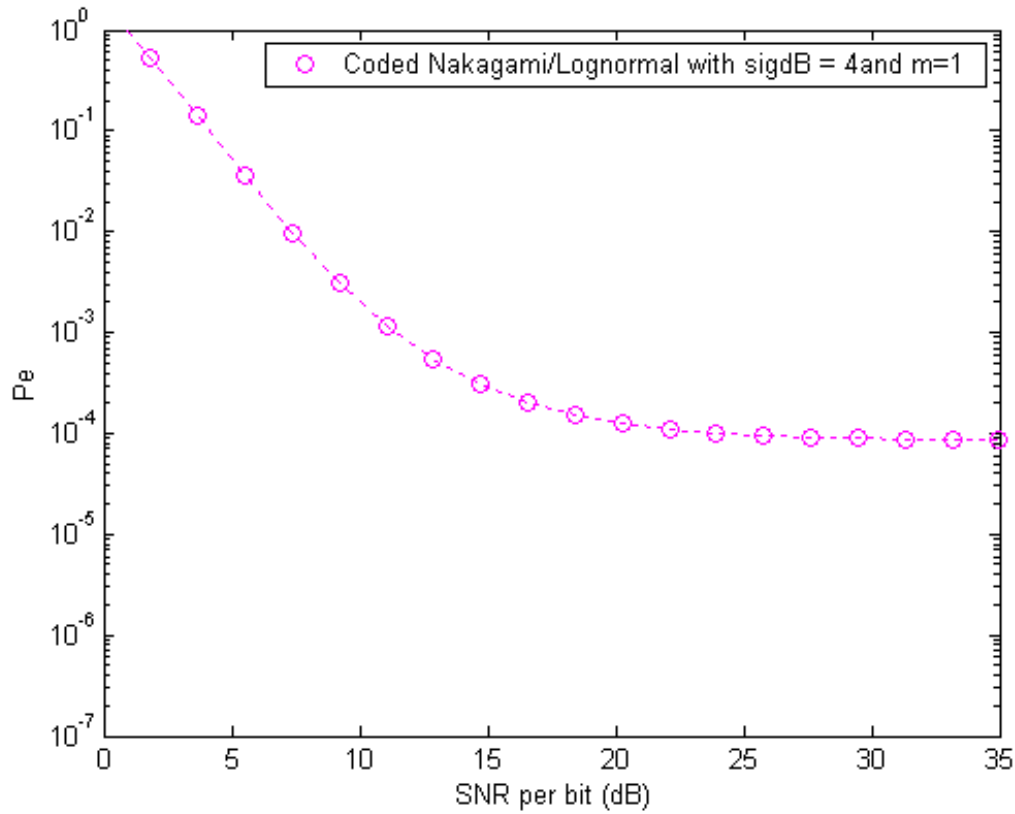


Figure 6.1. Coded Nakagami for 100 Users per Cell with  $120^\circ$  Sectoring, Lognormal Shadowing  $\sigma = 7$ , Power Control Error  $\sigma_{1dB} = 4$  and  $m=1$ .

As seen from Figure 6.1, the probability of error for high values of SNR (SNR=30dB) achieves  $P_e = 10^{-4}$  while for SNR=15dB the value of probability of bit error is  $P_e \approx 2 \cdot 10^{-4}$ .

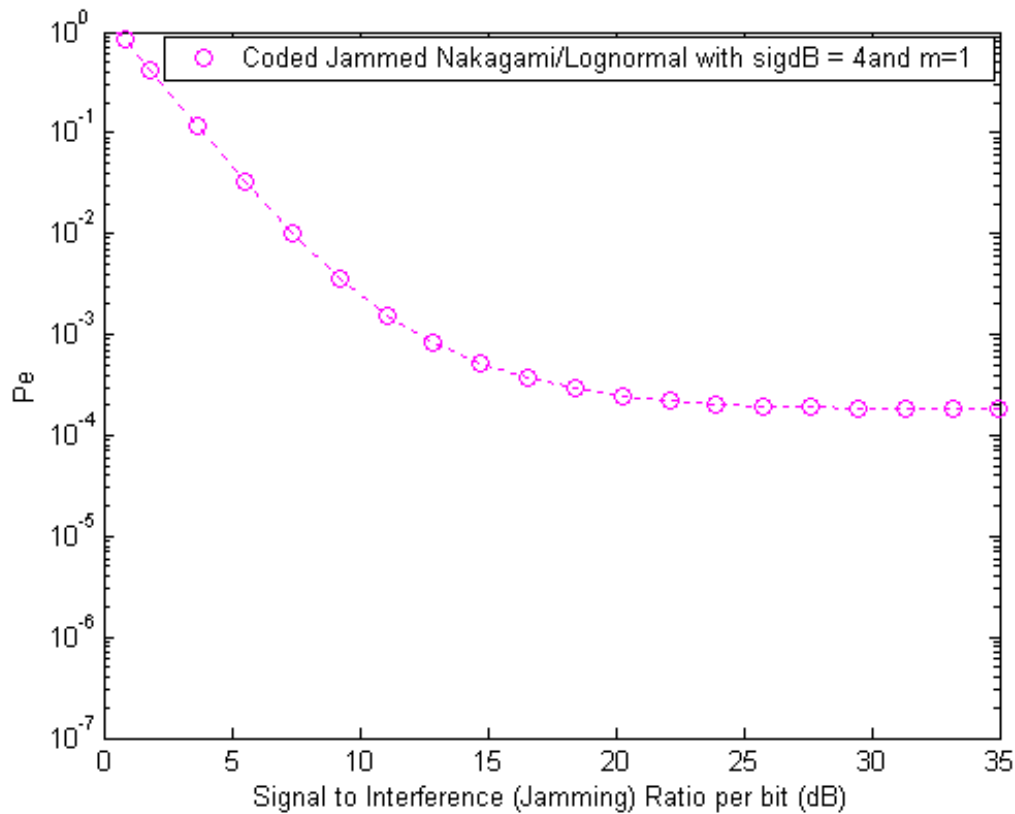


Figure 6.2. Coded Jammed Nakagami for 100 Users per Cell with 120° Sectoring, SNR=15, Lognormal Shadowing  $\sigma = 7$ , Power Control Error  $\sigma_{1dB} = 4$  and  $m=1$ .

It can be seen that for high values of Signal-to-Interference-Ratio (Signal-to-Jamming Power Ratio), when the jamming power is too small compared to the Signal Power and the Noise Power, the value of the probability of bit error is  $P_e \approx 2 \cdot 10^{-4}$ . So for high values of Signal-to-Interference-Ratio the results in Figure 6.2 converge to the same  $P_e$  that can be found in Figure 6.1 for SNR=15 dB.

## VII. CONCLUSIONS

In this thesis, the performance of the reverse channel of a DS-CDMA cellular system with FEC and sectoring in a Nakagami-fading environment with lognormal power control error and use of a Rake receiver at the base station was explored.

In Chapter II, the advantages of a Spread Spectrum communication system over the conventional BPSK system were discussed. The properties of PN sequences and Walsh codes and their use in spreading the information data signal were also demonstrated.

In Chapter III, a reverse channel for the DS-CDMA cellular system was developed and the effects of lognormal shadowing and power control error in a Nakagami-fading channel were examined. Also, the composite signal that the base station of the center cell receives was developed which includes the desired signal from mobile user one (which is in the coverage area of the center cell), the signals from the other active users in the center cell (intra-cell interference), the signals from all the active mobile users that are in the coverage area of the six adjacent cells (inter-cell or co-channel interference) and also the Additive White Gaussian Noise (AWGN).

In Chapter IV, FEC with convolutional code  $(n,k) = (1,2)$  and soft decision decoding was applied and then the Signal-to-Noise plus Interference Ratio (SNIR) and the bit error probability for the aforementioned communication system was developed. The performance (probability of bit error) of our system for several values of the Nakagami  $m$ -variable ( $m = 0.5, 0.75, 1, 1.5, 2$ ) and for various numbers of users per cell (10, 30, 60, 100) were then simulated by using Monte Carlo techniques. It was observed that as the value of the Nakagami  $m$ -variable increases, the better the performance and the performance degrades as the number of users increases. It was also observed the benefits, in performance, for using sectoring and that for small values of the standard deviation of the lognormal power control error, the system had a probability of bit error less than 0.001 even for a great number of users.

In Chapter V, the use of a Rake receiver at the base stations and the technique of sectoring was implemented and a dramatic improvement in performance was noticed.

Chapter VI demonstrated that our Spread Spectrum cellular communication system had better resistance than a typical BPSK system. Finally, the effects of barrage noise jamming in our communication system for a typical value of  $\frac{E_b}{N_0} = 15\text{dB}$  were observed.

## LIST OF REFERENCES

- [1] J. E. Tighe, "Modeling and Analysis of Cellular Forward System," Ph.D Dissertation, Naval Postgraduate School, Monterey California, March 2001.
- [2] T. S. Rappaport, *Wireless Communications: Principles & Practice*, Upper Saddle River, New Jersey: Prentice Hall PTR, 1996.
- [3] K. S. Gilhousen, I. M. Jacobs, R. Padovani, A. J. Viterbi, L. A. Weaver, Jr., C. E. Wheatley, "On the Capacity of a Cellular CDMA System," IEEE Transactions on Vehicular Technology, Vol. 40, No. 2, May 1991.
- [4] R. C. Robertson, *Class Notes from EC 4560 Communications ECCM*, NPS, Monterey, California.
- [5] R. L. Peterson, R. E. Ziemer, D. E. Borth, *Introduction to Spread Spectrum Communications*, Upper Saddle River, New Jersey: Prentice Hall PTR, 1995.
- [6] J. G. Proakis, *Digital Communications*, Boston, Massachusetts, WCB/McGraw-Hill, 1993.
- [7] S. B. Wicker, *Error Control Systems for Digital Communication and Storage*, Upper Saddle River, New Jersey: Prentice Hall PTR, 1995.
- [8] R. C. Robertson, *Class Notes from EC 4580 Coding and Information Theory*, NPS, Monterey, California.
- [9] J. S. Lee, L. E. Miller, *CDMA Systems Engineering Handbook*, Boston-London, Artech House Publishers, 1998.
- [10] M. P. Lotter, Pieter van Rooyen, "Cellular Channel Modeling and the Performance of DS-CDMA Systems with Antenna Arrays," IEEE Journal on Selected Areas in Communications, Vol. 17, No. 12, December 1999.

THIS PAGE INTENTIONALLY LEFT BLANK

## INITIAL DISTRIBUTION LIST

1. Defense Technical Information Center  
Ft. Belvoir, Virginia
2. Dudley Knox Library  
Naval Postgraduate School  
Monterey, California
3. Chairman, Department of Electrical of Computer Engineering  
Naval Postgraduate School  
Monterey, California
4. Chairman, Department of Information Sciences  
Naval Postgraduate School  
Monterey, California
5. Professor Tri T. Ha, Code EC/Ha  
Department of Electrical and Computer Engineering  
Naval Postgraduate School  
Monterey, California
6. CDR Jan E. Tighe  
Naval Information Warfare Activity  
Ft. Meade, Maryland
7. Professor David Jenn  
Department of Electrical and Computer Engineering  
Naval Postgraduate School  
Monterey, California
8. Embassy of Greece, Naval Attaché  
Washington, DC
9. Petros Klitorakis  
Chrisanthemon 68 Zografou, 157 72  
Athens, Greece